Spring 5-1997

Binding of Cobalt (III) to Nucleic Acids via Reaction with [Co(NH3)5(OH2)]3+

David M. Calderone
Seton Hall University

Binding of Cobalt (III) to Nucleic Acids
via Reaction with $[Co(NH_3)_5(OH_2)]^{3+}$
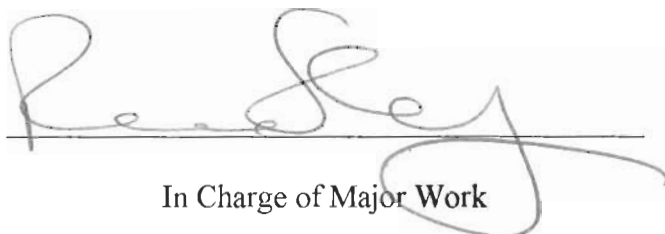
by

David M. Calderone

DISSERTATION

Submitted to the Department of Chemistry of Seton Hall University in partial
fulfillment of the requirements for the degree of Doctor of Philosophy.
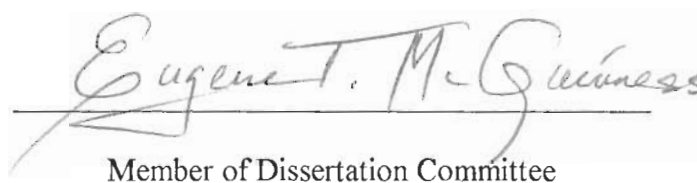
May 1997

We certify that we have read this thesis and that in our opinion it is adequate in scientific scope and quality as a dissertation for the degree of Doctor of Philosophy.
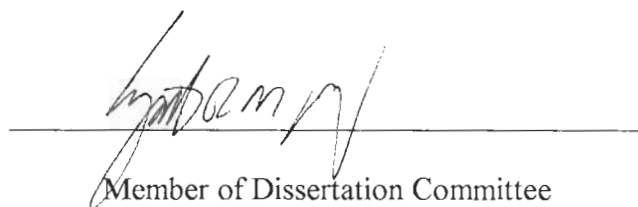
APPROVED

In Charge of Major Work

Eugene T. McGuiness

Member of Dissertation Committee

Member of Dissertation Committee

Daniel H. Huchital

Approved for the Chemistry Department
Chairperson, Department of Chemistry

ii

To the memory of
Joseph P. Calderone, Sr., M.D.

Τισ ανωεθαι ταυτα γενεστι

And to my Family
and Friends

ACKNOWLEDGMENTS

TABLE OF CONTENTS

LIST OF TABLES

vi

LIST OF FIGURES

viii

ix

ABSTRACT

Binding of Cobalt (III) to Nucleic Acids via Reaction with $[Co(NH_3)_5(OH_2)]^{3+}$

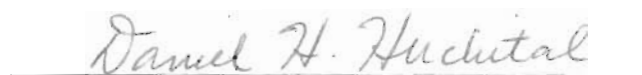David M. Calderone, Ph.D.

Seton Hall University, 1997

Mentor: Richard D. Sheardy

Treatment of five different synthetic DNA oligomers and a natural DNA polymer (sonicated calf thymus DNA) with $[Co(NH_3)_5(OH_2)]^{3+}$ resulted in irreversible modifications of all DNA samples. Standard protocol for preparing DNA samples calls for heat-annealing the oligomer in phosphate buffer in the absence or presence of cobalt(III)ammine complex for two minutes at 80 °C followed by slow cooling. An alternative method for treatment, in which the DNA remains fully duplexed, is incubation of oligomer in the presence of complex at 37 °C followed by exhaustive dialysis against 0.2 M NaCl and then water. The interaction specificities of cobalt(III)ammines with the self-complementary eight base pair oligomer (5medC-dG)$_4$, or **Z8**, have been investigated. The conformational properties of **Z8** were determined by inspection of the UV and CD spectra at 25 °C and 95 °C and thermal denaturation studies. With heat-annealing in the absence of any cobalt (III) complex, **Z8** assumes a double stranded, right-handed B conformation at 25 °C. Upon heat-annealing in the presence of 200 µM $[Co(NH_3)_6]^{3+}$, **Z8** assumes a double stranded, left-handed Z conformation at 25 °C. In contrast, the CD and UV spectra of **Z8** heat-annealed in the presence of 200 µM $[Co(NH_3)_5(OH_2)]^{3+}$ is consistent with a distorted B-like conformation at 25 °C. Incubation of **Z8** in the presence of $[Co(NH_3)_5(OH_2)]^{3+}$ results in modification of the conformational properties of the oligomer at both 25 °C and 95 °C relative to the

x

untreated oligomer. The extent of modification depends upon the incubation concentration of complex and reaction time. Atomic absorption (AA) analysis of these treated **Z8** samples indicate a high degree of cobalt association to the oligomer. The salt dependence of melting temperature, shown through linear T_m versus log [NaCl] plots, can be used to calculate (from the slope) the differential ion binding term, Δn, which represents the release of counterions per duplex upon denaturation. For oligomers **Z8**, **Z8** heat-treated, and **Z8** incubated, the Δn terms are 0.92, 0.48, and 0.28, respectively, indicating fewer Na+ released upon melting. This is indirect evidence that the two methods of modification result in cobalt being tightly bound to the DNA. These studies suggest that $[Co(NH_3)_5(OH_2)]^{3+}$ reacts with the oligomer resulting in tight binding of the cobalt (III) metal center to the DNA lattice.

Thermal denaturation studies on three oligomers which possess GpC sites (**Z8**, 12-mer and GC-site) indicated higher T_m values and dramatically decreased hyperchromism upon melting relative to the untreated oligomers. However, identical treatment of two oligomers (24-mer and CG-isomer) with G bases, but no GpC sites, resulted in lower T_m values and only slightly reduced hyperchromism. Thermal denaturation studies on sonicated calf thymus DNA prepared at three different cobalt to DNA ratios resulted in irreversible melting profiles of lower T_m than untreated DNA polymer. However, the sample prepared at high DNA and cobalt complex concentrations did not fully dissociate and gave a quasi sigmoidal remelting profile. The combined results of these studies are interpreted in terms of covalent attachment of the cobalt (III) metal center to N7 of guanine, which is then followed by an interstrand GN7-Co-GN7 crosslink in those DNA samples which possess GpC sites.

CHAPTER I

INTRODUCTION

Forty-four years ago Watson and Crick (1953) proposed the double helical structure of deoxyribose nucleic acid along with an elegant scenario for how that form allowed the cell to copy and excerpt the messages contained within the sequences. Over the last two decades hardy versions of nuclease and polymerase enzymes have become commercially available in kits for the methodical tagging, selecting and cutting specific pieces or whole genes of DNA in order to splice, transfer or express those messages. However, the complexity at the molecular level of the multitude of possible structures of DNA remains, to a large extent, hidden.

DNA Structure

This polyelecrolyte has three types of interactions which contribute to its duplex structure in solution. Hydrogen bonding, as depicted between the bases (Figure 1) but also involving water molecules with many groups on the DNA, is an attractive interaction. Secondly, hydrophobic interactions are attractive in nature by involving not only the stacking of the aromatic rings of the bases but also the van der Waals shape fitting of any two structures which can exclude solvent. Lastly, electrostatic repulsion between the phosphate groups keeps them separated and also makes the DNA molecule sensitive to different counter ions and the ionic strength of the surrounding medium. Very large DNA molecules behave as rigid rods in solution because of the high charge density from the many phosphate repeats, but small oligomers are more flexible in that aspects of local conditions can more than

1

compensate the effects of charge. In the cell, DNA is always attended by a whole entourage of chromatin, proteins and the like. When a section of the chromosome is, say, "unwrapped" for transcription, it is possible that the target portion of DNA would share more physical properties with a small oligomer than with an unnaturally "naked" long molecular salt.

A molecule of DNA can be described with global parameters which result from calculations relative to the overall helix axis. The pitch of the helix, or number of bases per turn, derives from the average rise (D_z) and helix rotation (Ω) per base-pair. The tilt angle (τ) measures the average sideways tilting of the base-pairs, allowing for the separation of the bases along the helical axis to appear to be smaller than the van der Waals distance of 3.4 Å. The displacement of the base-pairs from the helical axis contributes, in part, to the size of the major and minor grooves. The handedness of the helix is a right-spiral except for left-handed Z-DNA. The five membered ring of the sugar can pucker two ways: either with C2'-endo (i.e. C2' is on the same side of the ring plane as C5') or with C3'-endo. The base can be oriented principally across from the sugar with respect from the C1' bond, an *anti* conformation, or oriented above the sugar as in the *syn* position. The oxygen of carbon 2 limits pyrimidines to the *anti* form. Studies show that guanine prefers the *syn* orientation, but this can only occur in a helix if it is left-handed (Blackburn & Gait, 1996).

B-DNA is the classic double-helical structure in which the base pairings are in the middle of the helix and are oriented nearly perpendicular to the axis (Watson & Crick, 1953). This right handed helix has a rise of 3.4 Å, helix rotation of 36°, and a pitch of ten residues per turn. When the nucleic acid is dehydrated, the A-DNA structure results in which the bases tilt 20° and are displaced 4.5 Å from the center of the axis. With a pitch of 11 residues

per turn and a smaller rise (2.8 Å), A-DNA is a more compact structure. It has been suggested that the B-form occurs in high humidity because it requires two water molecules to bridge the gap of 0.66 nm between adjacent phosphates. At lower humidity, the A conformation occurs in which only one water molecule now can span the 0.53 nm between adjacent phosphates (Saenger et al., 1986).

X-ray determinations of many examples of DNA molecules have provided groupings of DNA types with differing secondary structure characteristics. Decamer and dodecamer B-DNA crystal structure analyses have provided examples for about one quarter of the 136 unique tetrads or four-base pair sequences found in the double helix (Dickerson, 1992). From such detailed studies, local helix axis parameters can be determined for how individual bases are distorted from expected averaged positions. Often the bases pair up in Watson-Crick fashion, but their orientations can vary slightly by translational displacement or by rotation about the x, y, or z axes (Dickerson, 1989). The bases can rise in a displacement up the z axis, slide along the y axis toward the sugars, or shift along the x axis into one of the grooves (Figure 1). The bases can rotate about their short (x) axis, called tilting, or turn about their long (y) axis, which is called rolling. If two paired bases roll in opposite directions, the base-pair assumes a propeller twist. Rotation about the z axis, perpendicular to the plane of the bases, constitutes the base twist. The average of all the base twist angles results in the global helix rotation. Should the hydrogen bonding between the bases depart from the preferred angles or separating distance between donor and accepter, then even more possible base movements arise. These seemingly unfavorable adjustments occur to allow for better stacking of the bases. The π - π interactions of overlapping bases are so strongly an attractive force

3

MAJOR GROOVE

G:C

A:T

MINOR GROOVE

MINOR GROOVE
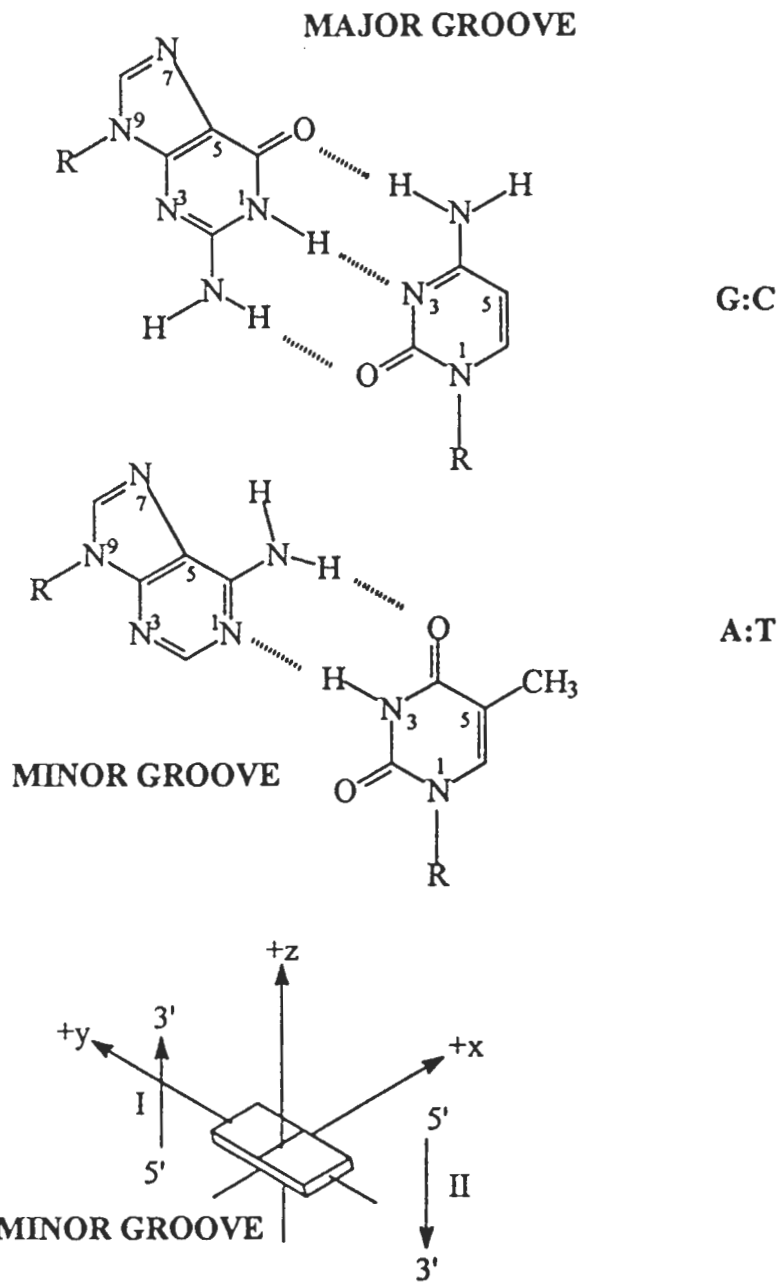
Figure 1. Watson-Crick Base Pairing and the Base Pair Coordinate Frame

4

that the base sequence predominantly determines both base orientation and helix conformation (Dickerson et al., 1994).

Many of these base movements are restricted because the duplex is a relatively compact structure. Propeller twist can cause a purine-purine clash in either groove. Calladine's rules describe the four likely responses that B-DNA structures undergo to minimize the sequence-dependent base clashes (Calladine et al., 1988). The propeller twist can flatten locally for either or both base-pairs. The base-pairs can roll (y axis) away from their clashing edges. One or both of the base-pairs can slide (shift) along their x axis to push the purine away from the helical axis. Lastly the helix axis can unwind locally to diminish interstrand purine-purine overlap. Altering the helical twist angle is principle among the adjustments to relieve base rolling steric clash. Depending upon sequence, the local helical twist angle can vary from $27.7°$ for ApG to $40.0°$ for GpC (Kabsch et al., 1982). This highlights the sequence-dependent irregularity of the helix.

The sequence also causes a deformation to the sugar phosphate backbone. How compact or elongated the helix is varies as well as the nature of the grooves in terms of width and depth. The binding of water to the particularly oriented phosphates and the solvation of functional groups in the grooves can present a local shape which is recognized by proteins or preferred by small molecules.

DNA in the left-handed Z form conformation usually requires a sequence of alternating pyrimidine-purine bases and is facilitated by bromination or methylation of the C-5 of cytosines, as in $(dG-5medC)_n$. High salt concentrations or specific counter ions can induce the flip to the left handed helix. In Z-DNA all the purine bases are in the *syn* conformation

5

and the sugars alternate between C-2'-endo and C-3'-endo pucker. In Z-DNA the helical repeat unit consists of two successive base pairs, a purine and pyrimidine. The GpC step has a helical twist angle of -50.6° and a base pair slide (y-axis) of -1.1 Å, which is in contrast to a -9° twist and a slide of 5.4 Å of the CpG step. These very distinct conformations, which cause the sugar-phosphate backbone to zig-zag, allow for greater base overlap. The minor groove of Z-DNA is so deep that it contains the helix axis. What would be the major groove is a convex surface, exposing cytosine-C5 and guanine-N7 and -C8. Certain base sequences then form specific conformational domains. If the two domains which differ greatly in conformation are juxtaposed, as in the case of a strictly B-DNA sequence next to a sequence capable of the Z-form at high salt, then the intervening residues are part of neither a right nor left helical region, but are considered to comprise a junction (Sheardy, 1988; Lu et al., 1992).

Early work in protein crystallography raised the question of whether the conformation of the molecule in the crystals might differ from that in solution (Matthews, 1977). Observing catalysis from crystallized enzymes and obtaining identical structures with crystals grown from very different solutions indicated that the examined crystal-locked proteins were not distorted from their native conformation (Eisenberg, 1970). It is accepted that x-ray studies of proteins produce a time-averaged image of the crystal which represents the stable equilibrium conformation of the molecule held within it (Blundell & Johnson, 1976). However, the dynamic conformations which nucleic acids are capable of are an intrinsic part of their structure and function. A prominent or critical motif present in the DNA, while in solution, may be literally squeezed out when the molecules are constrained in a crystal lattice. Although sensitive to changes, CD spectropolarimetry can at best indicate an averaged view

6

of secondary structure. Some NMR techniques can show agreement or differences with the x-ray depiction. The CpG twist angle has been found to be 29.8° from x-ray crystal structures (Kabsch et al., 1982), but a study adds perspective to the sensitivity of the CpG step toward its flanking sequences in two decamers (Lefebvre et al., 1995). Comparison of the solution structures by NMR illustrates the malleability of CpG, which has a helical twist of 42° and a roll (y-axis) of -1° for the sequence -ACGT- while the -TCGA- oligomer has a 35° twist and a 3.7° roll. Early reports on many synthetic oligonucleotides often revealed crystals of the A-type DNA structure. Some of these oligomers, mostly octamers, in fact appear to assume the B-form in solution as determined by NMR. Trends indicate that the crystal packing may favor A-DNA for octanucleotides (Blackburn & Gait, 1996). In addition to dynamic behavior in solution, native DNA in the cell is attended to by various counter ions, positively charged nucleoproteins and nucleosomes. Any DNA studies with clinical implications should be considered in a general sense and with caution.

DNA Sources and Synthesis

While DNA can be obtained from any cell, it has been traditionally extracted from sources rich in material, such as animals (calf thymus), bacteria (*e. coli*) and viruses (lambda phage). The polymerase chain reaction (PCR) allows for an extremely small amount of DNA to be amplified geometrically until necessary quantities are obtained. If a large DNA sequence, gene, or group of genes is required in great abundance, the desired sequence is cloned by means of a vector into a cell line. Cultivating the cells makes exact copies of the inserted DNA. While these sources of DNA have their applications, the studying of nucleic acid structure at the molecular level often requires small molecules of DNA which are

7

synthesized one nucleotide at a time. Commercially available automated solid support DNA synthesizers can make DNA molecules of less than 100 bases in useful micromolar scale quantities.

The phosphoramidite chemistry for solid support synthesis was worked out by Caruthers (1985). The breakthrough in this phosphite triester method is the highly efficient coupling reaction between a 5'-hydroxyl group of a deoxynucleoside and an alkyl 5'-DMTr-(N-acylated)-deoxynucleoside 3'-O-(N,N-diisopropylamino)phosphite. Nanogram quantities of nucleoside, producing micromoles of base pairs, are employed for every milligram of column resin. Silica or control pored glass is used with a 10-20 atom linker to the 3' end residue. The ester linkage to the 3'-oxygen is base labile, but less so than the protecting groups. The 3'-hydroxyl is a secondary alcohol which can be chemically modified with a phosphitylating reagent. The resins with linked tritylated bases and the phosphoramidites for the base building blocks are commercially available and stable if kept dry and at a basic pH. The order of synthesis is 3' end to 5' end, which is the reverse of the convention for writing sequences, i.e. 5' end to 3' end. The automation involves a cycle of four steps: 1) detritylation of the 5' end, 2) activation and coupling, 3) capping any failed sites, and 4) oxidation of phosphite to phosphate. The reagent lines and column are washed with acetonitrile in between each step. The synthesis scheme is depicted in Figures 2 A, B, and C. The 5'-hydroxyl group is a primary alcohol which is protected with a 4,4'-dimethoxytriphenylmethyl group (or dimethoxytrityl or DMTr-) by means of DMTr-Cl and pyridine (Figure 2 A iv).

8

(i)

isobutyryl chloride

$$\xrightarrow{}$$

$$\xleftarrow[-(CH_3)_2CHCOOH]{NH_4OH}$$

(ii)

benzoyl chloride

$$\xrightarrow{}$$

$$\xleftarrow[-PhCOOH]{NH_4OH}$$

(iii)

benzoyl chloride

$$\xrightarrow{}$$

$$\xleftarrow[-PhCOOH]{NH_4OH}$$

5'-OH Protection

(iv)

$$\xrightarrow{Et_3N}$$

DMTr   Nucleoside Monohydrate

Protected 5'-OH
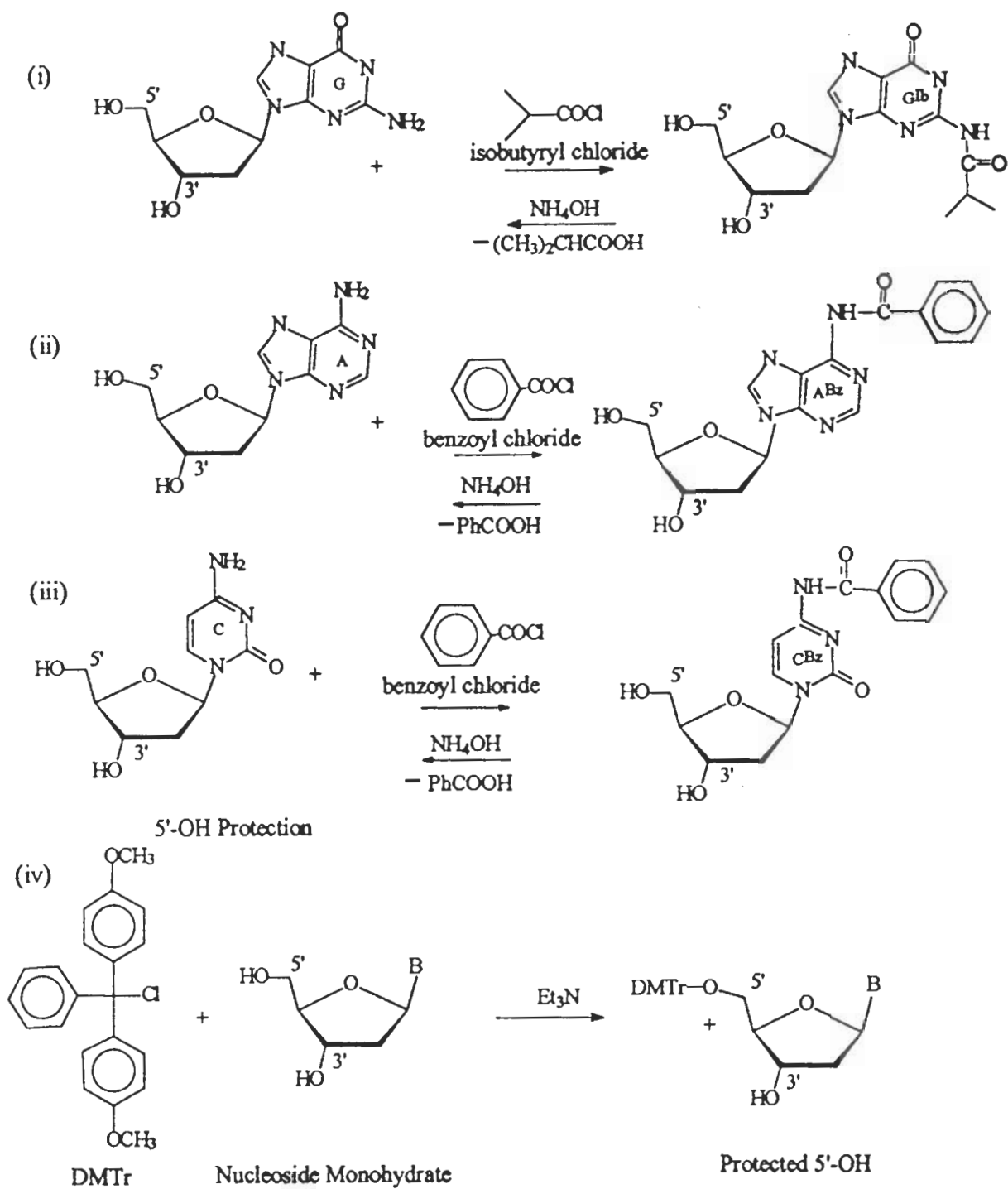
Figure 2 A: Protection/Deprotection of the nucleoside bases G, A, C and the sugar 5' primary hydroxyl group.

9
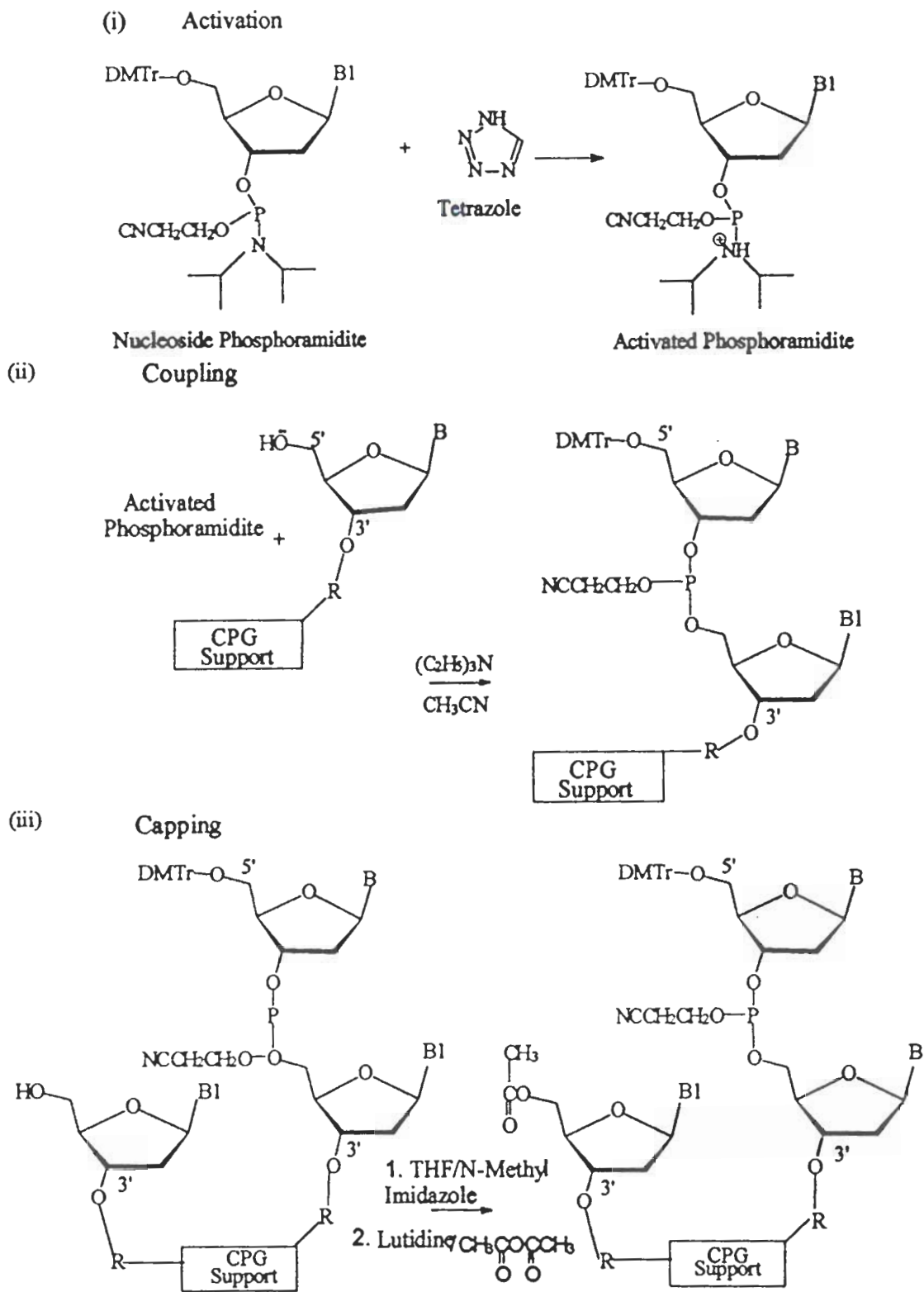
Figure 2 B: Phosphoramidite Activation (i), Coupling (ii), and Capping of the failure sequences (iii).

(i)   Oxidation of Phosphite to Phosphate
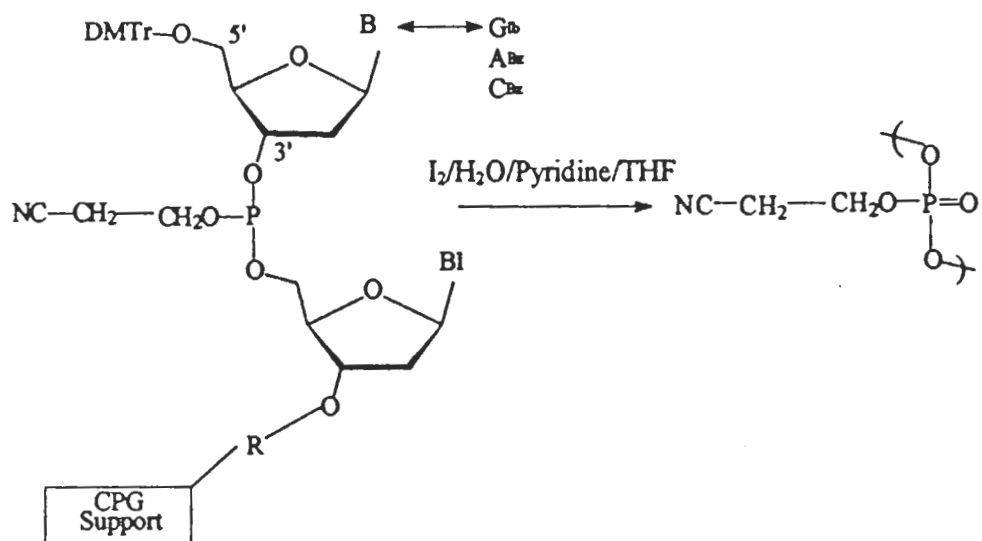
(ii)   Removal of B-cyanoethyl group
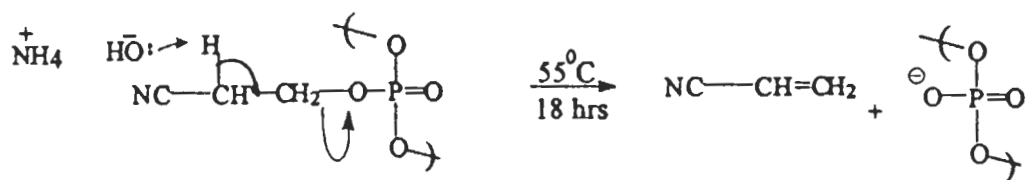
(iii)   Detritylation

Protected 5'-OH   DMTr—OH
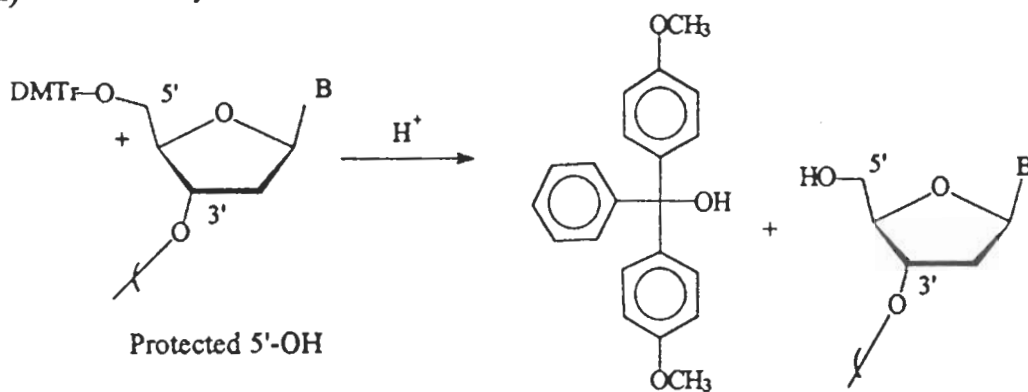
H⁺ is CCl₃COOH during synthesis

H⁺ is acetic acid during purification

Figure 2 C: Oxidation of Phosphite (i), Removal of the cyanoethyl group (ii), and Removal of DMTr group.

11

The support is activated by detritylating the initial tethered nucleoside and freeing its 5'-hydroxyl with trichloroacetic acid, TCA (Figure 2 C iii). Exposure to TCA should be for less than three minutes to ensure deprotection of only the chain terminal trityl group and to avoid depurination. Activation of the phosphoramidite building block occurs when tetrazole protonates the tertiary amine (Figure 2 B i). With triethylamine to deprotonate the 5'-oxygen, efficient coupling occurs by nucleophilic attack and loss of diisopropylamine, forming the phosphite linkage (Figure 2 B ii). The coupling efficiencies need to be 99.6% or better in order to obtain good yields of a 30 base or longer oligonucleotide polymer. In the third step of the cycle the coupling failures are capped on their 5'-OH with an acetyl group via acetic anhydride, tetrahydrofuran (THF), lutidine (2,6-dimethylpyridine), pyridine, and nucleophilic catalyst N-methylimidazole (Figure 2 B iii). The acetyl group cap will not be removed during the subsequent detritylating activation steps which stops the failure strands in their tracks. Originally the capping chemistry utilized DMAP which bound irreversibly to guanine and gave rise to a fluorescence. The phosphite is oxidized to a phosphate triester with iodine, pyridine, water, and THF (Figure 2 C i). This ends the cycle, leaving a resin supported dinucleotide with a dimethoxytrityl group on the 5' end. The cycle is repeated until the programmed sequence is completely coupled and oxidized.

The exocyclic nitrogens on the bases other than thymine need to be protected in order not to be modified by the cycle chemistry. Isobutyryl chloride (or anhydride) is employed for blocking the amide of carbon-2 of guanine (Figure 2 A i). The bulk of the protecting group shields N1 as well. The oxygen of carbon-6 can also react and become blocked. The amide of carbon-6 of adenine is protected with benzoyl chloride (Figure 2 A ii). The same reagent

is used for cytosine to react with the amine of carbon-4. The oxygen of carbon-2 of cytosine is also reactive toward benzoyl chloride. The benzoyl group can react with an OH on the sugar, but it is readily removed in base. Concentrated ammonia (NH_3, 11.8-M) is added to the column at the end of the sequence completion, cutting the linker ester and removing the DNA from the support to the collection vial. The base initiates removal of the nucleic acid protecting groups (isobutyl and benzoyl amides, Figure 2 A), as well as removal of the beta-cyanoethyl groups from the phosphate triesters to form phosphate diester links (Figure 2 C ii).

The remaining protecting groups are removed by treatment with concentrated ammonium hydroxide (11.8-M) in an oil bath at 55 °C for 18 hours (or three days at room temperature). These reagent conditions convert every phosphate triester to a diester and released acrylonitrile, $CH_2=CH-CN$. The still tritylated (full sequence) strands are separated from failure sequences and cleaved protecting groups by a trityl select reverse phase HPLC as described in the methods (Sheardy, 1988). Acetic acid (0.1-M) detritylates the full strands within an hour (Figure 2 C iii). A final reverse HPLC preparative run separates any dimethoxytrityl alcohol from the very pure oligonucleotide. In this manner, very pure DNA can be obtained for studies. The purity can be checked by running a native or denaturing polyacrylamide electrophoresis gel (PAGE) and observing a single band upon staining. To check the sequence, two additional avenues are available. A Maxam-Gilbert sequencing gel, with a ^{32}P end label or fluorescence tags, will provide a complete readout of the base sequence. One set of reactions are selective for the purines while another set of reactions pick out the pyrimidines. Secondly, an enzymatic digest with snake venom phosphodiesterase

13

(SVPD) and bovine alkaline phosphatase (BAP), at 37 or 40 C°, will convert the strands to mononucleosides. Those monomers can, in turn, be separated on C-18 Novapac RP HPLC to verify content, to determine the ratios of the bases, or even to quantify them by peak heights or areas.

The Duplex State

Whether on single strands or in a duplex, adjacent bases readily stack at moderate temperatures, as determined by optical and NMR studies (Cantor & Shimmel, 1980, p.1121). The process of two complementary single strands joining together is even more sensitive to environmental conditions and several factors. The attractive forces of hydrogen bonding and hydrophobic interactions overcome the repulsive electrostatic forces in complementary strands of three or more bases. Duplex stability depends upon the nature of the DNA. The G:C base-pair has three hydrogen bonds and is held together better than the two hydrogen bonds in A:T pairs. Generally duplex stability increases with the percent GC content. Conversely, AT rich regions are more readily separated and are involved in the initiation of replication and transcription. There is a sequence dependence on duplex stability as well. Purine-purine stacking is the most stable overlapping interaction, followed by purine-pyrimidine which is more stable than pyrimidine-pyrimidine stacking (Saenger, 1984). Recalling the earlier discussion, many conformational distortions are undergone to maximize base overlap. The adjacent bases have a pronounced effect on base stacking and helix stability. The nature of the solvent can also promote or discourage helix formation in several ways. A change in pH can alter the tautomeric form of the bases and thus their interactions. The ionic strength of the solvent can stabilize the duplex by shielding the phosphate

14

repulsions. Studies which vary the salt concentration are, therefore, useful techniques.

The thermodynamics of helix formation can be addressed as a two-state transition even though it is understood that both paired and single strands are dynamic structures of various conformations. The observed equilibrium constant for the formation of a double stranded structure, D, out of two single strands, S_1 and S_2, is K_{obs}.

$$K_{obs} = (D)/(S_1)(S_2) \quad \text{or} \quad \Delta G_{obs} = -RT \ln K_{obs} \tag{1,2}$$

The change in free energy of duplex formation, ΔG_D^0, depends upon the change in heat capacity or enthalpy of helix formation, ΔH_D^0, and the entropy of double strand formation, ΔS_D^0.

$$\Delta G_D^0 = \Delta H_D^0 - T \ \Delta S_D^0 \tag{3}$$

The entropic component of the helix to coil transition is a source of the temperature dependence. Raising the temperature separates the strands in what is classically termed "melting" of the DNA because the transition can be as dramatic as a phase change. The midpoint of the thermal denaturation is called the melting temperature, T_m. The two-state model for duplex formation does not give a good fit with small oligomers because the effects of fraying ends, more readily separated AT-rich strings, and looped regions are not negligible.

When the bases are stacked, their excitation dipoles are coupled, which reduces the UV absorption. In the melted single strand, the bases are more free to be unstacked and their absorbance more closely resembles that of the mononucleotides. This hyperchromicity is one way to monitor the helical duplex to coil transition as a function of temperature. For small oligomers the melting transition is reversible. The duplex separation (melting) and reformation (reannealing) is quite cooperative. For longer DNA molecules reannealing is

15

more problematic in that the two DNA strands must find the correct register (Geiduschek, 1961). There are many possible incorrect reformations, including interstrand loops and slipped sequences. Once some region has joined up in a nucleation duplex, the bases can adjust by separating on a local, short range basis called breathing. The rate at which the incorrect pairings separate to single strands and then rejoin as correct double strand is so slow that the large DNA simply remains in a denatured random coil state.

Reversible Interactions of Small Molecules with Nucleic Acids

Reversible interactions occur between nucleic acids and many species, including: water, metal ions, metal complexes, small organic molecules, and proteins. These molecules and ions usually stabilize the DNA duplex and in some cases induce big changes in conformation. There are three modes of binding to nucleic acids: exterior electrostatic binding, groove-binding and intercalation. First and foremost one should consider electrostatic binding.

Nucleic acids are highly charged polyelectrolytes, so they are very sensitive to changes in the ionic environment. In developing polyelectrolyte theory, Manning (1978) showed that simple cations interact with nucleic acids in two ways. The ions can undergo direct binding or condensation to the polymer, or ions can be a part of the counterion atmosphere which provides electrostatic shielding for the net remaining charge on the polymer. The counterion binding is approached with a dimensionless parameter ξ, defined as:

$$\xi = e^2 / \epsilon kTb \tag{4}$$

where e is the charge on the electron, ϵ is the solvent dielectric constant, k is the Boltzmann's constant, T is the absolute temperature, and b is the average spacing between charges along

16

the length of the polymer. In water at 25 °C the value of $e^2 / \epsilon kT$ is 7.14 Å. When $\xi < 1$, no ions condense, but if $\xi > 1$, condensation of counterions will occur until ξ is reduced to the value of one. The fraction of a counterion condensed per polymer charge is

$$\theta_M = 1 - \xi^{-1}. \tag{5}$$

For double stranded B-form DNA, two phosphates are between each base pair, at 3.4 Å, so b is 1.7 Å. A net negative charge of $1 - \theta_M$ remains on each phosphate. So $1 - \theta_M = \xi^{-1} = 1 = b / 7.14$, resulting in one net negative charge remaining at every 7.14 Å after counterion condensation. This remaining charge is shielded by ions in the Debye-Huckel counterion atmosphere to the degree of ξ^{-1}, the net fractional charge on each phosphate.

Ionic strength has an effect on the equilibrium of duplex formation via the measurable role of monovalent cation M. For the transformation

$$S_1^{(0)} + S_2^{(0)} + \Delta n M \rightleftharpoons D^{(0)}, \tag{6}$$
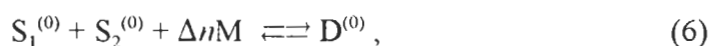
in which Δn is the counterion uptake upon double helix formation, the true equilibrium constant is $K_T^{(0)}$.

$$K_T^{(0)} = (D^{(0)})/(S_1^{(0)})(S_2^{(0)})(M)^{\Delta n} \quad \text{or} \quad \Delta G_T^{(0)} = -RT \ln K_T^{(0)} \tag{7,8}$$

The superscript (0) denotes a particular reference state which can be chosen as the polymer with a complement of condensed counterions. The difference between K_{obs} and $K_T^{(0)}$ is due to two factors, the change in free energy involved in the uptake of counterions, and the change in free energy of the ion atmosphere shielding between the double and single strands. Shielding is more important for single stranded nucleic acid than for double stranded polymer because the net charge after counterion condensation is much higher for single strands than for double strands. Conversely, the double stranded forms bind more condensed ions than

17

the single strands because the duplex has a higher charge density than single strands by virtue of a more compact structure and two strings of phosphate. With increasing salt, the effect on the equilibrium of the interactions of cations with DNA act in opposition. Condensation favors the duplex form while shielding favors the single strands. The Δn above is the counterion uptake or release with respect to a cooperative unit in the melting process, which is not easily known. Record (1978) has shown the dependence of melting temperature, T_m, on salt concentration.

$$\delta T_m/\delta \log [NaCl] = \{2.303RT_m^2/\Delta H\}\Delta n \tag{9}$$

Here Δn is the differential ion binding term which represents the release of counterions per duplex oligomer upon denaturation. There is a linear relationship between T_m and log [NaCl] which reflects the linkage between sodium ions binding and the duplex to single strand transition. The enthalpy change per phosphate, ΔH, reflects the intrinsic heat of helix formation as well as the heat of any small molecule binding or release. The differential ion binding term (Δn) is a reflection of the sensitivity of DNA to the ionic strength of the solution.

Groove-binding interactions involve direct interactions between the bound molecule and the edges of the base-pairs in either the major or minor grooves. The size of the minor groove favors small molecule binding, while proteins have been found to interact with both grooves. Many natural antibiotics, such as netropsin and distamycin, are minor groove binders which curve to fit the space and displace bound water molecules (Kopka et al., 1985; Pelton & Wemmer, 1989). Because of the nuances of base structure, the shape of the groove can be a handle for sequence-specific recognition. Some groove-binders are positively charged, adding an electrostatic component to the binding free energy.

18

The model for intercalation involves a molecule containing planar aromatic rings which inserts between the adjacent base-pairs after the bases have separated and become unstacked. Separating the bases along the helical (z) axis unwinds and lengthens the double helix. These changes can be determined by hydrodynamic methods, such as viscosity which is sensitive to helix length, or by circular dichroism spectropolarimetry. Some natural products are charged groove-binders with aromatic rings which intercalate. Thermodynamic studies are able to separate the proportion due to each of the binding modes (Chaires, 1990; Chaires et al., 1993).

It has been observed that intercalators reach saturation upon binding a maximum of one intercalator per two base-pairs. This is termed the neighbor exclusion principle, which states that intercalators can at most bind at alternate possible sites. Once a non-specific intercalator binds to a site, the sites on both sides of the occupied position become unfavorable toward further binding (Carlson et al., 1993). One possible explanation is that the intercalator induces conformational changes in the adjacent sites which prevents binding there. Another explanation by Friedman and Manning (1984) is that upon binding of the intercalator, some of the charge of the DNA is neutralized and the elongated local helix has a slightly lower charge density. As intercalators bind, the favorable release of condensed ions is reduced, lowering the observed equilibrium constant as well. This model is not only consistent with that predicted by neighbor exclusion, but it also applies to any non-specific binding mode.

Binding of Metal Complexes to Mononucleosides

Investigators have looked at the interactions of metal complexes with nucleosides and nucleotides as studies in their own right and for insights into interactions with DNA. The pentaammineruthenium complex preferentially coordinates to N7 of the imidazole ring of guanine with stabilizing hydrogen bonds from the ammines to O6 (Clarke & Taube, 1974; Clarke & Taube, 1975; Clarke, 1977). Substitution inert complexes between cobalt (III) ammines and ATP and ADP which have been studied by ^{31}P-NMR all indicate covalent binding between the metal and oxygens of the charged phosphate groups (Cornelius et al., 1977). The monomeric nucleotide unit has metal binding sites in the base, sugar, and phosphate groups. In polynucleotides, those binding sites are altered. The phosphate group has decreased charge and another sugar ester linkage. The sugar has a second ester linkage, and lastly, the base undergoes hydrogen bonding with its complementary base while embedded in the helix (Marzilli, 1981). The double helix is more constrained compared to single stranded oligonucleotides, in which the bases are not hydrogen bonded and there are more varied possible conformations that allow for base stacking. Therefore making predictions even between single and double stranded structures is problematic (Kozelka & Chottard, 1990).

In a study of inert metal-purine complexes in which alkylation reactions were employed, the coordination sites of the pyrimidine ligands were directed by steric factors (Marzilli et al., 1975). Steric repulsions result in adjustments in conformation for the ligand in a cobalt (III) glycinate complex (Buckingham et al., 1974). Steric repulsions also play a role in the interligand interactions between the exocyclic group on the bases and the chelated

20

polyammines, which indicated binding might lead to specificity among the different bases (Marzilli et al., 1974). The small size of these simple cobalt complexes lend themselves well both for binding to regions of DNA and for substitutions of one or more ligands. Cobalt (III) complexes have a very high preference for binding to nitrogen over oxygen donor sites on nucleic acids and nucleotides because it is a soft metal with a lower charge-to-radius ratio and more polarizable electron shells (Marzilli, 1981). Evidence for the binding of simple cobalt (III) complexes to nucleoside bases indicate outer sphere coordination in both crystal structure and solution (Marzilli, 1977; Marzilli, 1981). Additional evidence for such interactions of purine nucleotides with $[Co(NH_3)_6]^{3+}$ or cobalt (III) hexaammine, $[Co(NH_3)_5Cl]^{2+}$ or cobalt (III) pentaammine chloride, and $[Co(NH_3)_4Cl_2]^+$ or cobalt (III) tetraammine dichloride has been put forth from FT-IR and NMR studies (Tajmir-Riahi, 1991).

Early studies of the structures of cobalt (III) complexes with adenine and theophylline indicated hydrogen bonding altered the conformation of the product (Kistenmacher et al., 1973; Marzilli et al., 1973). They suggest that octahedral complexes with hydrogen donor ligands attached may achieve selectivity for guanine over adenine bases. It was further indicated that the reaction of the cobalt complex *trans*-$[Co(en)_2Cl_2]^+$ with a DNA polymer should not severely disrupt the intermolecular Watson-Crick hydrogen bonding for G:C (Marzilli et al., 1973).

Interactions between Select Metal Complexes and Nucleic Acids

It is well known that the inert complex cobalt (III) hexaammine induces the B to Z transition in appropriate DNA polymers (Behe & Felsenfeld, 1981) and in synthetic oligomers (Winkle & Sheardy, 1990; Lu et al., 1992). The stabilization of Z-DNA by $[Co(NH_3)_6]^{3+}$ has

21

also been attributed to specific hydrogen bonds between three of the ammine groups with guanine and phosphate accepter sites on the DNA helix (Gessner et al., 1985). While all cations are drawn to DNA to neutralize the negatively charged lattice, monovalent cations are bound in a nonspecific way at a mobile layer, termed "territorial," in close proximity to DNA (Friedman & Manning, 1984). In contrast, divalent and trivalent cations bind with specific interactions with individual moieties. In some such fashion cobalt (III) hexaammine induces the B to A transition in oligomers of sequence dCCCCGGGG (Xu et al., 1993). This cobalt complex also induces an unusual non-Z like structure in a DNA oligomer which contains a $(dC-dG)_4$ segment (Winkle et al., 1992). Cobalt (III) hexaammine has been shown to bind to natural occurring DNA with a preference for regions rich in GC content (Braunlin & Xu, 1992; Braunlin et al., 1987). Various cobalt complexes have been synthesized for binding studies with nucleosides (Sorrell et al., 1977). The candidate molecules are screened for novel, informative or useful model complexes between metal ions and nucleic acids.

A number of reports have been published of metal cations binding to RNA and DNA. Transition metals such as manganese (Jack et al., 1977) and complexes of cobalt, platinum, and iridium (Karpel et al., 1975) have been studied in the binding to RNA. A nickel(II) macrocyclic complex bound to DNA and facilitated oxidative cleavage of the polymer (Muller et al., 1992). There is a report of x-ray evidence of manganese bound to N7 of guanosine 5'-monophosphate (de Meester et al., 1974). A study of the effect of the carcinogen chromium on the thermal denaturation of DNA was limited in that at a pH of greater than 6, the hydroxychromium species precipitates (Pett et al., 1985).

22

A number of small metal complexes with appropriate ligands have been shown to interact with DNA by covalent attachment of the nitrogenous bases to the metal via loss of a labile ligand from the metal. For example, $[Ru(NH_3)_5(OH_2)]^{2+}$ has been shown to bind to calf thymus DNA primarily at N7 of guanine bases (Clarke et al., 1986). It has been suggested that *cis*-$[Ru(NH_3)_2Cl_2]^{2+}$ behaves in a manner similar to the anti-tumor drug cisplatin (Clarke, 1980).

Cisplatin, *cis*-diamminedichloroplatinum(II), also selects sites rich in G bases, covalently attaching to the N7 position (Murry et al., 1992; Brabek et al., 1992; Hopkins et al., 1991; Bruhn et al., 1990). Echoing the modeling studies of *trans*-$[Co(en)_2Cl_2]^+$, plausible structures for cisplatin and double stranded DNA could involve either intact Watson-Crick base-pairing or disrupted Watson-Crick base-pairing consisting of weaker hydrogen bonds or bifurcated hydrogen bonds (Kozelka & Chottard, 1990). Both intrastrand and interstrand crosslinking by cisplatin have been observed, with intrastrand crosslinking predominant at 5'-GG-3' sites (Pinto & Lippard, 1985; Rahmouni & Leng, 1987; Bruhn et al., 1990) and interstrand crosslinking occurring at 5'-GC-3' sites (Hopkins et al., 1991). Both cisplatin (*cis*-$Pt(NH_3)_2Cl_2$) and *cis*-dichloro (ethlenediamine) platinum(II) platinate the following DNA sequences in an interstrand fashion: GpG, 65%; ApG, 25%; GpNpG, 6%. The AG adduct invariably occurs with adenine on the 5' end of the duplex (Eastman, 1983; Eastman, 1986). The distances between nitrogens in the sequences can account for some of the observed specificity. With some uncertainty arising from the differences in the local helical twist, there is approximately 4.5 Å separating N7's in GpG sites and a 4 Å distance in ApG sites. Also the N7 of guanine is more nucleophilic than N7 on adenine. The guanine nitrogens in a

23

GpNpG sequence are spaced at 8 Å, but that can vary with a bend or wedge step in the helix conformation. The distance between the N7's of interstrand G's in GpC sites is also 8 Å, but in this case the separating vector makes an angle of about 15° with the helical axis and that vector is at least 2 Å away from the helical axis. In contrast, the interstrand distance between nitrogens in CpG sites is 9 Å, but because of the turn of the helix, those nitrogens are on the floor of the major groove on *opposite* sides of the helical axis. These two nitrogens are actually in a straight line with a third point that is on the helical axis. The resulting steric hindrance prevents the metal complex from getting close enough to both guanines in the CpG sequence.

In our preliminary experiments, it was found that pentaammineaquocobalt(III), $[Co(NH_3)_5(OH_2)]^{3+}$, bound to a small oligomer differently from cobalt (III) hexaammine. The replacement of one of the ammine groups on the metal with a more labile ligand appeared to cause an irreversible modification of the DNA (Calderone et al., 1995). Since this cobalt complex seemed to be a novel modifier of DNA, we undertook an investigation to delineate the interactions of pentaammineaquocobalt(III) with nucleic acids.

24

CHAPTER II

EXPERIMENTAL SECTION

2.1   MATERIALS

A.   DNA Preparation

DNA oligomers were synthesized via the phosphoramidite method (Caruthers, 1985) on an Applied Biosystems 380B DNA synthesizer (Foster City, CA). The remaining protecting groups are removed by treatment with concentrated ammonium hydroxide (11.8 M) kept at 55 °C for 18 hours. After incubation the acetonitrile and ammonia are removed, together with ethanol and triethylamine, by rotovap reduced pressure distillation. Ethanol helps remove water azeotropically, while triethylamine vaporizes last, keeping the pH basic. Without triethylamine, any water present would be acidic enough to detritylate the nucleic acid product after the ammonia is removed. The failure sequences have hydroxyl groups at both ends as a result of the removed linker at the beginning 3' residues and the removed acetyl cap at the 5' positions (which are missing the dimethoxytrityl group, DMTr). Complete strands are purified by trityl select reverse phase HPLC on a Waters two pump (Model 510) Chromatography system utilizing Baseline Acquisition Software (version 2.1) with a microBodapak C-18 RP Plastic Radial (Z-module) semi-prep column. Acetic acid (0.1-M) detritylates the full strands within an hour. Most of the free dimethoxytrityl alcohol, DMTr-OH, is removed by extraction with diethylether. A final reverse HPLC preparative run removes any DMTr-OH from the very pure oligonucleotide. Product purity was checked by analytical HPLC and native and denaturing polyacrylamide gel electrophoresis (PAGE).

25

Prior to any studies, oligomers were dissolved in buffer, heated at 80 °C for two minutes and allowed to cool slowly for a uniform heat annealing.

Calf thymus DNA (Sigma Chemical Co., St. Louis, MO.) was sonicated in phosphate buffer (for 1 minute in 5 second intervals, on ice), dialyzed against water and lyophilized. The natural DNA was reconstituted in phosphate buffer and a portion melted to check the sample batch. Sonicated calf thymus DNA was strictly not heat annealed as this would denature the sample.

B.   Cobalt Complex Preparation

Pentaammineaquocobalt(III) perchlorate was synthesized from the carbonato-pentaamminecobalt(III) nitrate salt (Basolo and Murmann, 1953). Clean air was bubbled for 24 hours through a mixture of 300 grams of cobalt nitrate hexahydrate in 150 ml. water and 450 grams of ammonium carbonate in 45 ml. water and 750 ml. concentrated aqueous ammonia (11.8 M). After cooling in an ice bath, the crystals were collected on a filter, washed sparingly with ice cold water, alcohol and ether, and dried at 50 °C. The product (crude) was recrystallized once from water, following a couple hours on a steam bath, and dried as before.

The carbonato complex was dissolved in hot water and treated with 60% perchloric acid, with magnetic stirring, until all carbon dioxide evolution ceased. The wet residue, collected by filtration through fritted glass, was redissolved at 90 °C, and again treated with 60% perchloric acid. Cooled to 0 °C for twelve hours, the complex was further recrystallized by dissolving it in water at 90 °C, adding 60% perchloric acid, and digesting on a steam bath for a couple hours. The product was filtered, washed sparingly with ice cold water, ethanol

26

and ether, and dried in a vacuum desiccator.

C.   Reagents and Buffers

Cobalt (III) hexaammine was purchased from Aldrich and used without further purification. Phosphoramidites were purchased from Applied Biosystems Inc. (Foster City, CA) or Cruachem (Dulles, VA). HPLC grade solvents were obtained from Aldrich. Nucleosides and mononucleotides were from Sigma. Solutions and buffers were made from water that had been deionized, passed through Barstead Thermolyne Organic Removal and Ultrapure Mixed Bed cartridges, distilled with a Wheaton Autostill 5, and filtered through 0.45 micron cellulose membrane (Millipore). Phosphate buffer (5 mM, pH 7) with 50 mM NaCl and 0.05 mM EDTA was used throughout (standard phosphate buffer), except when otherwise noted.

2.2   METHODS

A.   UV Spectra and Melts

Spectroscopy of all samples were obtained with a Gilford Response II spectrometer (Ciba-Corning, Oberlin, OH) with a thermostated cell holder. Absorbance readings and spectra were obtained at 25 °C, except when otherwise noted. The thermal program used to obtain a melt absorbance profile monitored a specific wavelength while the samples were slowly heated at about 0.3 C°/minute from a native temperature to a denaturing temperature, typically from 20 °C to 95 °C. To degas the solutions, the room temperature eppendorf tubes were placed in a Savant SpeedVac Concentrator under vacuum for 1-2 minutes. Some small oligonucleotide sequences can readily form structures other than the duplex (i.e. hairpins) if left in solutions of low ionic strength. In order to maximize the duplex state in the case of **Z8**,

27

$(5medC-dG)_4$, the oligomer solutions were loaded hot and annealed in the cells right before starting the melt. The empty cells were heated in the sample holder to 76 °C while the solutions, in eppendorf tubes, were heated to 80 °C in a dry bath. The hot oligomer solutions were pipetted into the hot cells which were then inserted into the 76 °C holder. Thermal programming was run from 95 °C to 20 °C at about 4.0 C°/minute to anneal the samples. Not only does this "loading hot" procedure minimize hairpin structures, but also the thorough degassing of the solution and the cooling of the cell dead volume air bubble can result in improvement in lower and upper base lines.

The melt profiles were transferred to an external PC as an ASCII file via Procomm Software version 2.4.1 (Datastorm Technologies Inc., Columbia, MO), sorted and reheaded in order to be analyzed by GOMELT and GODIFF software (Turbo-Basic, Borland International) for transition temperatures and thermodynamic parameters (Marky & Breslauer, 1987). The program GOMELT can be used to obtain melting temperatures, T_m, provided the lower and upper base lines are low in noise and well indicated. The midpoint of the transition is calculated after left and right margins, typically at 35 °C and 90 °C respectively, are used to define the baselines. The program GODIFF can be used to calculate the first derivative, or T_{max}, of the melt profile. Large DNA, such as sonicated calf thymus, melts in a cooperative fashion. The big duplex polyelectrolyte separates into single strands while spanning approximately a 10 C° change or less in temperature. The phase transition is a sharp one and the first derivative analysis is unambiguous. In the case of small oligomers, the fraying ends or end effects are not negligible, making its thermal transition less concerted than that of large DNA. The resulting first derivative often is a small change hidden by noise.

28

The options in the GODIFF program offer flexibility when applied to the uncertain first derivatives of small oligomers. This program allows local pseudo maxima, which arise from noise in the melt, to be removed one at a time. Thus, a melt which has ambiguous baselines and relatively high noise can be analyzed provided the transition is dramatic enough. GODIFF uses an NPI, or number of points interval, to calculate the first derivative. A higher interval results in a more smoothed derivative curve. Depending on the data set, values for NPI can be set at intervals of 5 degrees through the range from about 20 to 100, or higher. The derivative sets, for which a good representative apex value surfaces, can number as many as 15. Removing false maxima eliminates the effects of obvious noisy points. Small subtle errors from noise can remain and affect the calculated T_{max}. By smoothing with a range of NPI values, unnoticed bad points are calculated in with different sized averages. The highest and lowest figures then are likely to be unrepresentative of the set of derivative values because of how the noise near the true derivative of the curve slants the analysis. So in addition to averaging all the derivatives, removing the highest and lowest extreme numbers (in a manner similar to jury selection) before averaging can produce a T_{max} which is less affected by noise.

In the case of nucleosides, a series of spectra were taken after the temperature was increased 10 °C and allowed to equilibrate for 10 minutes. This set of thermal scans was an alternative to a programmed melt in order to monitor the effect of temperature on solutions.

B.   Circular Dichroism Spectroscopy

CD spectra were recorded on an Aviv 62A DS circular dichroism spectropolarimeter (Aviv Associates Inc., Lakewood, NJ). Each spectrum was usually taken as a single scan

29

with a time averaging constant of 2.0 seconds and a 1.0 nm step size. After the buffer background was subtracted, the zero offset was checked against 320 nm where no absorbance occurs. Aviv Software (version 4.1t) was used to smooth the curve by least squares polynomial fit (up to 10th order). Nearly all spectra were obtained with temperature control.

C.   Equilibrium Dialysis

Dialysis was carried out in Spectrum Spectra/Por molecular porous membrane tubing. Tubing #6, with molecular weight cutoff of 1,000, was used with 12-mer or smaller oligomers, while tubing #3, MWCO 3,500, was used with larger oligonucleotides. Calf thymus DNA, sonicated or not, required the higher MWCO 8,000 of Spectra/Por tubing #7. In addition to Spectra/Por closure clips, the dialysis tubing was also tied on the outside of the clips with dental floss to keep sample loss to a minimum. When divalent or trivalent cations were involved with oligonucleotides, the dialysis was run first against three changes of 0.2 M NaCl followed by three changes against distilled water.

D.   Atomic Absorption

Graphite furnace atomic absorption spectra were recorded at the Analytical Research Department of Merck and Co. Inc. (Rahway, NJ) with a Polarized Zeeman Spectrometer Z-8270 from Hitachi using a platform graphite tube with Argon purge. The temperature program involved drying from 80 °C to 140 °C for a 30 second hold, and then atomizing at 2700 °C and reading the absorbance at 240.7 nm. Readings were performed in triplicate using a standard SSC-300 Hitachi Autosampler and compared to an external standard curve at 20, 50, and 100 ppb.

E.   HPLC

DNA oligomers were purified with a Radial Pak reverse phase C-18 HPLC column. The still tritylated (full sequence) strands are separated from failure sequences and protecting groups by a trityl select reverse phase HPLC using triethylammonium acetate buffer (0.1 M, pH 7.0) in which the amount of acetonitrile, CH_3CN, was varied between 15% and 35% (Figure 3). Acetic acid (0.1-M) detritylates the full strands within an hour. Most of the free dimethoxytrityl alcohol is removed by extraction with diethylether. A final reverse HPLC preparative run, which uses an CH_3CN range of 8% to 20%, removes any DMTr-OH from the pure oligonucleotide (Figure 4).

Mononucleosides were analyzed with a Radial Pak reverse phase Novapak HPLC column. Adequate separation of the peaks of the principle mononucleosides was obtained by varying the acetonitrile between 2% and 15% (Figure 5). It should be noted here that under the conditions used, 5medC eluted just before dG, with a slight peak overlap in that there was not a return to baseline. The elution order is: dC, (5medC), dG, dT, 5BrdC, dA.

31
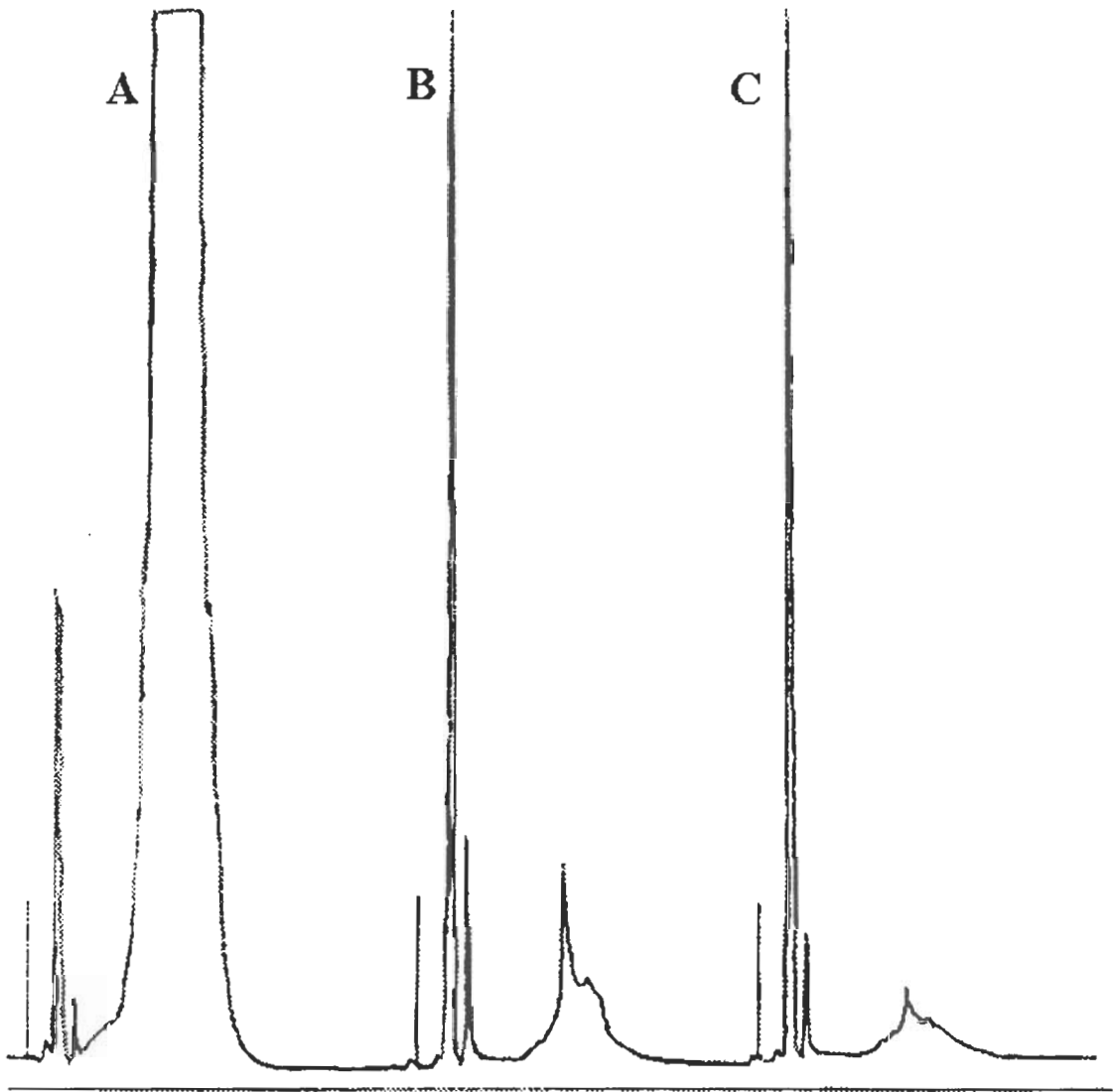
Figure 3. Preparative HPLC of DMTr-**GC-site** and Analytical Runs of **GC-site** detritylation.

Preparative RP C-18 HPLC of DMTr-**GC-site** (A) shows peaks for the detritylated failure sequences, protection groups, and tritylated product. Preparative runs are typically monitored with the least sensitive detector range of 2.0 AUFS at 280 nm, for which the DNA extinction coefficient values are about half that at 260 nm. Analytical HPLC traces follow the acid-catalyzed detritylation of **GC-site**, in which (B) the peaks correspond to trityl-free oligonucleotide, protection groups, and DMTr-DNA. After 15 minutes (C) the peak profile differs in that the last peak cluster is smaller.

32
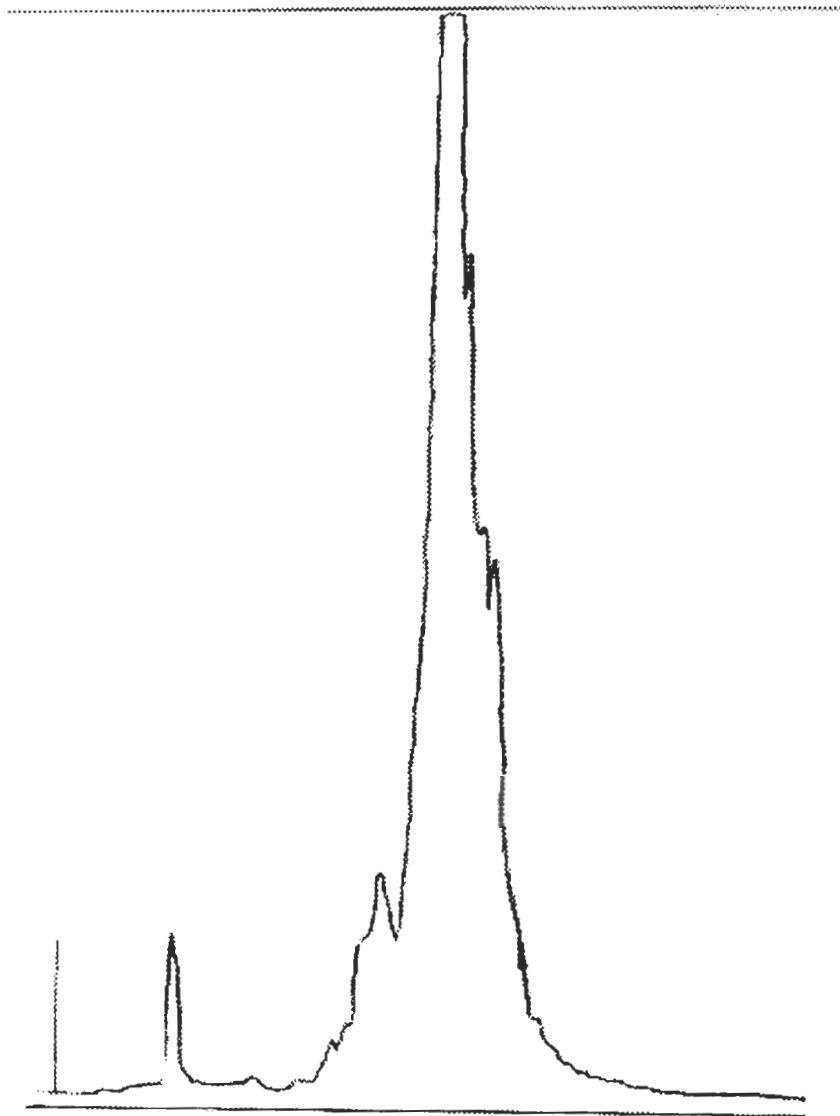
Figure 4. Preparative HPLC of **GC-site.**

The center portion of the preparative RP HPLC, which contains the best cut of oligonucleotide product, is surrounded by various peaks and shoulders. The material contained therein is cut into separate fractions. All absorbances are collected since the high concentrations of unique polymers can result in unforeseen HPLC anomalies and unexplainable elutions (N. Kallenbach, conversation in person). Analytical HPLC is used to determine the peak purity of secondary fractions.
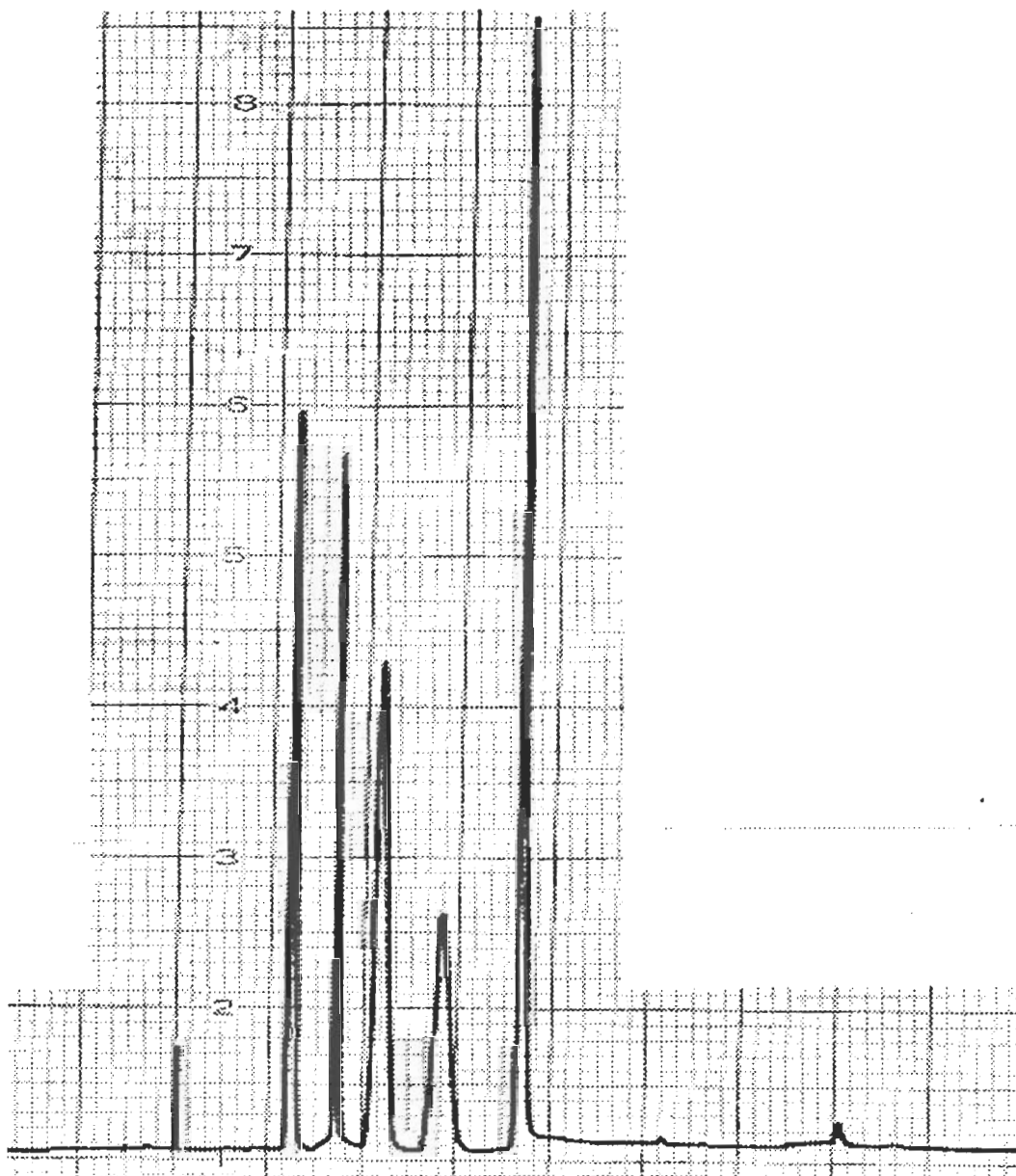
Figure 5. Analytical RP NovaPak C-18 HPLC of a mixture of nucleosides which elute in the order dC, dG, dT, 5BrdC, and dA.

The chart paper was scrolled at 0.5 centimeters per minute and the absorbance was monitored with a sensitivity range set at 1.0 AUFS at 260 nm.

34

CHAPTER III

RESULTS AND DISCUSSION

The interactions of the cobalt complex pentaammineaquocobalt(III), $[Co(NH_3)_5(OH_2)]^{3+}$, with DNA has been examined by UV absorption, circular dichroism, HPLC, atomic absorption, and melting temperature (T_m of helix-coil transition) studies. The results are presented below.

3.1   A Labile Cobalt Complex

The preliminary work focused on the interaction of pentaammineaquocobalt(III), $[Co(NH_3)_5(OH_2)]^{3+}$, with a known Z-forming DNA oligomer, (5medC-dG)$_4$, or **Z8** (Table I). Circular dichroism (CD) studies indicated that this oligomer will assume a right-handed B conformation at low NaCl concentrations (a monovalent salt) and a left-handed Z conformation at a NaCl concentration of 2.0 M or at a $[Co(NH_3)_6]^{3+}$ concentration of 200 µM. This can be seen for the most part in UV spectra as the Z form of **I** has a larger absorbance shoulder at about 280 nm than the B form (Figure 1, dash). Heat-annealing (2 minutes at 80 °C, followed by slow cooling) **Z8** in the presence of 200 µM of $[Co(NH_3)_6]^{3+}$ produces a CD spectrum (Figure 2, dash) characteristic of Z-DNA with a trough at 295 nm and a peak at 275 nm (Sheardy, 1991). During heat-annealing, the temperature is raised enough so that all strands separate. Upon slow cooling, the oligomers form the most stable structure possible, which for **I**, is a duplex. However, after heat-annealing **Z8** with 200 µM pentaammineaquocobalt(III), the UV spectrum is hyperchromic throughout but it does not have the pronounced Z-shoulder at 280 nm (Figure 1, dash-dot). CD spectra confirmed that

35

Table I

Synthesized DNA Oligomers

	Oligonucleotide Sequence	Shortened Name
I.	(5medC-dG)$_4$	**Z8**
	(dG-5medC)$_4$	
II.	CGCGATATCGCG	**12-mer**
	GCGCTATAGCGC	
III.	(ACTG)$_6$	**24-mer**
	(TGAC)$_6$	
IV.	AATATAATAGCTATTAT	**GC-site**
	TATTATCGATAATATAA	
V.	AATATAATACGTATTAT	**CG-isomer**
	TATTATGCATAATATAA	

$[Co(NH_3)_5(OH_2)]^{3+}$ at 200 µM did not induce the B to Z transition in **Z8**, but rather leaves the oligomer in an altered B-like structure with a peak at 279 nm and a trough at 255 nm (Figure 2, dash-dot). This suggests that this reagent is modifying the DNA oligomer in such a manner as to prevent the B to Z conformational transition.

When this heat-annealed treated **Z8** was subjected to exhaustive dialysis against 200 mM NaCl and then water to remove excess cobalt complex, the resultant CD spectrum remained that of an altered B-like structure. Hence, the modification apparently is irreversible. For comparison, oligomer **I** with inert hexaamminecobalt(III) sample was dialyzed two ways. One portion underwent equilibrium dialysis versus water alone, while another was dialyzed against 200 mM NaCl and water as above. The CD spectrum of the water-only dialyzed oligomer retained its Z-like character, indicating the inert complex remained bound to **Z8** (Gessner et al., 1985), while the CD spectrum of the salt-dialyzed oligomer completely returned to B-like conformation. Since the salt dialysis is able to remove all of the electrostatically bound trivalent cations from DNA (Hicks et al., 1997b), and the structure and charge density of the two cobalt complexes are nearly identical, then the differences are due to the labile ligand. This suggests that the pentaammine complex is covalently bound to the DNA.

The transition of **Z8** from B form to Z form can be monitored via CD spectra of the oligomer which was heat-annealed in increasing concentrations of hexaamminecobalt(III) (Figure 8). A $[Co(NH_3)_6]^{3+}$ concentration of 150 µM or higher results in the loss of the B form trough at 255 nm and a conversion of oligomer to the Z form. Thermal denaturation of the duplex oligomer in these conditions by a programmed melt, which is a slow heating of

37

the sample to 95 °C followed by a slow cooling back to 25 °C, has no effect on the conformation of the oligomer as depicted by CD. Taking heat annealed **I** in the presence of $[Co(NH_3)_6]^{3+}$ slowly to the single stranded state with denaturing temperature and back to the duplex is reversible. Heat-annealing **Z8** in increasing concentrations of $[Co(NH_3)_5(OH_2)]^{3+}$ induces a conformational transition which is complete at 150 μM in cobalt complex (Figure 9). However, the new conformation is not left handed Z but still "B-like." The trough at 255 nm is deeper at the low cobalt concentrations that in the absence of cobalt complex. This may indicate a tightening of the helix turn by the binding of the trivalent complex at low concentrations. Subsequent melting of heat-annealed **Z8** in the presence of this labile cobalt complex alters the secondary structure further only at the lower cobalt concentrations. The spectra at 150 and 200 μM cobalt complex are quite similar before and after melting, following a smooth trend from "completely" altered-B form to untreated **I**. This indicates that both processes of heat-annealing and thermally denaturing of **Z8** in the presence of pentaammineaquocobalt(III) modify the DNA oligomer in an irreversible fashion. This two part process, when carried out consecutively with the reactive cobalt complex, is referred to here as melt treatment, heat treatment, or heat-annealing treatment.

Since the water ligand is labile at elevated temperatures and the nucleophilic N7 of guanine bases is accessible in B form DNA and single stranded DNA, it is suggested that this modification is through covalent attachment of the cobalt complex to the DNA molecule via displacement of the water forming a cobalt-to-G:N7 linkage.

38

3.2   Mononucleoside Studies

The possibility of a reaction between guanine N7 and pentaammineaquocobalt(III) prompted us to investigate the behavior of this cobalt complex in the presence of nucleosides under similar conditions as above. Samples of nucleoside (i.e., dA, dC, dG, dT, and 5medC) in buffer with 200 μM [Co(NH$_3$)$_5$(OH$_2$)]$^{3+}$ were placed in a UV/VIS spectrophotometer and gradually heated, in 10 C° increments, from 25°C to 85°C. After equilibration for 15-20 minutes at each temperature, the UV spectrum was recorded. At temperatures above 55°C, spectral changes were observed for deoxyguanosine only: a dramatic hypochromism (circa 50%) at all wavelengths from 240 to 290 nm. Upon cooling back to 25°C, the spectrum remained unchanged from the higher temperature spectra, i.e., the dG sample remained hyperchromic (Figure 10). No precipitate was visible in the cell, eliminating the possibility that less material was simply in the pathlength. The dG solution, after heating, was placed in eppendorf tubes and centrifuged. After 20 minutes there was no precipitate visible. The spectrum of dC showed little difference (Figure 11). The other nucleosides, dA, dT, & 5medC, also exhibited only the slight change found with deoxycytosine. In a separate study, the absorbance of a new deoxyguanosine sample in 200 μM pentaammineaquocobalt(III) at two different wavelengths was monitored as a function of time at 75°C. At both wavelengths, the absorbances dropped off to minimum values in approximately 15 minutes. These results suggested a possible heat induced modification of the G nucleoside, but only the G nucleoside, by the cobalt complex.

There are studies (Marzilli et al., 1974) of cobalt complexes binding to mononucleotides. The structures resolved by NMR all show binding to the charged

39

phosphate. This gives an indication of the interaction with phosphate buffer of the cobalt complex. The interactions between $[Co(NH_3)_5(OH_2)]^{3+}$ and phosphate, both in the DNA backbone and as the buffer, had to be examined more.

Mononucleosides were separated on a NOVA Pak reverse phase HPLC column. The peaks were resolved and eluted at reproducible times (Table II). The monomers which were heated in the presence of pentaammineaquocobalt(III) had identical elution times as the control monomers. When a new sample of deoxyguanosine was heated up to 75 °C with the complex, exhibiting the UV spectral changes, an aliquot was cooled slightly and then injected onto the column, the resultant elution time of the single peak remained unchanged. If a charged metal complex were to bind to an uncharged monomer one would expect a noticeable difference in elution time on a reverse phase HPLC column. The modification at high temperatures to the dG which is indicted by UV spectra may be only a reversible binding interaction. The interaction between deoxyguanosine and the labile cobalt complex must be different from the interaction of the complex to a DNA oligomer by virtue of the polyelectrolyte lattice (Drew & Dickerson, 1981).

3.3   Pentaammineaquocobalt(III) And Other Buffers

Since the interaction of various cobalt complexes with phosphate had been reported (Marzilli et al., 1974), the effect of phosphate on the labile complex was a concern. Perhaps another biological range buffer could be used in the presence of the labile cobalt complex. The common pH 7 buffers HEPES, MES, PEPES, and TRIS were examined by UV spectra with pentaammineaquocobalt(III) at increased temperatures. TRIS buffer is a poor candidate for temperature studies since the pH can change with temperature. All exhibited great

40

Table II

Mononucleoside HPLC Retention Times

Monomer	ϵ at 260 nm $(cm^{-1}M^{-1})$*	λ_{max}	retention time (minutes)
dC	9,000	271 nm	1.47
5medC	-	277 nm	2.14
dG	13,000	259 nm	2.16
dT	9,650	267 nm	2.43
5BrdC	-	288 nm	3.24
dA	15,000	259 nm	4.17

*(Cantor & Washaw, 1970)

changes in their absorbance profiles as binding interactions caused energies of transitions to enter into the monitored range (240-350 nm). Pentaammineaquocobalt(III) will form oxo-bridged complexes and precipitate out of solution if kept basic. The synthesis of the cobalt complex ended with crystallization out of perchloric acid. To evaluate if the large absorbance changes were due to a change in the complex other than binding, acetate (pH 3.5) and borate (pH 10) buffers were used. Equally large spectral changes were the result. Compared to ligand properties of the alternative buffers, phosphate at the concentration of 5 mM exhibits a small interaction with $[Co(NH_3)_5(OH_2)]^{3+}$ as monitored by UV spectroscopy. In a buffered solution of an oligonucleotide, the polyelectrolyte has the advantage over the phosphate ion with respect to a persistent encounter with the cobalt complex. The interaction between pentaammineaquocobalt(III) and phosphate does not occur much when the phosphate buffer concentration is 5 mM.

Spectra of the complex dissolved in water alone, in the pH range 5 to 7.5, indicate changes at elevated temperatures comparable to that observed in standard phosphate buffer. These are due to the cobalt complex forming dimers and polymers (Cotton & Wilkinson, 1988) and precipitating from solution. The extent to which the cobalt complex reacts with itself in water is small at concentrations of less than 400 μM provided that there is a polyelectrolyte oligomer in solution to compete with self-chemistry. Thus the blanks which contained cobalt, but no DNA, distorted the melting profiles of an oligomer (Figure 12). At pentaammineaquocobalt(III) concentrations of 300 μM or higher, enough precipitate is produced that some of it remains in the bottom of the cell or eppendorf tube after heating or incubating near room temperature. The precipitate is a very fine powder which readily passes

42

through the membrane and gets dialyzed away. Stock solutions of $[Co(NH_3)_5(OH_2)]^{3+}$ in water at millimolar concentrations will form a precipitate if kept at room temperature rather than 5 °C. For this reason, stock solutions of $[Co(NH_3)_5(OH_2)]^{3+}$ were made fresh and the concentrations were checked spectrophotometrically with an epsilon at 492 nm of 47.5 cm^{-1} M^{-1} (Dixon et al., 1981).

3.4   Sequences Subject to Crosslinking

The effect of this potential modification on the thermodynamic stability of specific DNA oligomers was examined by a series of thermal denaturation studies (melts). The following molecules were included: self-complementary $[(5medC-dG)_4]_2$ or **Z8**, self-complementary $[(CG)_2ATAT(CG)_2]_2$ or **12-mer**, and the a and b strand duplex $[(ACTG)_6]:[(TGAC)_6]$, designated **24-mer**. The 24-mer is distinguished by not having a G as a neighbor to G on either strand (Table 1). All oligomers gave very unusual melting profiles (after heat-annealing) in the presence of 200 μM $[Co(NH_3)_5(OH_2)]^{3+}$. The thus treated oligomers were subjected to exhaustive dialysis against water to remove excess cobalt complex, lyophilized to powder, dissolved in fresh buffer, and remelted. The melt profiles of the treated (heat-annealed, melted, then dialyzed) samples indicate a much lower degree of hyperchromism upon denaturation than the analogous untreated controls. The actual melting profiles in the presence of 200 μM cobalt complex indicate the cobalt complex in the blank, finding no DNA, is more readily undergoing chemistry with itself and with phosphate. During the melt, the dimerizing and polymerizing of the cobalt complex through an oxo-bridge (Cotton & Wilkinson, 1988) forms the light scattering clouds of settling precipitate.

43

UV spectra of an oligonucleotide at 20°C and 95°C reveals hyperchromicity of the bases (Figure 13). At low temperature, the paired (hydrogen-bonded) and stacked structure restricts the bases, allowing their transition dipoles to interact which in turn reduces the absorbances. Though linked by the sugars, at high temperature the strands are fully separated and the bases are free to move. The transition dipoles then are parts of independent chromophores that absorb nearly as readily as the mononucleotides.

Comparing the UV spectra at 20°C and 95°C of untreated and treated **Z8** shows a large reduction in hyperchromicity, as well as an elevated or distorted low temperature profile, in the treated case (Figure 14). Temperature difference spectra, obtained as absorbance at 95 °C minus 25 °C, highlight only the reduction in hyperchromicity (Figure 15). The UV spectra and difference profiles for **12-mer** and **24-mer** show changes that are less dramatic than those in **I** (Figures 16-21). The difference spectra of **Z8** and **12-mer** (Figures 15 & 18) both have reductions at about 280 nm. This "GC shoulder" region is a result of the run of alternating cytosine and guanine bases common to both molecules. While the temperature difference spectra of **24-mer** also shows a reduction in hyperchromicity after treatment, it is not centered around 280 nm (Figure 21). Close examination of the 95 °C spectra of both untreated and treated **24-mer** reveals that they are nearly identical. That indicates that, at denaturing conditions, what can be expected to be single stranded **24-mer** shows no UV spectral changes when modified by the cobalt complex. The change in the temperature difference spectra (Figure 21) is due to a slight hyperchromism in the 20 °C spectrum of treated **24-mer** with respect to the control **24-mer**. Treatment of 24-mer with $[Co(NH_3)_5(OH_2)]^{3+}$ causes a modification which distorts the oligomer when it is the duplex

44

state, but not when the modified oligomer is single stranded.

A thermal denaturation monitors the change in hyperchromicity with incremental increases in temperature. The optimal wavelength at which to record the melt is apparent from temperature difference spectra. The melt of treated **Z8** changes much less than that of untreated (Figure 22). The third trace is the absorbance of the pentaammine complex and the oligomer as it undergoes melt treatment. The unusual melt profile is due to the formation of inorganic dimer and polymer precipitate. **12-mer** also has a largely reduced transition upon treatment (Figure 23), while **24-mer** does not (Figure 24). The differences in the third traces reflect the change in formation of the cobalt precipitate. The fact that precipitate forms early in the melt during treatment of **24-mer** indicates that the complex binds less to that oligomer, which allows more of the cobalt to find itself in solution and dimerize/polymerize.

III not only binds less cobalt, but also is less affected upon treatment. Since this oligomer has its G bases on the same strand separated by three bases and those on the opposite strand separated by one base, a cobalt complex can only modify an isolated "single-hit" site. These results suggest that all the duplex and single strands have been permanently modified by pentaammineaquocobalt(III). One possibility for this modification, in the strands containing neighboring G bases, is either interstrand or intrastrand crosslinking. Intrastrand crosslinks occur between bases from within the same strand, as in GpG and GpNpG sequences. Interstrand crosslinks, formed only in a duplex, would occur between a base on the Watson strand and a base on the Crick strand, such as the guanines in a GpC site. Both oligomers **I** and **II** have -GC- in their sequences. Crosslinking with $[Co(NH_3)_5(OH_2)]^{3+}$ requires two binding sites on the metal, however, and would only be possible through initial

45

loss of water followed by loss of an ammine.

It has been demonstrated that cisplatin crosslinks DNA at GpC sites in an interstrand motif (Hopkins et al., 1991). Although compounds of platinum(II) are square planar and those of cobalt(III) are octahedral, the geometries reveal the possibility of interstrand crosslinking at GpC sites in our oligomers with pentaammineaquocobalt(III) (Figure 25). As in cisplatin, the leaving ligands could be at 90 ° to each other. Also, the ammines occupying the positions above and below the plane occupied by the leaving groups should not interfere with the interaction due to their small van der Waal's radii. In fact, the binding may even be enhanced by their presence due to possible hydrogen bonding interactions between these ammines and acceptor sites on the GpC dinucleotide subunit as observed in the binding of cobalt (III) hexaammine to $(dC-dG)_3$ (Gessner et al., 1985; Seeman et al., 1976).

To test the possibility of crosslinking, we synthesized two DNA oligomers that have been used to model the interstrand crosslinking of DNA by cis-$Pt(NH_3)_2Cl_2$ (Hopkins et al., 1991). These oligomers, designated **GC-site** and **CG-isomer**, are 17 bases long and have a self-complementary string of 14 bases (Table I). Oligomer **IV**, or **GC-site**, has a single GpC site while oligomer **V**, or **CG-isomer**, has a single CpG site. Like **24-mer**, **CG-isomer** contains no GpC sites.

The difference in the middle two base pairs alone affects the helix stability. The pur-pyr-pur-pyr run of the -ACGT- sequence in **V** has better base stacking than the pur-pur-pyr-pyr sequence (-AGCT-) found in **IV** (Saenger, 1984; Dickerson et al., 1994). After heat treatment and dialysis, these two oligomers were melted along with control strands (Figure 26). At the same conditions, **CG-isomer** oligomer melts at a temperature nearly 6 degrees

higher than **GC-site** (30.3 °C and 24.5 °C, respectively).

As for the effect of heat-annealing with $[Co(NH_3)_5(OH_2)]^{3+}$, treated **GC-site** shows much lower hyperchromism than the untreated **GC-site**. In contrast, treated and untreated **CG-isomer** show little difference in their melt profiles. This result indicates that **CG-isomer** is modified by pentaammineaquocobalt(III) in a different way than **GC-site** oligomer. As in the case of cisplatin, this rules out the 15 A's and T's as reaction sites for this cobalt complex since these residues are the same in both molecules. Comparisons of percent hyperchromicity are listed in Table III. Oligomer **V** is the only molecule which, after treatment, showed little change in hyperchromism between double stranded and single stranded denaturing conditions.

While the treated **24-mer** exhibits an absorbance increase comparable to the treated oligomers **II** and **IV**, it has characteristics which set it apart from the other duplexes. The 24-mer has 12 guanine bases, each a possible single binding site for $[Co(NH_3)_5(OH_2)]^{3+}$. The six-fold repeating sequence also makes **III** a more uniform polymer in a conformational sense. The -ACTG- sequence, with its pur-pur-pyr-pyr repeat, could be more readily distorted by a bound charged complex than the other oligomers, even if the modification was only via single hits (Saenger, 1984). If the -ACTG- sequence has some local feature, such as a wedge step conformation, the repeated motif would enhance the quirky nature of the structure (Crothers et al., 1990).

The first differentials of the thermal denaturations reveals the inflection point or T_{max} temperature of quickest melting (steepest slope). Treated **GC-site** melts over six degrees higher than the **GC-site** control (Figure 27). This noteworthy stabilization of the double stranded helix is due to the modification by pentaammineaquocobalt(III). It is unlikely that

47

Table III

Percent Hyperchromicity in Untreated and Treated Oligomers

		CONTROL	TREATED	λ_{obs}	FRACTION CG
I	**Z8**	34%	12.8%	280 nm	1
II	**12-mer**	31%	14%	280 nm	2/3
III	**24-mer**	34%	17.5%*	272 nm	1/2
IV	**GC-site**	24%	11%	260 nm	1/8
V	**CG-isomer**	21%	18%	260 nm	1/8

(* 28% according to Gilford files #0222 S#2 & #0223 S#2)

48

the presence of 1 or 2 cobalt complexes bound to the central guanine bases in **GC-site** would stabilize the helix by shielding electrostatic repulsive forces. If this were the case, then for the same reasons the **CG-isomer** pair would exhibit a similar shift in T_m, which they do not (Figure 28). The unaltered hyperchromism and the similar melts in **CG-isomer**, which lacks a GpC, indicate that the GpC unit allows for a distinct modification by the cobalt complex in oligomers **Z8 (I)**, **12-mer (II)**, and **GC-site (IV)**. The mathematical analysis of the thermal denaturation data is in Table IV as T_m values or midpoints of the transitions (Markey & Breslauer, 1987). The oligomers which contain GpC sites, **I, II, & IV**, exhibited higher melting temperatures in their treated samples than for their control strands. The other molecules, one containing a CpG site **(V)** and **III** which has separated guanines, had lower melts with the treated samples. These sequences are limited to only singular binding modes with the cobalt complex. A single hit modification of the DNA may distort the nucleotide, but the presence of the bound trivalent cation would not stabilize the two strands as much as an interstrand crosslink would. When the 24-mer data are analyzed by inflection point or T_{max}, the control melts at or just slightly lower than the treated sample. This change in the determined melting temperatures is due to the strange shape of the melt of **24-mer**. The unsymmetric denaturation of this oligomer (Figure 29) alters the drawn baselines for the determination of the transition midpoint T_m. There is the possibility that the nature of the repeated sequence in **III** simply is manifested in this way.

Table IV

Melting Temperatures of Untreated and Treated Oligomers

		T_m ($\pm$0.3 °C)	λ_{obs}
I	**Z8**	61.3	280 nm
	Treated **Z8**	63.0	
II	**12-mer**	66.0	280 nm
	Treated **12-mer**	67.5	
III	**24-mer**	59.6*	272 nm
	Treated **24-mer**	59.1*	
IV	**GC-site**	24.5	260 nm
	Treated **GC-site**	31.0	
V	**CG-isomer**	30.3	260 nm
	Treated **CG-isomer**	28.8	

*Via first derivative (Godiff) : **24-mer** 61.6 °C, Treated **24-mer** 61.9 °C.

50

3.5   Sonicated Calf Thymus DNA

In order to test for the possibility of crosslinking, sonicated calf thymus DNA was treated in a fashion with $[Co(NH_3)_5(OH_2)]^{3+}$ at various DNA to cobalt ratios (Table V). The high temperature treatments employed earlier could not be applied to the long polymer since the heat would irreversibly disrupt the large duplex structure. Destroying the target DNA would prevent the analysis of any cobalt chemistry modifications via the thermal denaturation method. Instead, the treated samples were incubated at 37 °C for 48 hours, exhaustively dialyzed versus water to remove excess cobalt complex, evaporated to dryness and then reconstituted in the same buffer without any added cobalt complex.

All samples were vortexed both at the start and finish of the incubation. Some fibrous precipitate remained in the dialysis bags after harvest, but these amounts were small and were discarded. Some precipitate is to be expected with the combination of multivalent cations and long polyelectrolytes (Braunlin et al., 1987). Sample 5, with high end amounts of both DNA and cobalt, showed some precipitation upon addition of the cobalt complex and, therefore, was diluted with water and vortexed before dialysis. Another sample, which contained 400 μM cobalt and 1,000 μM DNA, was unworkable after the incubation. At the end of the incubation period, the higher ratio samples were vortexed and even sonicated briefly in an attempt to transfer the most amount of material onto dialysis against water, where it is reasonable that most purely electrostatic associations due to the trivalent complex would be reversed. Some precipitated material may have clung to the dialysis membrane during the harvest, reducing the yield. Only solubilized product was quantified and used in the melts.

51

Table V

Calf Thymus DNA and $[Co(NH_3)_5(OH_2)]^{3+}$ Incubations

Sample	[DNA] μM	[Co] μM	DNA/Co	T_m °C ($\pm$0.3 °C)*
1.	280	0	--	75.2
2.	560	200	2.8	70.6
3.	280	200	1.4	69.2
4.	140	200	0.7	65.9
5.	560	400	1.4	86.1

*Melts were done after dialysis against water and reconstitution in standard buffer.

For the thermal denaturation experiments, the concentration of DNA was adjusted to ca. 1.0×10^{-4} M in base pairs and the resultant melting profiles are shown. As means of normalizing the transitions, the melting data is plotted as θ (fraction of absorbance change) $= (A_T - A_{25})/(A_{95} - A_{25})$ where A_T is the absorbance at temperature T and A_{25} and A_{95} are the initial and final absorbances at 25 °C and 95 °C, respectively (Figure 30). Samples 2, 3, and 4 indicated lower melting temperatures than untreated DNA, in which the increase in the cobalt to DNA ratio correlated with the extent of destabilization. On the other hand, sample 5 had a higher T_m than untreated DNA (Table V). Thus at the higher total DNA and pentaammineaquocobalt(III) concentrations, the modification of the DNA was quite different from the other samples. Here the transitions are cooperative and sharp, so the T_m values are the inflection points from the first derivative. Sample five never reached an upper baseline, so the Gomelt program for transition midpoints could not be applied. The other profiles are symmetric enough that either method of analysis gave similar transition values.

All five samples were reannealed by slow cooling to room temperature and allowed to equilibrate at 4 °C for several days. The samples were then melted once again. The remelting profiles are shown with all experimental conditions and sample numbers identical to that for the previous data (Figure 31). Inspection of these profiles reveals that only sample 5 showed some sigmoidality, indicating quasi reversibility in its reannealing. Reversibility in the denaturation of polymeric native DNA could only be possible through interstrand crosslinking, which would allow the bases to pair with their original partner upon reannealing (Geiduschek, 1961). From the slope of the first melt of sample 5 (in contrast to the flat upper baselines of the other samples), it is apparent that the strands had not fully denatured even at

53

95 °C. The extent of modification apparently retained some duplex structure and allowed the DNA to return to register upon renaturation. The heterogeneous length and sequence of this natural DNA made for an imperfect target to demonstrate the effect of reactive complex. However, these samples did indicate that pentaammineaquocobalt(III) would modify DNA in a reasonable amount of time at the gentle conditions of a 37 °C incubation.

There are some studies on the interactions of multivalent cations with large DNA (Pett et al., 1985; Thomas & Bloomfield, 1983). The concern is that the trivalent metal complex in appreciable concentrations causes aggregation and possibly precipitation of the DNA. At the most extreme scenario, should any crosslinking then occur, it is possible that inter*molecule* interstrand residues could be involved. There was some precipitation while mixing the samples with higher Co/DNA ratios, but after vortex-mixing until pseudohomogeneity, the samples were set afloat in the temperature bath. These samples after incubation were dialysed against water and *not* versus a sodium chloride solution. It is likely that electrostatically bound pentaammineaquocobalt(III) remained associated with the polymer after dialysis removed the cations from the bulk solvent. The possibility exists that complexes, which were only reversibly bound, underwent reactions with the DNA during the thermal denaturation. This is a valid criticism which raises the question if the modification occurs here strictly during the 37 °C incubation. However, this does not diminish the conclusion that sonicated calf thymus DNA was modified by $[Co(NH_3)_5(OH_2)]^{3+}$ in an irreversible manner.

3.6   **Z8** Incubated with Pentaammineaquocobalt(III)

The modification of sonicated calf thymus DNA demonstrated that incubation treatment with pentaammineaquocobalt(III) can modify oligonucleotides during conditions that allow the DNA to remain fully duplexed. This should be beneficial in demonstrating that crosslinking is occurring since having all the nucleic acid in a duplex would promote the maximum amount of interstrand crosslinks. Oligomer **IV** melts too low to be double-stranded during the incubation. **Z8** and **12-mer** both have a high enough melting temperature, but **I** has three -GC- sites compared to only two in the 12-mer. The effect of concentration of cobalt complex on DNA modification was examined by incubating one "OD" of Z8 in one milliliter (approximately 40 μM in basepairs) for 48 hours at 37 °C at concentrations of 100 to 400 μM $[Co(NH_3)_5(OH_2)]^{3+}$, followed by exhaustive dialysis against salt solution, then against water. An "OD" or optical density is the amount of DNA contained in one milliliter of solution such that it gives an absorbance of 1.00 at 260 nm and in a one centimeter pathlength cell.

UV spectra at 25 °C and 95 °C of oligomer **I** follows the hyperchromicity of the bases (Figure 32). Note the difference in temperature from the spectra taken in the heat treatment studies (Figure 13). Again less hyperchromicity was found with increasing concentration of cobalt complex in the incubation (Figure 33). There is a striking similarity between the spectra of the incubation at 300 μM $[Co(NH_3)_5(OH_2)]^{3+}$ (Figure 34) and that of the heat-annealed treated with 200 μM $[Co(NH_3)_5(OH_2)]^{3+}$ (Figure 14). An overview of the changes in the UV spectra can be depicted by taking the difference between the absorbances of each treated sample and the control at 25 °C (Figure 35) and at 95 °C (Figure 36). The spectra

55

were normalized at 260 nm (at 25 °C), so the apparent iso-point at $\Delta A=0$ is the consequence. In order to do this, an assumption had to be made that the molar extinction coefficients at 260 nm did not differ by much upon modification and through the range of modification that results from the complex reacting with the oligomer. The changes in hyperchromicity are shown through temperature difference spectra (Figure 37). The sample incubated at 400 µM in cobalt appears to be off trend and instead coincides with a sample of lower concentration.

Changes in the UV spectrum reflect the amount of stacked and paired (duplexed) bases. CD spectra are sensitive to changes in secondary structure. Though the base stacking is the dominant director in helix conformation (Dickerson et al., 1994), some differences might be better observed by CD. The CD spectra (Figure 38) indicate that increasing the concentration of $[Co(NH_3)_5(OH_2)]^{3+}$ from 100 to 300 µM increases the molar ellipticity at 255 nm relative to untreated **Z8**. The 255 nm trough becomes less negative as the right-handed B form becomes more altered. A similar overview of the changes in ellipticity is depicted by CD difference spectra at 25 °C (Figure 39) and at 95 °C (Figure 40). The changes in ellipticity that arise from the conformation at low and high temperatures (double and single strands) are shown through temperature difference spectra (Figure 41). The sample incubated at 400 µM is again off the trend.

Thermal denaturations were done on these samples. The reduction in hyperchromicity in the UV spectra and the increase in melting temperature depend upon increasing complex concentration up to 300 µM (Figure 42). The values for the incubation at 400 µM in cobalt appear in a reverse trend because the precipitation of pentaammineaquocobalt(III) dimers and

56

polymers occurs more readily at the higher concentrations of complex (Cotton & Wilkinson, 1988). Therefore the incubation sample which begins with 400 μM $[Co(NH_3)_5(OH_2)]^{3+}$, in time, has a time-averaged cobalt concentration which is lower than 300 μM because of precipitation. After centrifuging in an eppendorf tube, one can easily notice the red powdery precipitate of the cobalt complex dimers and polymers. The precipitate readily goes into suspension, but when put in the dialysis bags, it disperses and is dialyzed away through the membrane. It is unlikely that oligomer is precipitating with the red inorganic precipitate. The dialysis bags can hide precipitated losses, but the yields in the higher concentration samples were, at the most, only slightly lower. This suggested that the concentration of 200 to 300 μM pentaammineaquocobalt(III) was a good compromise between loss of sample and low degree of modification. This concentration seemed to offer greater promise for a more preparative scale application.

The incubation of **Z8** in the presence of 200 μM $[Co(NH_3)_5(OH_2)]^{3+}$ at 37 °C for the times ranging from 8 to 72 hours was carried out in order to assess the effect of incubation time on the alteration of the oligomer. As shown in Figure 43, increasing the time of incubation from 8 to 51 hours increases the molar ellipticity at 255 nm relative to untreated **Z8**. The degree of alteration apparently levels off after 51 hours. The incubation time has a similar effect on the T_m; the melting temperature increases with increasing reaction time and then levels off (Figure 44). At short reaction times (< 15 hours) the T_m does decrease. This demonstrates that the incubation conditions described, in two days, modifies **Z8** by covalent binding of cobalt in such a manner as to stabilize the duplex while altering the B-form character of the helix.

57

3.7   Direct Evidence of Binding by Atomic Absorption

Incubation of **Z8** in the presence of 200 μM $[Co(NH_3)_5(OH_2)]^{3+}$ at 37 $^\circ$C for times ranging from 8 to 72 hours, followed by exhaustive dialysis, was carried out in order to assess any uptake by the oligomer. In order to test for the presence of tightly bound cobalt, atomic absorption analysis was performed. The results presented in Figure 45 indicate a rapid uptake of cobalt by **Z8** at reaction times less than 30 hours with a leveling off in the uptake at longer reaction times. The amount of tightly bound cobalt increases with increasing time for the first two days of incubation. In addition, the oligomer is apparently saturated with cobalt at one cobalt for every 3.5 to 4 base pairs. Hence, the binding of one cobalt results in a site exclusion effect such as that noted for simple intercalators, including daunomycin, for which a site size of 2.8 to 3.6 base pairs has been reported (Chaires et al., 1987). Atomic absorption was done on samples of an oligomer that had been incubated with cobalt(III) hexaammine to eliminate the possibility of cobalt complex remaining because of electrostatic binding. After up to 96 hours of incubation, followed by dialysis against 0.2 M NaCl, then water, AA established that no $[Co(NH_3)_6]^{3+}$ had remained bound to the DNA (Hicks et al., 1997b). The directly observed trend of cation uptake that takes place during approximately two days is therefore the result of cobalt binding covalently to the DNA oligomer.

3.8   Salt Dependence of Melting Temperature

The shift in melting temperature in treated **Z8** and treated **GC-site** oligomer indicates the cobalt is stabilizing the duplex. The cobalt is bound and affecting the thermodynamics of the oligomer. Extensions of polyelectrolyte theory quantitatively describe the thermodynamic linkage between cation binding and charged ligand binding to the DNA lattice (Friedman and

58

Manning, 1984). The binding of a charged ligand affects cation binding, and the cation binding affects the ligand binding. By quantifying the release of sodium ions, it is possible to determine the presence of the +3 charged cobalt complex on the treated oligomer. The manner in which this experiment is carried out is by melting both the untreated and treated oligomer in various NaCl concentrations. The change in the melting temperature will show sensitivity to the salt concentration such that it can be quantified by means of a plot of T_m versus log [NaCl], which can be expected to give a straight line.

An indirect method to establish binding of cobalt to the DNA oligomers is determination of the T_m of a specifically treated sample as a function of Na^+ concentration. Three different samples were prepared in standard buffer with a range of NaCl concentrations, between 125 to 400 mM, and subjected to thermal denaturation. Control **Z8** was used in contrast to heat-annealed **Z8**, as well as **Z8** which had been incubated for 48 hours. Both treatments were done with 200 μM $[Co(NH_3)_5(OH_2)](ClO_4)_3$, followed by exhaustive dialysis. Plots of T_m versus log [NaCl] for the three samples are shown in Figure 46. Both treated DNA oligomers have lower T_m values than the untreated oligomer at NaCl concentrations greater than 125 mM. The slopes of the least squares regression lines ($r^2 > 0.955$ for all regressions) for the treated samples are quite different from that of the untreated sample as well as quite different from each other. Hence, the treated samples have a dramatic decrease in the salt dependence on their stabilities relative to the untreated sample.

The lower T_m values for the modified oligomers arising from the incubation of **I** with increasing concentrations of $[Co(NH_3)_5(OH_2)]^{3+}$ suggest that they are less stable than the unmodified oligomer. In order to evaluate the thermodynamic parameters of the untreated

59

and treated **Z8** samples, curve analyses of the melting profiles was carried out according to Marky and Breslauer (1987). For a self-complementary DNA oligomer

$$\Delta H^{\circ} = 6RT_m^2(\delta\alpha/\delta T)_{T=Tm} \tag{10}$$

$$\Delta G^{\circ} = \Delta H^{\circ}(1 - T/T_m) \tag{11}$$

$$\Delta S^{\circ} = (\Delta H^{\circ} - \Delta g^{\circ})/T \tag{12}$$

where ΔH° is the standard enthalpy change, T_m is the inflection point of the α versus T melting profile, α is the fraction of single stands, ΔG° and ΔS° are the standard free energy and entropy changes, respectively and T is 298 K. Thermodynamic comparisons of untreated **Z8,** heat-annealed **Z8,** or **Z8** incubated for 48 hours in the presence of 200 μM $[Co(NH_3)_5(OH_2)]^{3+}$ followed by exhaustive dialysis are revealed in Table VI. At 200 mM NaCl, the different samples have unique T_m values, but the enthalpies of thermal denaturations are quite similar. Hence, the T_m values alone cannot be used to assess thermodynamic stability.

The coordination of cobalt (III) metal to the DNA substrate would dramatically alter the charge density of the oligomer. According to the terms of the polyelectrolyte theories (Manning, 1978; Record et al., 1978; Record et al., 1981), this alteration should thus change the number of sodium counterions bound to the lattice. At low concentrations of NaCl (less than 400 mM), there is a linear relationship between T_m and log [NaCl]; the slope of the resultant line reflects the linkage between Na binding and the duplex to single strand transition. Record et al. (1978) have shown that

$$\delta T_m/\delta \log [NaCl] = \{2.303RT_m^2/\Delta H\}\Delta n \tag{13}$$

where Δn is the differential ion binding term. The Δn term represents the release of

60

Table VI

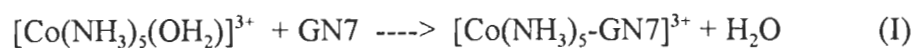Influence of NaCl on the Thermal Denaturation of

Untreated and Treated **Z8**[a]

Sample	T_m (°C)	ΔH° (kcal/mol)	$\delta T_m / \delta Log(NaCl)$	Δn
Z8 Untreated control	69.6 ± 0.4	45.2 ± 2.3	10.93	0.92
Treated **Z8** Heat-Annealed and Melt Treated	67.7 ± 0.4	48.0 ± 2.4	5.36	0.48
Treated **Z8**, Incubated	68.5 ± 0.4	45.0 ± 2.2	3.30	0.28

[a]Values determined for **Z8** in 200 mM NaCl

61

counterions upon denaturation (i.e., double stranded DNA has a higher charge density than single stranded DNA). With the experimentally determined slopes ($\delta T_m/\delta \log$ [NaCl]) for the oligomer samples untreated **Z8**, heat-annealed **Z8** and incubated **Z8**, combined with the values of T_m and ΔH at 200 mM NaCl, Δn values were determined (Table VI). There is a dramatic decrease in the differential ion binding term (Δn) for both treated DNA oligomers. For untreated **Z8**, $\Delta n = 1.83$, indicating that 1.83 sodium ions are released per 8 base-pair duplex upon melting. This value corresponds to 0.13 sodium ions released per phosphate, a value near to that reported (0.12) for 16 base-pair duplex DNA oligomers (Sheardy et al., 1994). In contrast, only 0.48 Na^+/duplex (0.034 sodium ions per phosphate) for heat-annealed **Z8** and 0.28 Na^+/duplex (0.020 Na^+/phosphate) are released for incubated **Z8**. These data also point to tightly bound cobalt.

The results presented here strongly suggest that $[Co(NH_3)_5(OH_2)]^{3+}$ binds to DNA in an manner consistent with coordination of G-N7 with the cobalt metal center. Tajmir et al. (1993) observed direct metal-base binding via IR spectroscopy when calf thymus DNA was treated with cobalt (III) pentaammine at high cobalt/base pair ratios. The UV and CD spectra at 95 °C and the dramatic decreases in hyperchromicity for **Z8** incubated with $[Co(NH_3)_5(OH_2)]^{3+}$ suggest that this DNA oligomer possessing contiguous GpC sites may also undergo interstrand crosslinking by $[Co(NH_3)_5(OH_2)]^{3+}$ in a manner similar to that of cisplatin. Binding to phosphate is ruled out due to the lability of the phosphate-cobalt bond (Cotton & Wilkinson, 1988) . The most likely site is N7 of guanine bases, such as that observed in the reaction of calf thymus DNA with $[Ru(NH_3)_5(OH_2)]^{2+}$ (Clark et al., 1986). This would allow the cobalt center to reside in the major groove where hydrogen bonding

62

from the ammines to the DNA would be favorable (Seeman et al., 1976). We propose a two step reaction:

$$[Co(NH_3)_5(OH_2)]^{3+} + GN7 \longrightarrow [Co(NH_3)_5\text{-}GN7]^{3+} + H_2O \qquad (I)$$

$$[Co(NH_3)_5\text{-}GN7]^{3+} + GN7 \longrightarrow [Co(NH_3)_4\text{-}(GN7)_2]^{3+} + NH_3 \qquad (II)$$

where GN7 is position N7 of a guanine base. The first step involving the loss of the labile aquo group is the fast reaction occurring at reaction times of less than 30 hours. The second step with loss of the less labile ammine group is a slow reaction requiring around 48 hours for completion. The GN7 of the second step must be unmodified and, should it be on the strand opposite the first GN7, then step 2 would result in a GN7:Co:GN7 interstrand cross link. The second guanine could be on the same strand, as in the prefered target for *cis*-Pt(NH_3)_2Cl_2, but the molecules studied here do not contain the d(-GG-) sequence (Eastman, 1986).

The pK_a of the $[Co(NH_3)_5(OH_2)]^{3+}$ complex is 6.2 (Hicks et al., 1997a; Hicks et al., 1997b). According to the Henderson-Hasselbach equation, at standard buffer conditions of pH 7, the aquo to hydroxo ratio is 0.16, or 84% ionized. That predicts that there is over six times more hydroxo complex, $[Co(NH_3)_5(OH)]^{2+}$, than there is aquo complex, $[Co(NH_3)_5(OH_2)]^{3+}$ present in solution. The first reaction step may then have hydroxide as the leaving group. The second step, in which the covalently bound ion now has a +2 charge in a formal sense, would still result in the loss of the ammine and formation of the bridged complex. However, in the vicinity of the DNA, it is likely that the complex will get (or remain) protonated because of the H+ ions that are associated with the polyelectrolyte. The environment in the grooves and near the phosphates differs from that found in bulk solution. For this reason one can expect that there is not six times more hydroxo than aquo complexes

63

near the DNA.

The same site selectivity was found by the behavior of pentaammineaquocobalt(III) toward DNA as is the case for that of cisplatin, namely, GpC sites are favored over CpG sites. As a result of the right handed helical twist, there are two features which distinguish these two pairs of interstrand guanine residues. The distance between N7's of the guanines in GpC sites is 8 Å, while that in CpG sites is 9 Å. The size of the gap, which the bridging complex has to span, is not the only consideration. The guanine nitrogens in a GpC sequence are both on the groove side of the helical axis, while the N7's of CpG sites are buried in the opposite sides of the axis from the major groove. To reach the two nitrogens of a CpG step, any complex would have to extend into the groove almost up to the helical axis, and in doing so it would encounter the steric hindrance of many functional groups. The CpG site has been reported to be especially malleable in solution structures, exhibiting a difference in twist angle (z axis) and base roll (y axis) depending upon the flanking base sequence (Lefebvre et al., 1995). It is worth asking the question if this observation can be extended to indicate accommodation, on the part of the CpG base overlap, in order to allow better GpC geometries of the guanines in **I** upon binding of the cobalt complex.

A covalent bond between N-7 of guanine and the Co (III) center, via displacement of the water, is highly likely. The data for **Z8**, **12-mer**, **GC-site**, and calf thymus DNA are also consistent with cobalt mediated interstrand crosslinking. As with cisplatin, the GpC sequence provides the crosslinkable site. Crosslinking through cobalt would only be possible through loss of one of the ammines.

The GpC sequence raises some questions. This sequence causes a 6 degree lower melting point when comparing **GC-site** to **CG-isomer** (Figure 26). One possible factor is the presence of a GpC step, at which the DNA conformation is altered to take advantage of improved base overlap. The shape of the grooves and phosphate backbone is altered by a large helical twist angle of 40° (Kabsch et al., 1982). This may present better geometries for metal to DNA bond formation. Another consideration is the bases that flank the central guanines. A less stable stack can be more available for binding and reactivity. The -AGCT-stacking of a pur-pur-pyr-pyr sequence (in **IV**) is less stabilizing than the pur-pyr-pur-pyr of -ACGT- (Saenger, 1984).

Lastly, in the heat annealing of **Z8** with cobalt (III) hexaammine, the guanine bases flip over, about their C1-N9 bonds (from *anti* to *syn*), to form a left handed Z helix. Whether this occurs while the oligomer is still single stranded or after reforming a B-form duplex is unclear. With the reactive pentaammineaquocobalt(III) complex, the oligomer retains the right-handed conformation when returned to the duplex state after reannealing. Since the first modification is likely a single hit of the cobalt to one or more of the 8 guanines, this can happen to the oligomer while in the single stranded state (at 80 °C or slightly cooler) or after reannealing. Either way, possibly the bound cobalt complex is too bulky to allow the G base to swing from the *anti* to *syn* conformation. It is plausible that the covalently bound cobalt complex could form specific interactions with the phosphate and the sugar, which favors the *anti* base orientation, and in turn maintains a B-like structure in the (formed or forming) duplex.

65

3.9   Future Directions

Other oligonucleotides, which can be used as better cobalt targets, would include sequences that contain single GpC, CpG, and GpG sites as well as isolated G's (G flanked by A and/or T). The design must consider the conflicting trends involving molecular size. It should be small enough so that NMR studies would be solvable and synthesis costs moderate, while it must be large enough to be a substrate for enzyme cleavage studies and to have a T_m well above room temperature, not withstanding so few G:C hydrogen bonds (Hicks et al., 1997a).

Modifying the best oligomer target on a preparative scale would allow for enzyme digest and isolation of the modified cobalt adduct by HPLC (Fichtinger-Schepman et al., 1984; Fichtinger-Schepman et al., 1985). Short of attaining that, enzyme cleavage studies could show inhibition by the complex, reduced rates of enzyme reaction, or even enzyme mediated complex removal.

Electrophoresis gels can reveal differences in enzymic cleavage of the treated and untreated oligomers. Polyacrylamide gel elecrophoresis (PAGE) may be able to demonstrate a change in migration of the complex treated oligomer itself due to the charge difference of the bound metal or by a conformational change in the DNA (Yohannes et al., 1993).

Thermodynamics of helix stability can be quantified by melting an oligomer at different concentrations of DNA. The midpoint of a bimolecular transition, such as a single strand annealing to double strand, is sensitive to concentration, and can be analyzed with van't Hoff plots. It also follows that a unimolecular transition, such as the melting of a hairpin structure, is insensitive to concentration. One half of the duplex stem is covalently bound by the loop

66

to its complementary strand. This is also encountered in a crosslinked oligomer. The two strands are covalently bound by some linking agent. Therefore, crosslinked strands, to the extent that the crosslinking reaction was complete, should show melting temperatures which are insensitive to concentration. After demonstrating the dependence of concentration on melting temperature for the controls, the treated oligomer would exhibit a different concentration dependence. This would indicate that, as in the case of a hairpin, the complementary strands are not free single strands but rather are linked by the rective complex because the transition is now unimolecular. In practice, this type of experiment has a fatal flaw. Modifications such as crosslinking reduce the hyperchromicity of the duplex to single strand transition since the final state is not fully single stranded. Thus the smaller change that one has to follow limits the range of useful concentrations of DNA which will give a measurable signal. With less of a transition to measure against noise, and a limited range available, the linear relationship is not supported by enough data. Perhaps a longer sequence, which can be crosslinked toward one end and thus allow for more than half of the molecule to melt, would be a more hairpin-like mimic and a better candidate for concentration effects in melting and modification.

A blocking study should be performed to demonstrate that the complex binds to N7 of guanine. Dimethyl sulfate is used to methylate N7 of guanines as a means to pick out the G bases in the Maxam and Gilbert sequencing method. If the complex only reacts and crosslinks through the N7 position, no modification will result in an oligomer whose guanines are blocked by methyl groups (Ezaz-Nikpay & Verdine, 1992).

67

The first anti-tumor drug, cisplatin, has been studied for nearly thirty years to determine the structure and mechanism of its interaction with DNA. There still are arguments and new perspectives on how it looks and acts (Takahara et al., 1995; Huang et al., 1995). Changing the other ligands in cisplatin was done over the years, but no substitution was more effective. In the case of octahedral cobalt(III), there are more positions to change than the four in square planar platinum(II). Varying the ammines with other ligands could change the binding selectivity or reactivity of the complex compared to $[Co(NH_3)_5(OH_2)]^{3+}$. A single change in a ligand could shift the pK_a of the leaving aquo group which could, even in the vicinity of the DNA, change the rates of the reactions with the organic bases. The continuation of these studies could lead to a useful therapeutic drug or simply a mechanism to explain the interaction between DNA and $[Co(NH_3)_5(OH_2)]^{3+}$.
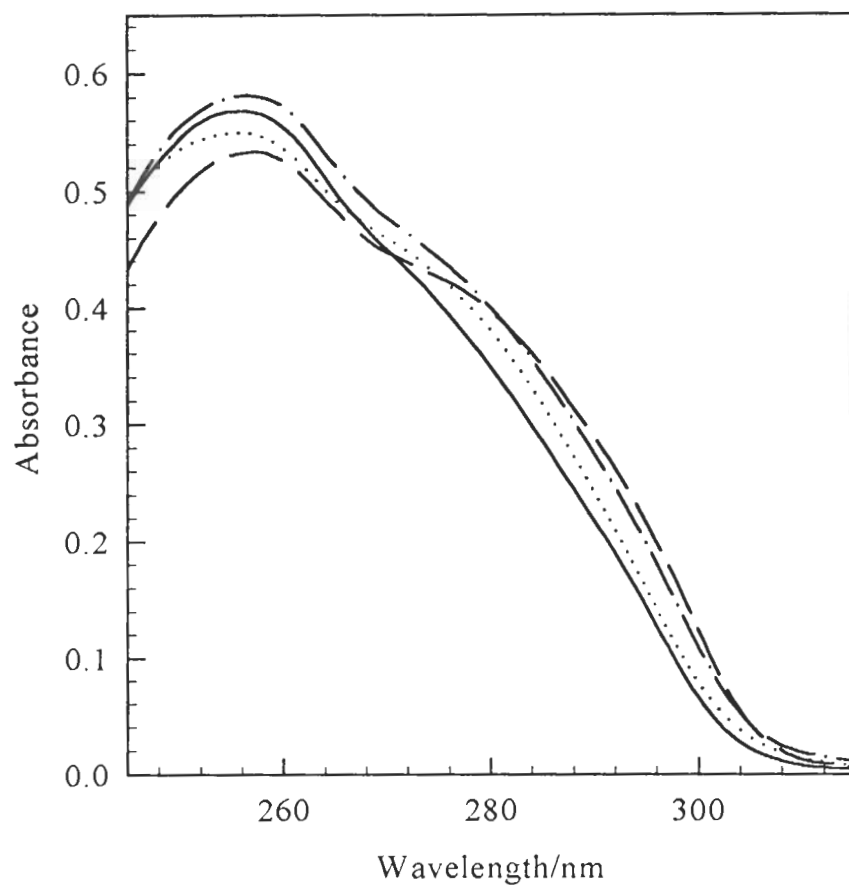
Figure 6. Dependence of the UV Spectrum of **Z8** on Cobalt Complex Treatment.

The UV spectra of **Z8** in standard phosphate buffer with 50 mM NaCl at 25 °C: in buffer alone (solid line); heat annealed in the presence of 200 μM $[Co(NH_3)_6]^{3+}$ without subsequent dialysis (dash); heat annealed in the presence of 200 μM $[Co(NH_3)_5(OH_2)]^{3+}$ (dash-dot); incubated in the presence of 200 μM $[Co(NH_3)_5(OH_2)]^{3+}$, followed by exhaustive dialysis, lyophilization and reconstitution in standard buffer with 50 mM NaCl (dot). The concentration of DNA for these samples was ca. 4.2×10^{-5} M in base pairs.

69
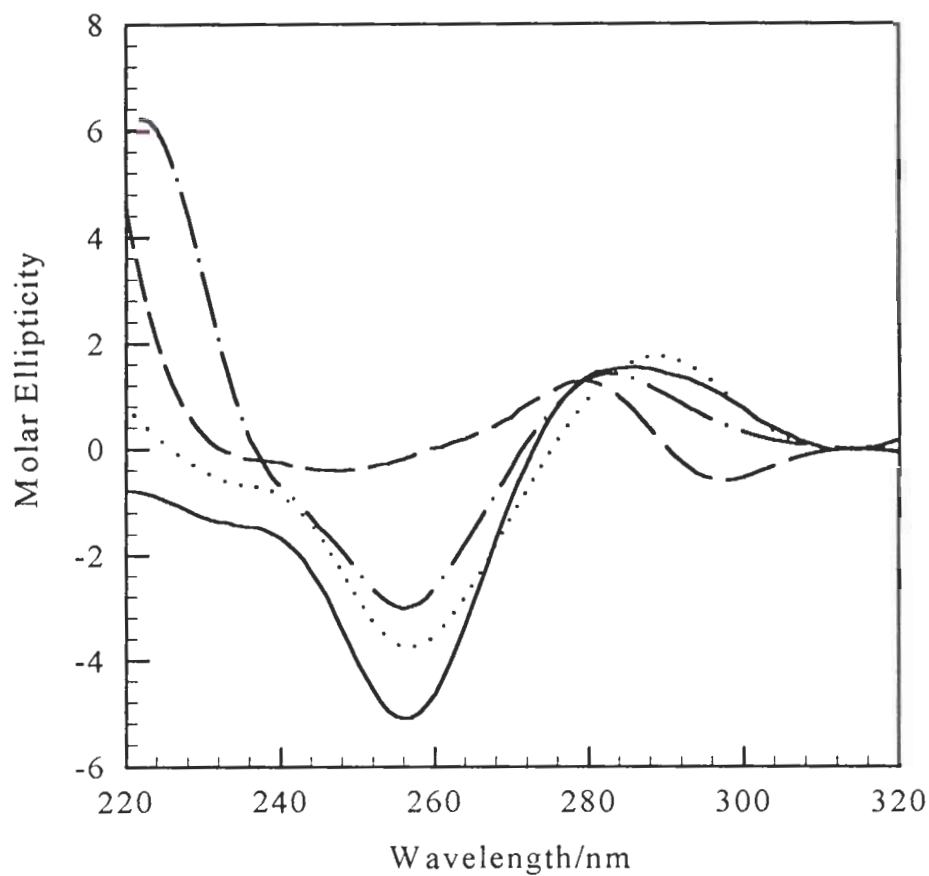
Figure 7. Dependence of the CD Spectrum of **Z8** on Cobalt Complex Treatment.

The CD spectra of **Z8** in standard phosphate buffer with 50 mM NaCl at 25 °C: in buffer alone (solid line); heat annealed in the presence of 200 μM $[Co(NH_3)_6]^{3+}$ without subsequent dialysis (dash); heat annealed in the presence of 200 μM $[Co(NH_3)_5(OH_2)]^{3+}$ (dash-dot); incubated in the presence of 200 μM $[Co(NH_3)_5(OH_2)]^{3+}$, followed by exhaustive dialysis, lyophilization and reconstitution in standard buffer with 50 mM NaCl (dot). The concentration of DNA for these samples was ca. 4.2×10^{-5} M in base pairs.

70
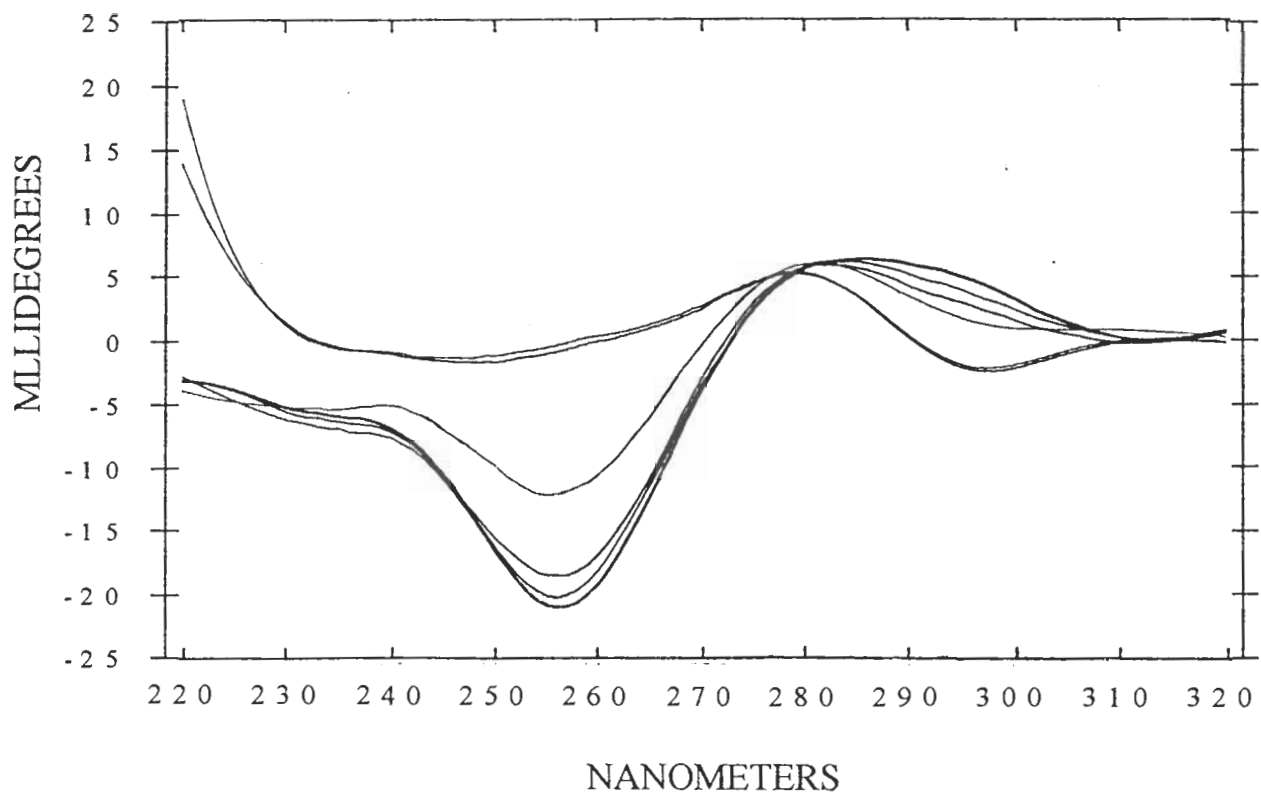
Figure 8. CD Spectra of **Z8** Heat-Annealed with Hexaamminecobalt(III)

The CD spectra at 25 °C of **Z8** which was heat annealed in buffer with $[Co(NH_3)_6]^{3+}$ at the concentrations 0 (bottom line at 255 nm), 25 μM, 50 μM, 100 μM, 200 μM and 150 μM (top line at 255 nm). The samples with the highest concentration of complex (150 μM & 200 μM) are virtually identical and indicate that the oligomer is in the Z-conformation.
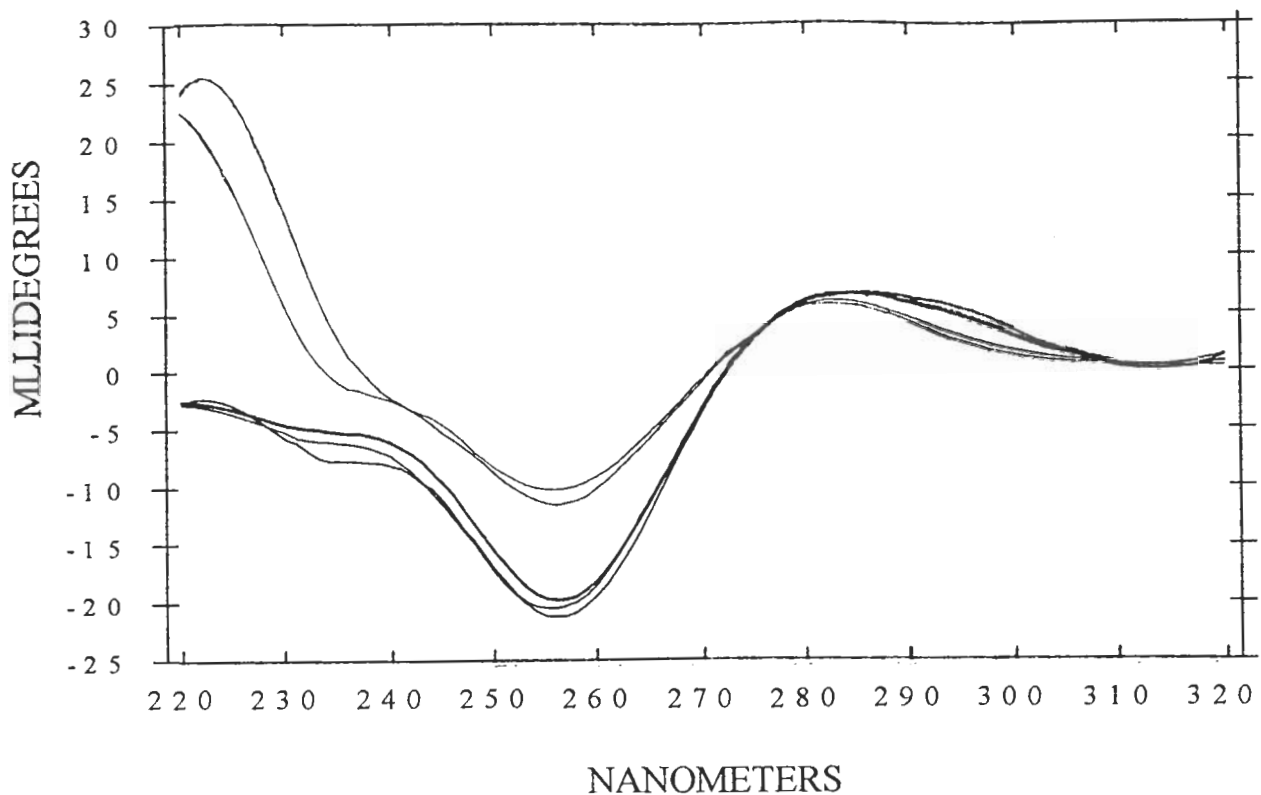
Figure 9. CD Spectra of **Z8** Heat-Annealed with Pentaammineaquocobalt(III)

The CD spectra at 25 °C of **Z8** which was heat annealed in buffer with $[Co(NH_3)_5(OH_2)]^{3+}$ at the concentrations 50 μM (bottom line at 255 nm), 100 μM, 0 (no added complex - middle line at 255 nm), 200 μM, & 150 μM (top line at 255 nm). At $[Co(NH_3)_5(OH_2)]^{3+}$ concentrations of less than 100 μM, the spectra are quite similar to that of the oligomer in the absence of any cobalt complex. The trough at 255 nm actually is deeper for the samples with 50 μM and 100 μM $[Co(NH_3)_5(OH_2)]^{3+}$. The samples with the highest concentration of complex (150 μM & 200 μM) are similar to each other, but quite different from the oligomer alone or with the hexaammine complex. The reactive cobalt complex also induces a conformational transition in **Z8** which is complete by 150 μM, but the oligomer remains in an altered B-like conformation.

72
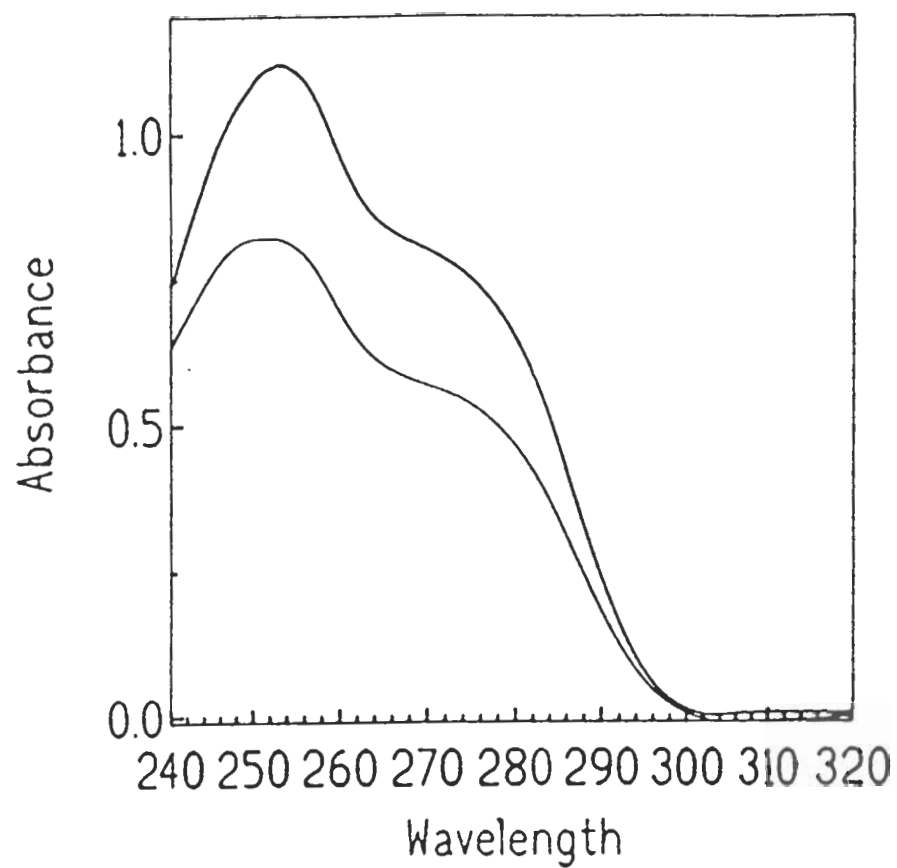
Figure 10. UV Spectra of dG with 200 μM $[Co(NH_3)_5(OH_2)]^{3+}$

    The UV spectra of dG in the presence of 200 μM $[Co(NH_3)_5(OH_2)]^{3+}$ before heating (upper line), and after slow heating and slow reannealing (lower).

73
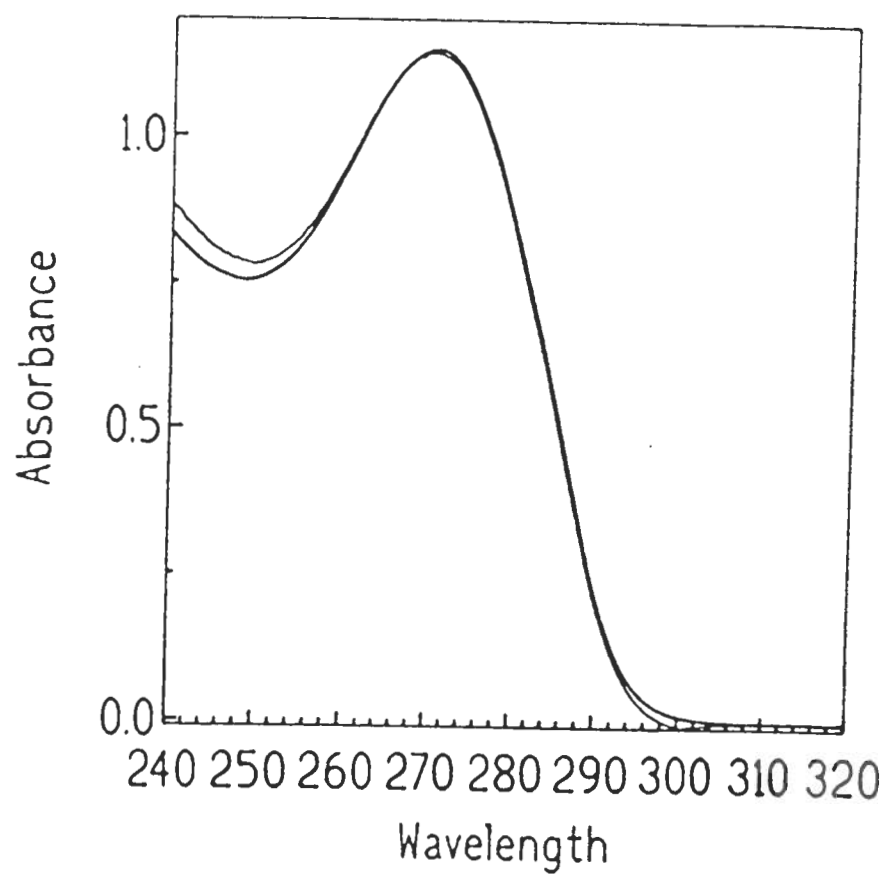
Figure 11. UV Spectra of dC with 200 μM $[Co(NH_3)_5(OH_2)]^{3+}$
    The UV spectra of dC in the presence of 200 μM $[Co(NH_3)_5(OH_2)]^{3+}$ before heating (lower line), and after slow heating and slow reannealing (upper).
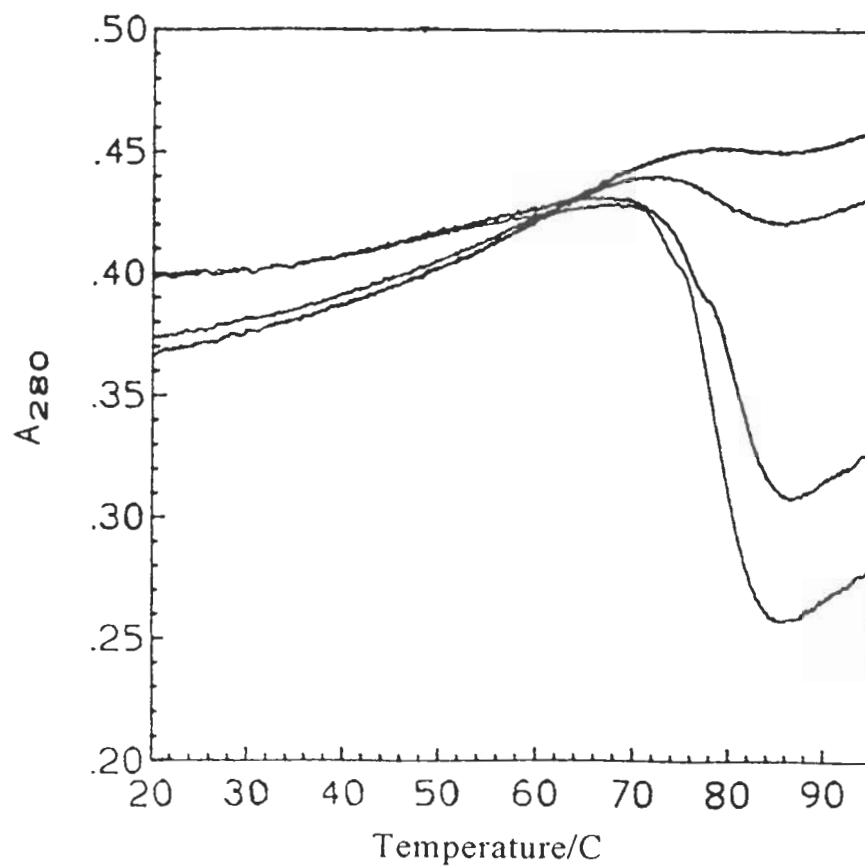
Figure 12. Melt of **Z8** and $[Co(NH_3)_5(OH_2)]^{3+}$ with Metal Added to the Blanks.

The thermal denaturation profiles for **Z8** in buffer with $[Co(NH_3)_5(OH_2)]^{3+}$ at the concentrations 25 μM (top line at 90°C), 50 μM, 150 μM, & 200 μM (bottom line) referenced against buffer with the corresponding cobalt complex concentration. The unusual profiles indicate that the cobalt complex is undergoing a reaction in the blank to a greater extent than is occurring in the solutions which also contain DNA. The cobalt complex is binding to the DNA, reducing the amount of free $[Co(NH_3)_5(OH_2)]^{3+}$ which can interact with $[Co(NH_3)_5(OH_2)]^{3+}$ or with phosphate.
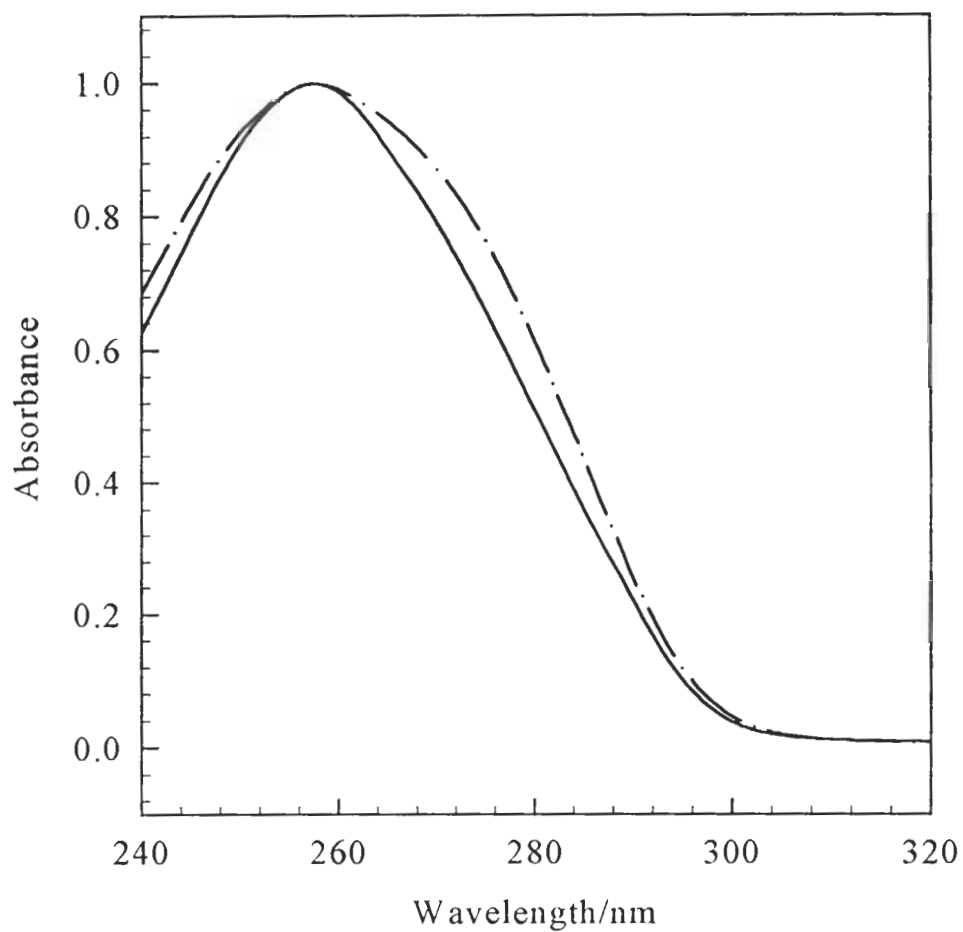
75
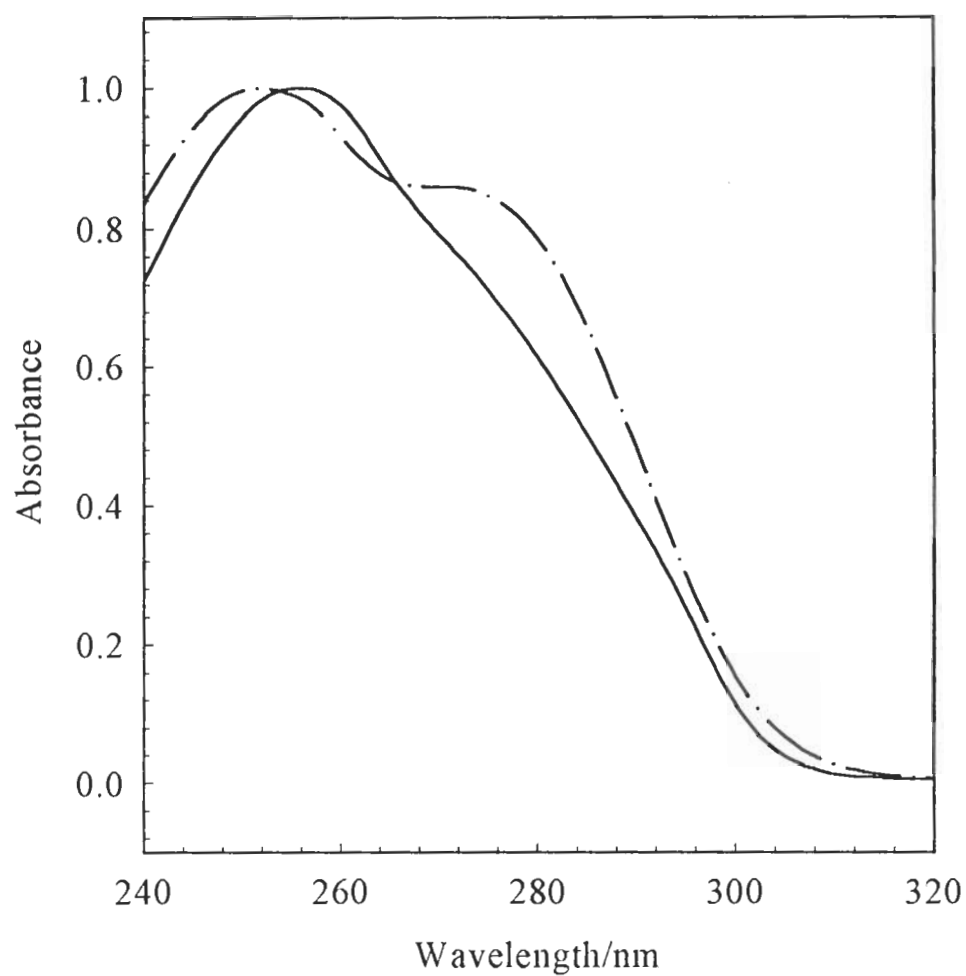
Figure 13. UV Spectra of Untreated **Z8** at 20 °C and 95 °C

The effect of temperature on UV absorption spectra of untreated **Z8.** The difference between the 20 °C (solid) and the 95 °C (dash-dot) spectra is due to hyperchromic shift. The concentration of DNA for these data was ca. 6.5×10^{-5} M in base pairs.
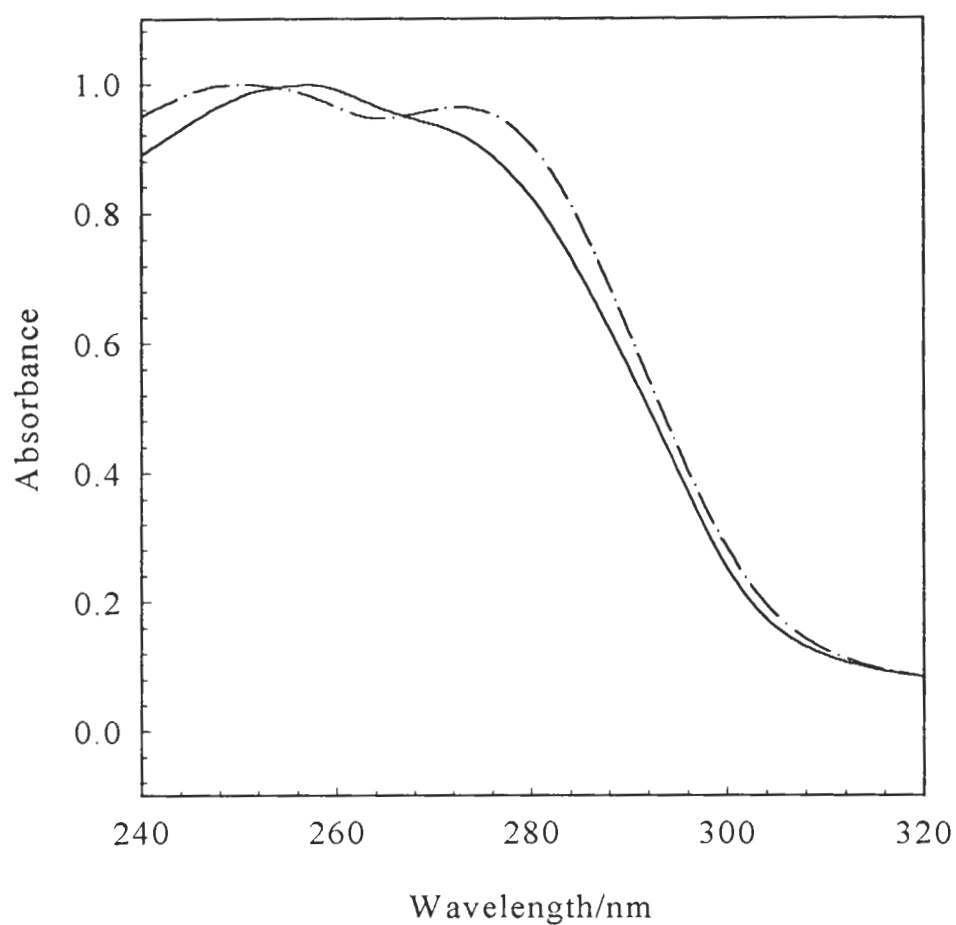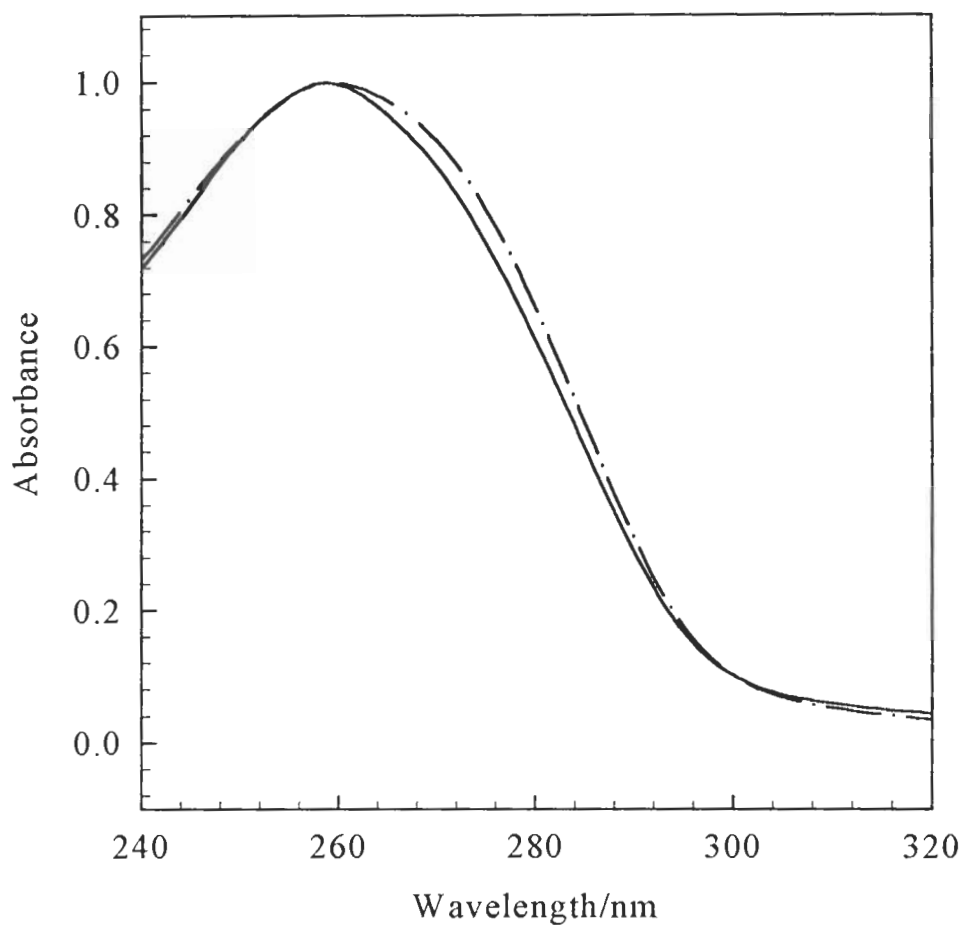
Figure 14. UV Spectra of Melt-Treated **Z8** at 20 °C and 95 °C

The effect of temperature on UV absorption spectra of **Z8** which was heat-annealed and melt-treated in the presence of 200µM $[Co(NH_3)_5(OH_2)]^{3+}$ and then exhaustively dialyzed. The difference between the 20 °C (solid) and the 95 °C (dash-dot) spectra is due to hyperchromic shift. The concentration of DNA for these data was ca. 6.5×10^{-5} M in base pairs.
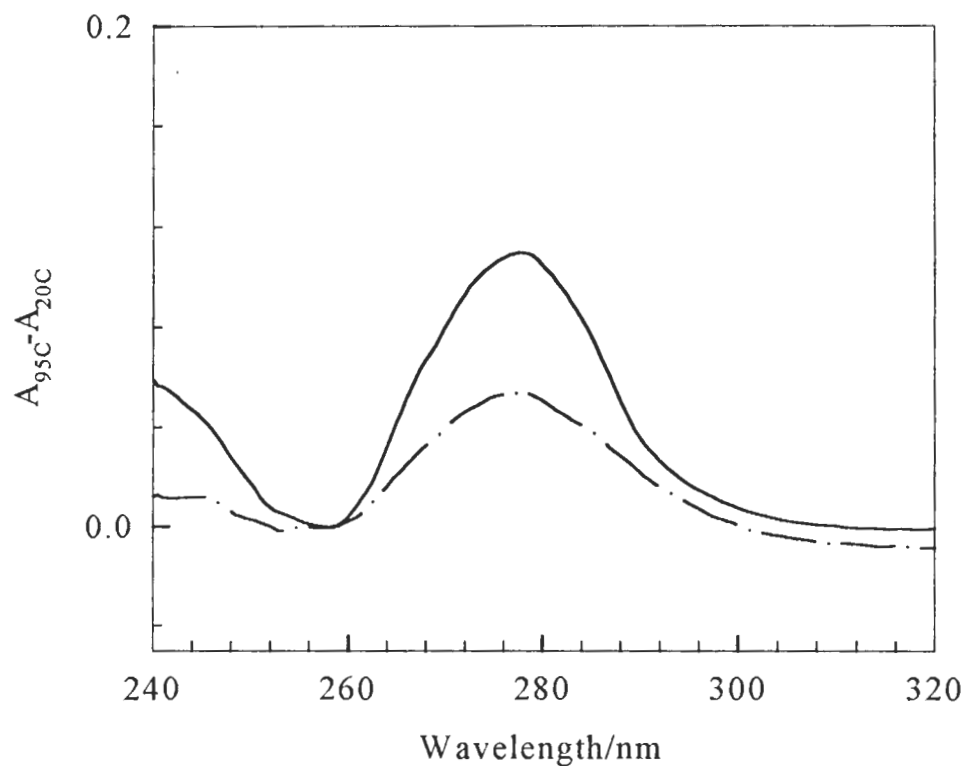
77

Figure 15. UV Temperature Difference Spectra of **Z8**

      The effect of temperature on UV absorption spectra of **Z8** which was heat-annealed and melt-treated in the presence of 200µM $[Co(NH_3)_5(OH_2)]^{3+}$ and then exhaustively dialyzed. The UV temperature difference spectra for untreated **Z8** (solid) and melt-treated **Z8** (dash) are plotted as: $\Delta A = A_{95C} - A_{20C}$, where the subscripts designate the temperature at which the spectra were recorded. The concentration of DNA for these data was ca. 6.5 x 10^{-5} M in base pairs.
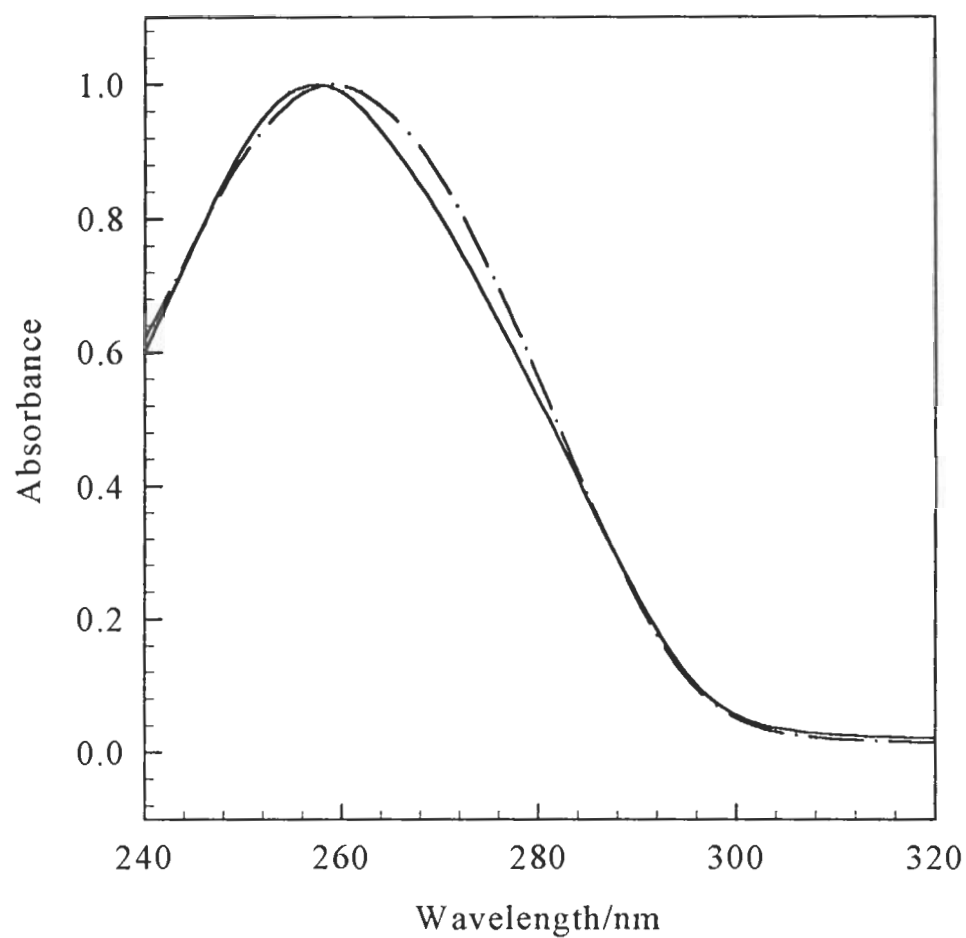
78

Figure 16. UV Spectra of Untreated **12-mer** at 20 °C and 95 °C

The effect of temperature on UV absorption spectra of untreated **12-mer.** The difference between the 20 °C (solid) and the 95 °C (dash-dot) spectra is due to hyperchromic shift. The concentration of DNA for these data was ca. 6.5×10^{-5} M in base pairs.
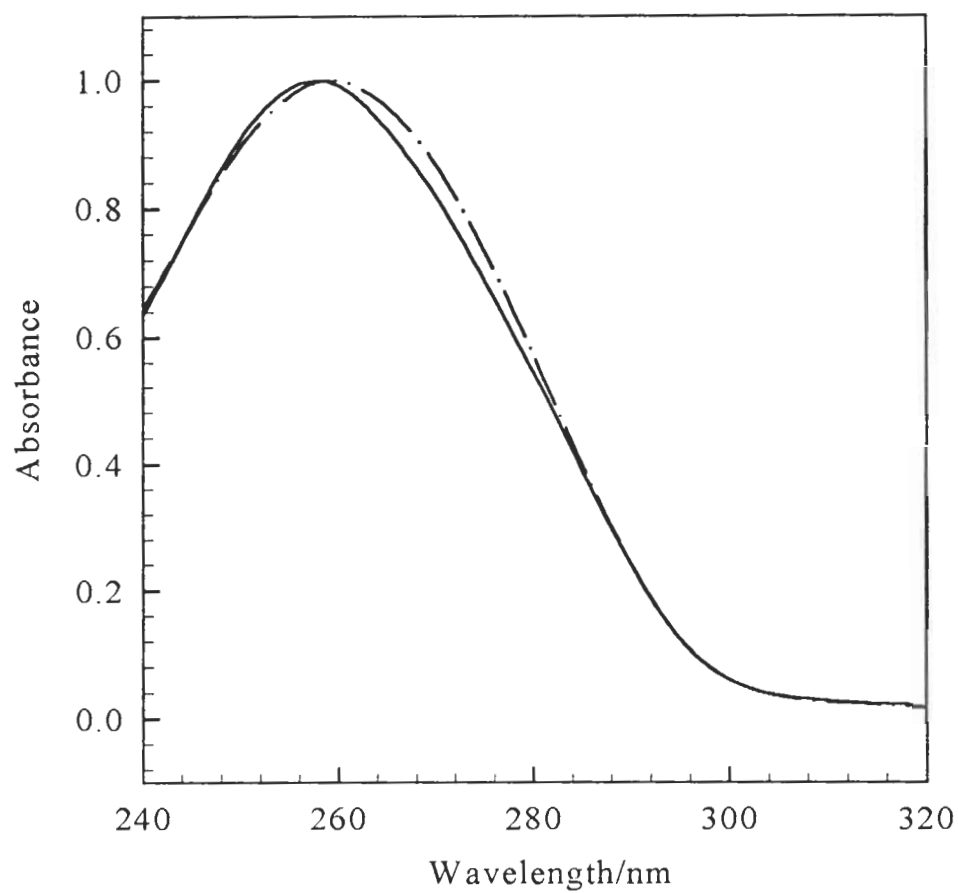
79

Figure 17. UV Spectra of Melt-Treated **12-mer** at 20 °C and 95 °C

The effect of temperature on UV absorption spectra of **12-mer** which was heat-annealed and melt-treated in the presence of 200μM $[Co(NH_3)_5(OH_2)]^{3+}$ and then exhaustively dialyzed. The difference between the 20 °C (solid) and the 95 °C (dash-dot) spectra is due to hyperchromic shift. The concentration of DNA for these data was ca. 6.5×10^{-5} M in base pairs.
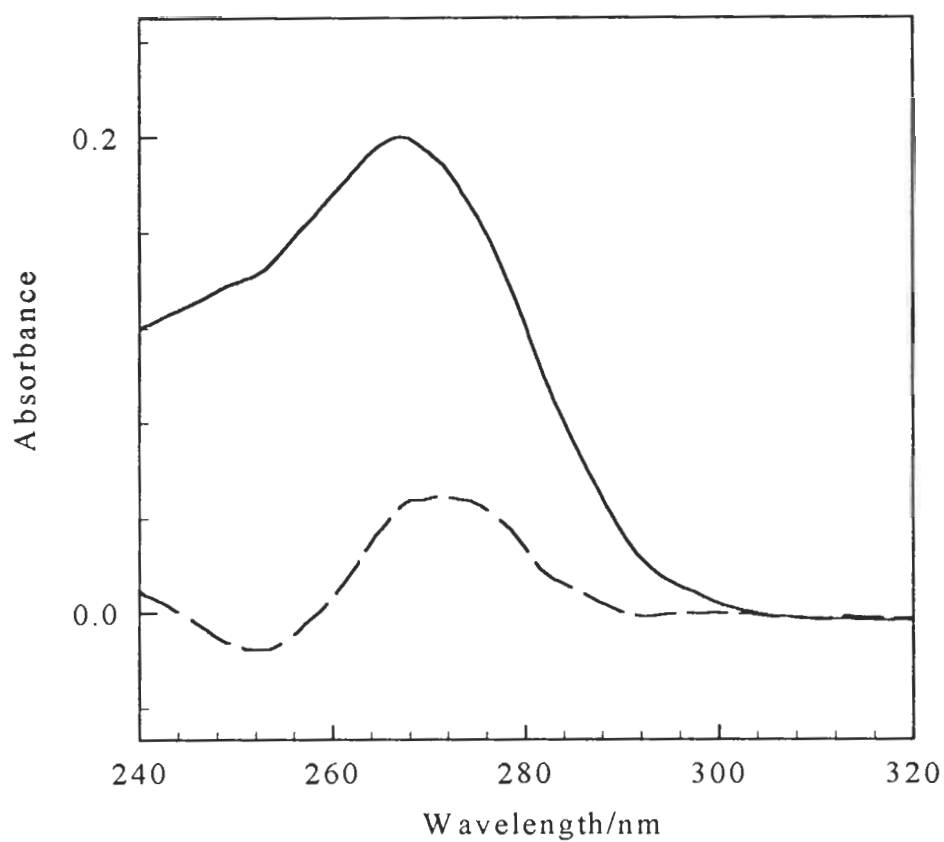
80

Figure 18. UV Temperature Difference Spectra of **12-mer**

The effect of temperature on UV absorption spectra of **12-mer** which was heat-annealed and melt-treated in the presence of $200\mu M$ $[Co(NH_3)_5(OH_2)]^{3+}$ and then exhaustively dialyzed. The UV temperature difference spectra for untreated **12-mer** (solid) and melt-treated **12-mer** (dash) are plotted as: $\Delta A = A_{95C} - A_{20C}$, where the subscripts designate the temperature at which the spectra were recorded. The concentration of DNA for these data was ca. 6.5×10^{-5} M in base pairs.

Figure 19. UV Spectra of Untreated **24-mer** at 20 °C and 95 °C

The effect of temperature on UV absorption spectra of untreated **24-mer.** The difference between the 20 °C (solid) and the 95 °C (dash-dot) spectra is due to hyperchromic shift. The concentration of DNA for these data was ca. 6.5×10^{-5} M in base pairs.

82

Figure 20. UV Spectra of Melt-Treated **24-mer** at 20 °C and 95 °C

The effect of temperature on UV absorption spectra of **24-mer** which was heat-annealed and melt-treated in the presence of 200μM $[Co(NH_3)_5(OH_2)]^{3+}$ and then exhaustively dialyzed. The difference between the 20 °C (solid) and the 95 °C (dash-dot) spectra is due to hyperchromic shift. The concentration of DNA for these data was ca. 6.5×10^{-5} M in base pairs.

Figure 21. UV Temperature Difference Spectra of **24-mer**

The effect of temperature on UV absorption spectra of **24-mer** which was heat-annealed and melt-treated in the presence of 200μM $[Co(NH_3)_5(OH_2)]^{3+}$ and then exhaustively dialyzed. The UV temperature difference spectra for untreated **24-mer** (solid) and melt-treated **24-mer** (dash) are plotted as: $\Delta A = A_{95C} - A_{20C}$, where the subscripts designate the temperature at which the spectra were recorded. The concentration of DNA for these data was ca. 6.5×10^{-5} M in base pairs.
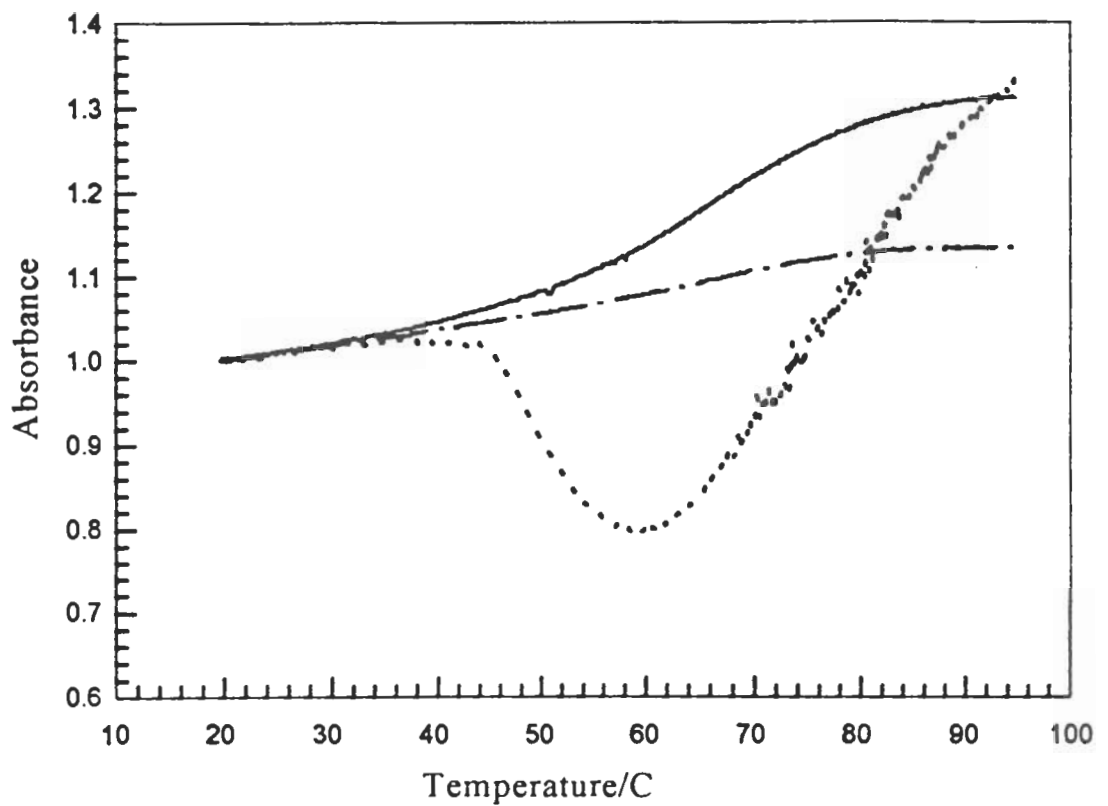
84
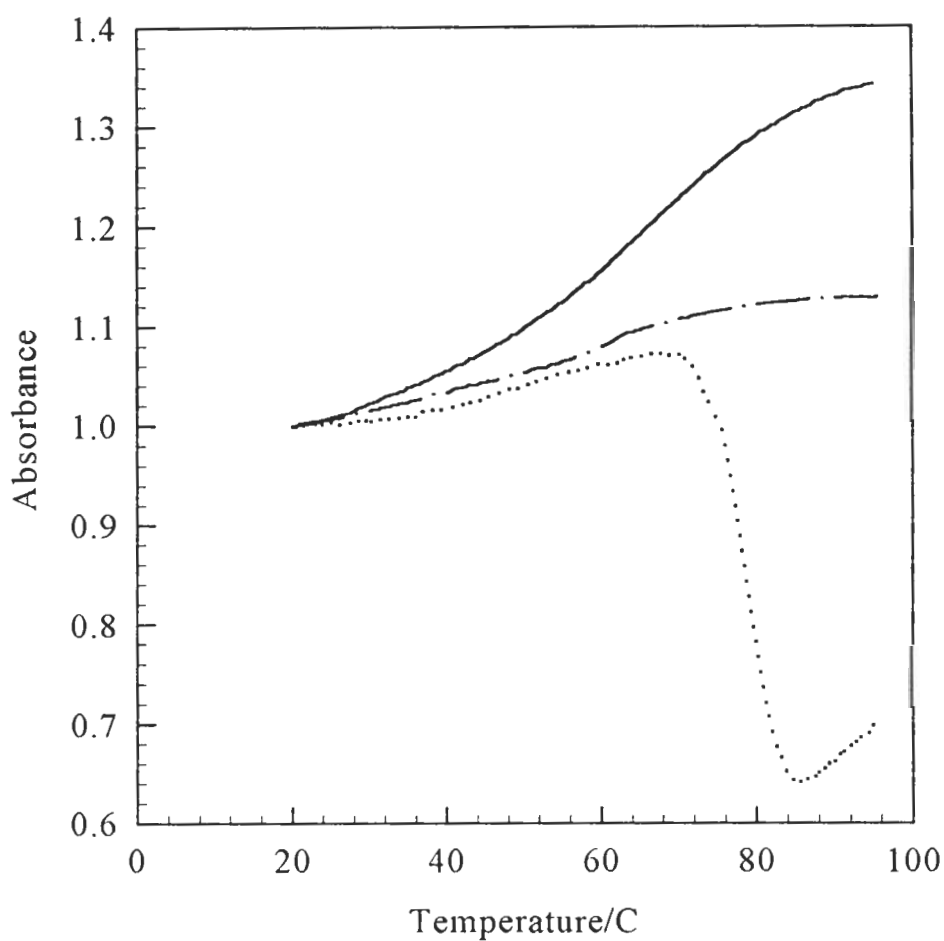
Figure 22. Melting Profiles of **Z8**

Normalized melting profiles, monitored at 280 nm while heated at about 0.3 C°/minute, of **Z8** before treatment (solid), after melt-treatment and exhaustive dialysis (dash-dot), as well as during the actual melting in the presence of 200µM $[Co(NH_3)_5(OH_2)]^{3+}$ (dot). The down turn above 70 °C in the melting-treatment profile reveals that the 200µM $[Co(NH_3)_5(OH_2)]^{3+}$ in the buffer solution of the blank is causing an increase in absorbance and/or turbidity at 280 nm as it undergoes dimerization and polymerization.
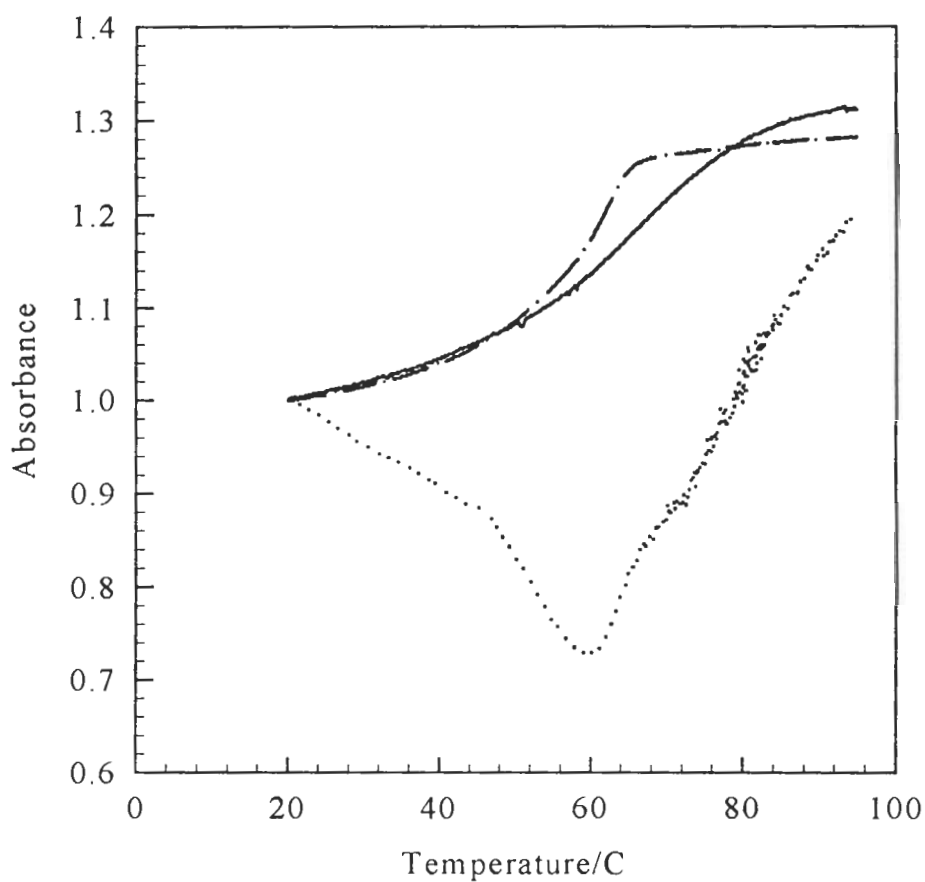
85

Figure 23. Melting Profiles of **12-mer**

Normalized melting profiles, monitored at 280 nm while heated at about 0.3 C°/minute, of **12-mer** before treatment (solid), after melt-treatment and exhaustive dialysis (dash-dot), as well as during the actual melting in the presence of 200μM $[Co(NH_3)_5(OH_2)]^{3+}$ (dot). The down turn above 40-45 °C in the melting-treatment profile reveals that the 200μM $[Co(NH_3)_5(OH_2)]^{3+}$ in the buffer solution of the blank is causing an increase in absorbance and/or turbidity at 280 nm as it undergoes dimerization and polymerization.

86

Figure 24. Melting Profiles of **24-mer**

Normalized melting profiles, monitored at 272 nm while heated at about 0.3 C°/minute, of **24-mer** before treatment (solid), after melt-treatment and exhaustive dialysis (dash-dot), as well as during the actual melting in the presence of 200μM $[Co(NH_3)_5(OH_2)]^{3+}$ (dot). The decrease at all temperatures and the down turn above 46 °C in the melting-treatment profile reveals that the 200μM $[Co(NH_3)_5(OH_2)]^{3+}$ in the buffer solution of the blank is causing an increase in absorbance and/or turbidity at 272 nm as it undergoes dimerization and polymerization.
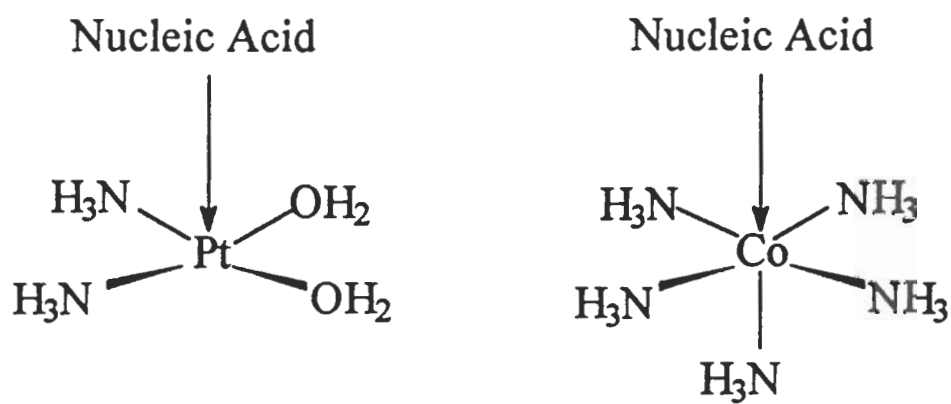
87

Nucleic Acid

Nucleic Acid

H_3N — Pt — OH_2 / H_3N / OH_2

H_3N — Co — NH_3 / H_3N / NH_3 / H_3N

Figure 25. Comparison of Ligand Orientation in Platinum and Cobalt Complexes

The octahedral cobalt(III) complexes can, upon binding, present DNA with a molecular structure of similar geometry to that found for the associative binding of square planer platinum(II) compounds.
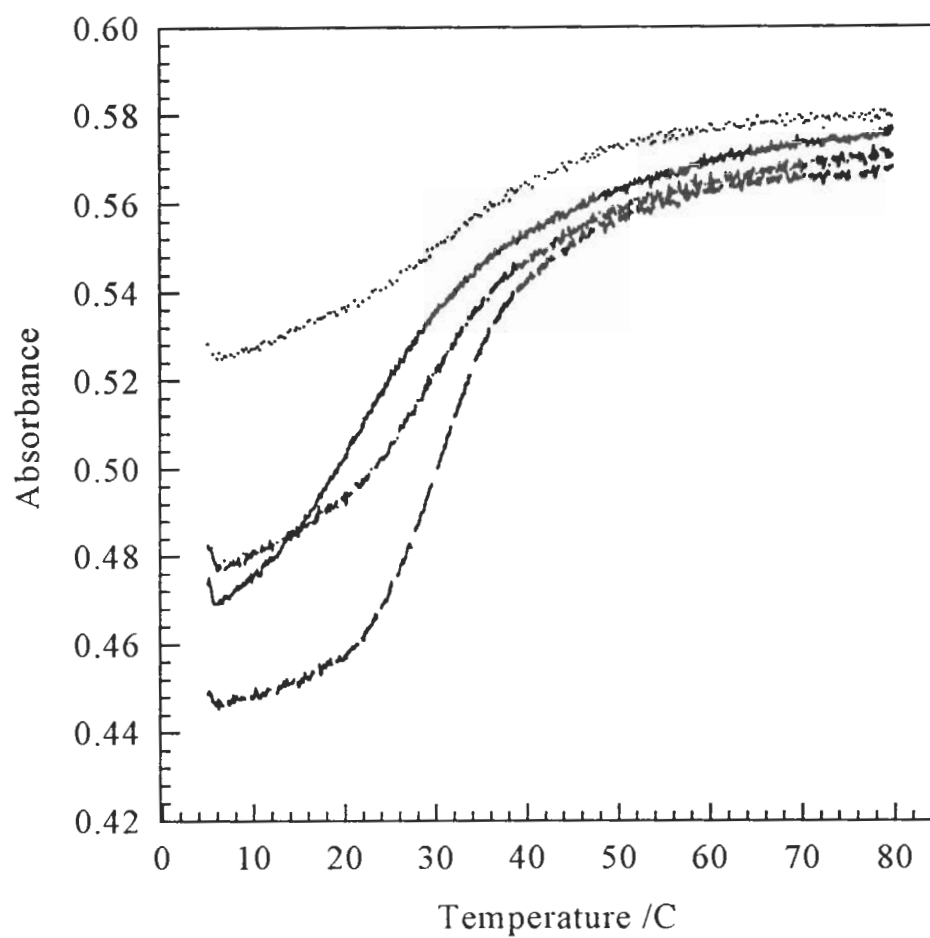
Figure 26. Melting Profiles of Untreated and Treated **GC-site** and **CG-isomer**

Melting Profiles, monitored at 260 nm while heated at about 0.3C°/minute, of **GC-site** before treatment (solid), **GC-site** after melt-treatment and exhaustive dialysis (dot, at top), **CG-isomer** before treatment (dash, at bottom), and **CG-isomer** after melt-treatment and exhaustive dialysis (dash-dot).
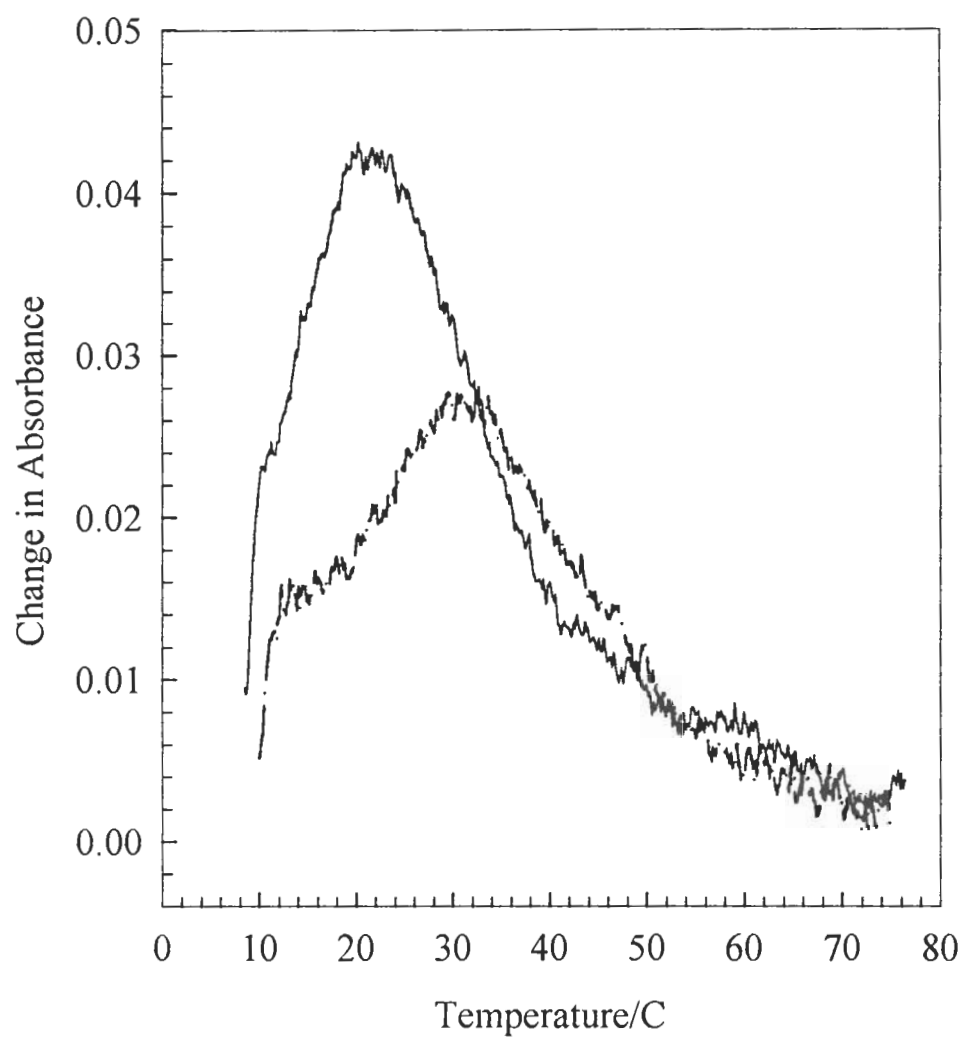
89

Figure 27. Differentials of Untreated and Treated **GC-site** Thermal Denaturation
    The first differentials of the melt profile of untreated **GC-site** (solid) and melt-treated **GC-site** (dash-dot). The maxima are the inflection point temperatures, or T_{max} .
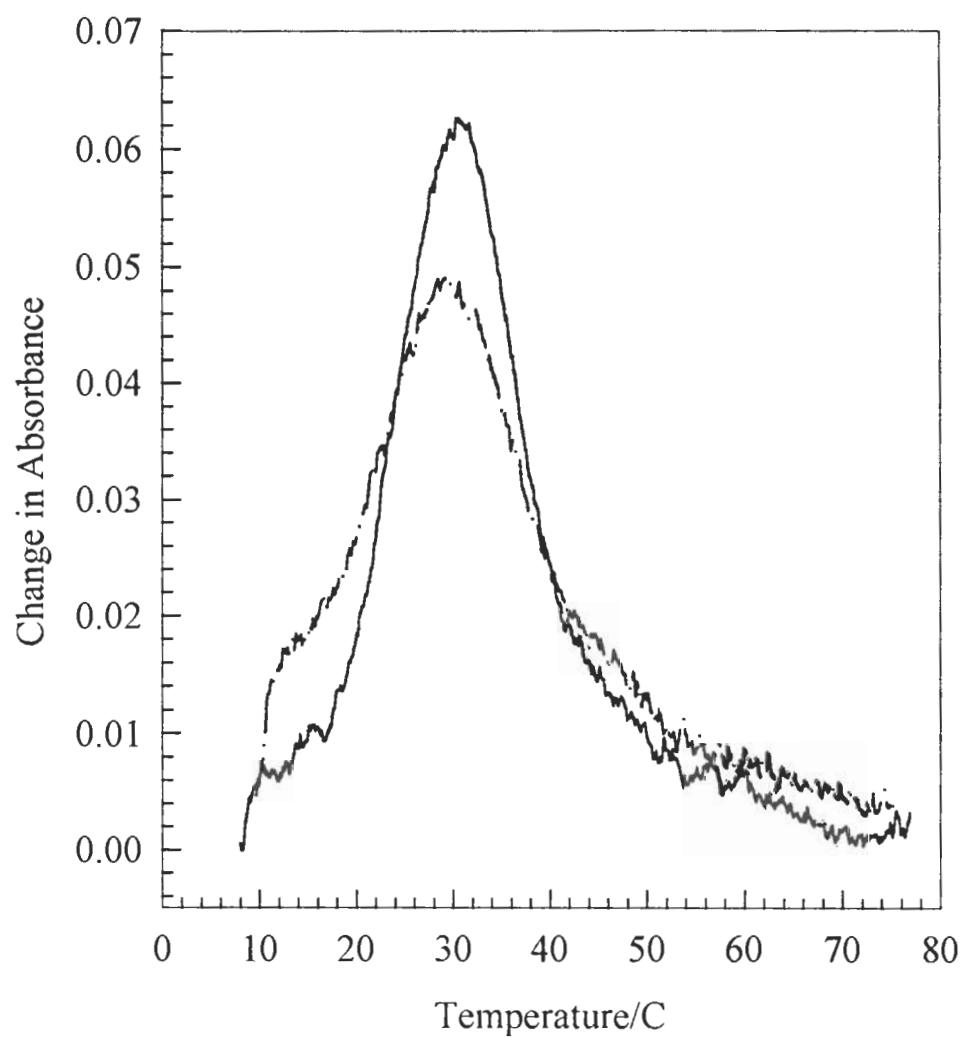
Figure 28. Differentials of Untreated and Treated **CG-isomer** Thermal Denaturation
The first differentials of the melt profile of untreated **CG-isomer** (solid) and melt-treated **CG-isomer** (dash-dot). The maxima are the inflection point temperatures, or T_{max}.
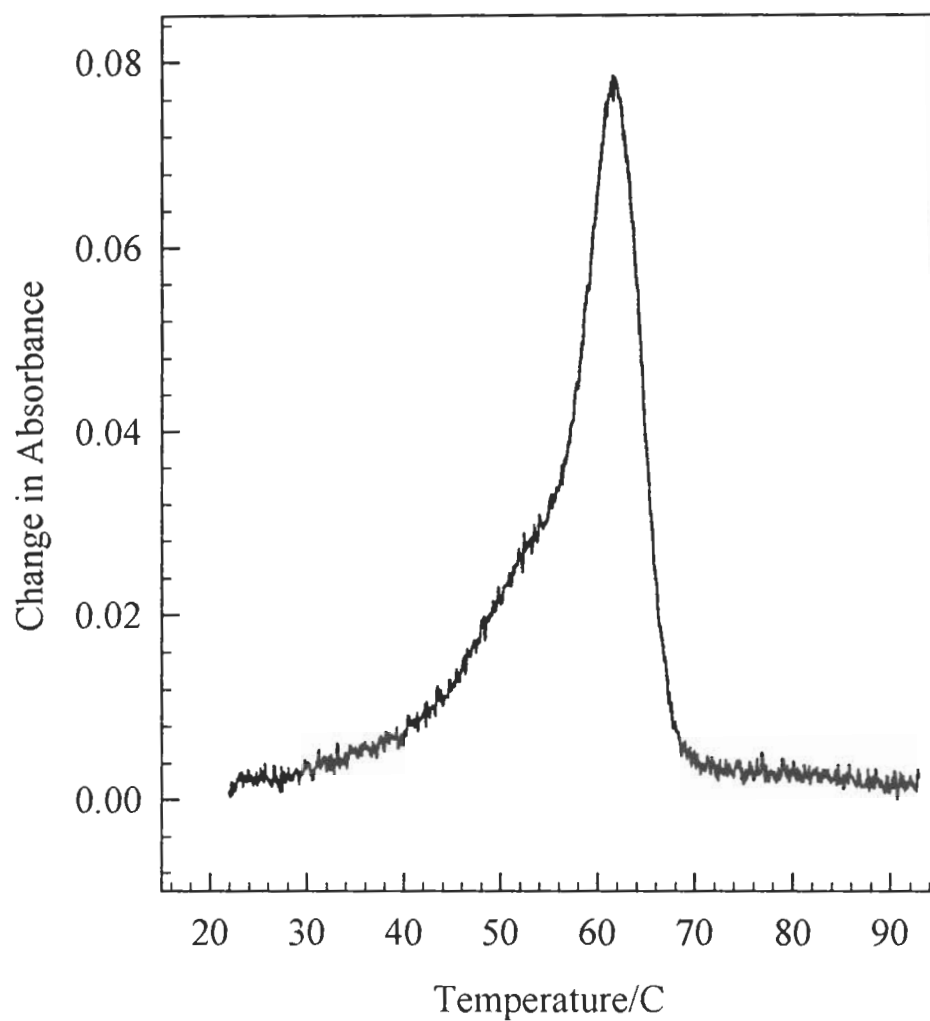
91

Figure 29. Differential of **24-mer** Thermal Denaturation

The first differential of the melt profile of untreated **24-mer** highlights the unsymmetric lower curve and baselines. The maximum is the inflection point temperature, or T_{max}.
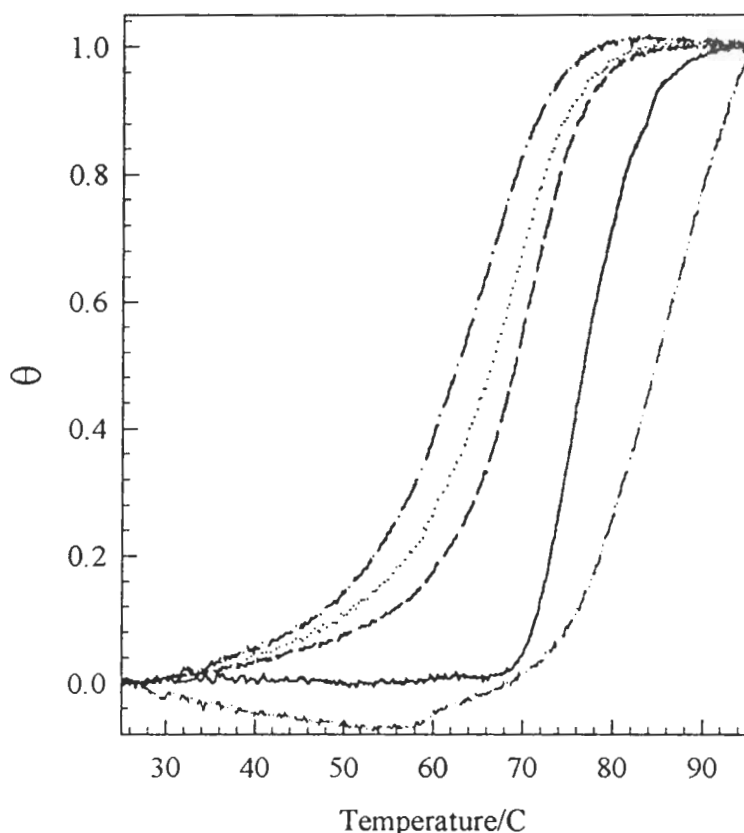
Figure 30. Melting Profiles of Incubation-Treated Sonicated Calf Thymus DNA

Sonicated Calf Thymus DNA samples were incubated at 37 °C for 48 hours in buffer with $[Co(NH_3)_5(OH_2)]^{3+}$ at the following concentrations (and **DNA/Co ratios**): {1} [CT-DNA] = 280 µM, Control, (--) {solid}; {2} [CT-DNA] = 560 µM, $[[Co(NH_3)_5(OH_2)]^{3+}]$ = 200 µM, **(2.8)** {dash}; {3} [CT-DNA] = 280 µM, $[[Co(NH_3)_5(OH_2)]^{3+}]$ = 200 µM, **(1.4)** {dot}; {4} [CT-DNA] = 140 µM, $[[Co(NH_3)_5(OH_2)]^{3+}]$ = 200 µM, **(0.7)** {dash-dot}; {5} [CT-DNA] = 560 µM, $[[Co(NH_3)_5(OH_2)]^{3+}]$ = 400 µM, **(1.4)** {dash-dot-dot}. After incubation, the samples were exhaustively dialyzed verses water, evaporated to dryness, and then reconstituted in buffer. Sample 5 had some precipitate, so it was diluted with water before dialysis. For the thermal denaturation experiments, the concentration of DNA was adjusted to ca. 1.0×10^{-4} M in base pairs. The temperature was ramped from 25 °C to 95 °C at 0.3 C°/minute while monitored at 260 nm. The melting data are plotted as θ (fraction of absorbance change) = $(A_T - A_{25})/(A_{95} - A_{25})$ where A_T is the absorbance at temperature T and A_{25} and A_{95} are the initial and final absorbances at 25 °C and 95 °C, respectively. The T_m values ($\pm$ 0.3 C°) obtained from the first derivative of the melt profiles are as follows: {1} 75.2 °C; {2} 70.6 °C; {3} 69.2 °C; {4} 65.9 °C; and {5} 86.1 °C.
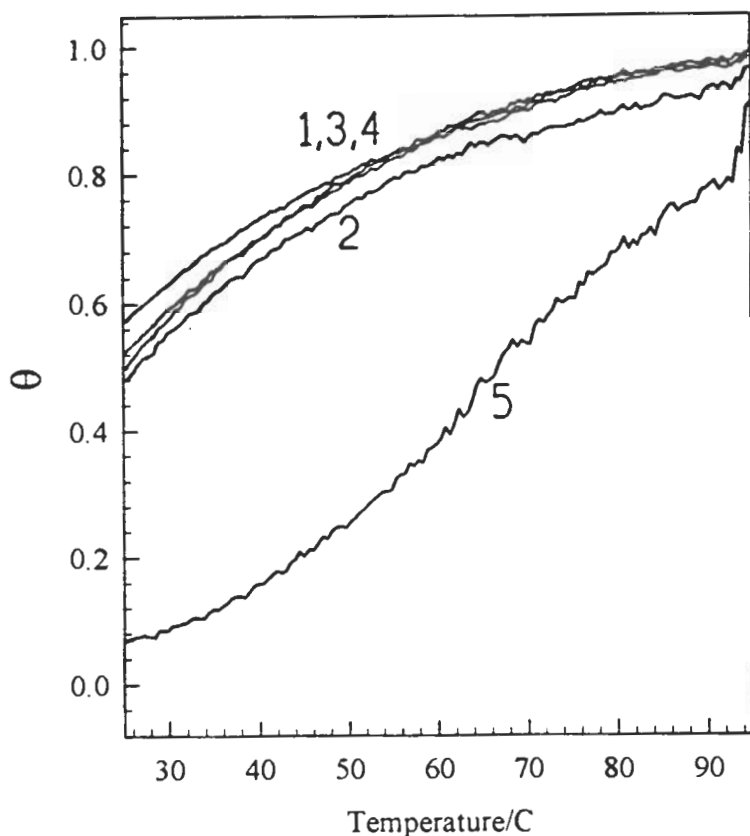
93

Figure 31. Remelting Profiles of Cobalt-Treated Sonicated Calf Thymus DNA

The samples of untreated and treated sonicated calf thymus DNA, from Figure 30, were slowly reannealed to room temperature under thermal control in the Gilford spectrophotometer following the initial denaturation. The samples equilibrated at 4 °C for several days before the second thermal denaturation. All the samples, with the same conditions in Figure 30, were remelted, as before, by ramping the temperature from 25 °C to 95 °C at 0.3 C°/minute while monitoring at 260 nm. The melting data are plotted as θ (fraction of absorbance change) $= (A_T - A_{25})/(A_{95} - A_{25})$ where A_T is the absorbance during the remelt at temperature T, and A_{25} and A_{95} are the initial and final absorbances from the initial melting (Figure 30) at 25 °C and 95 °C, respectively. Thus the remelt data is normalized according to the profiles of the initial melt.
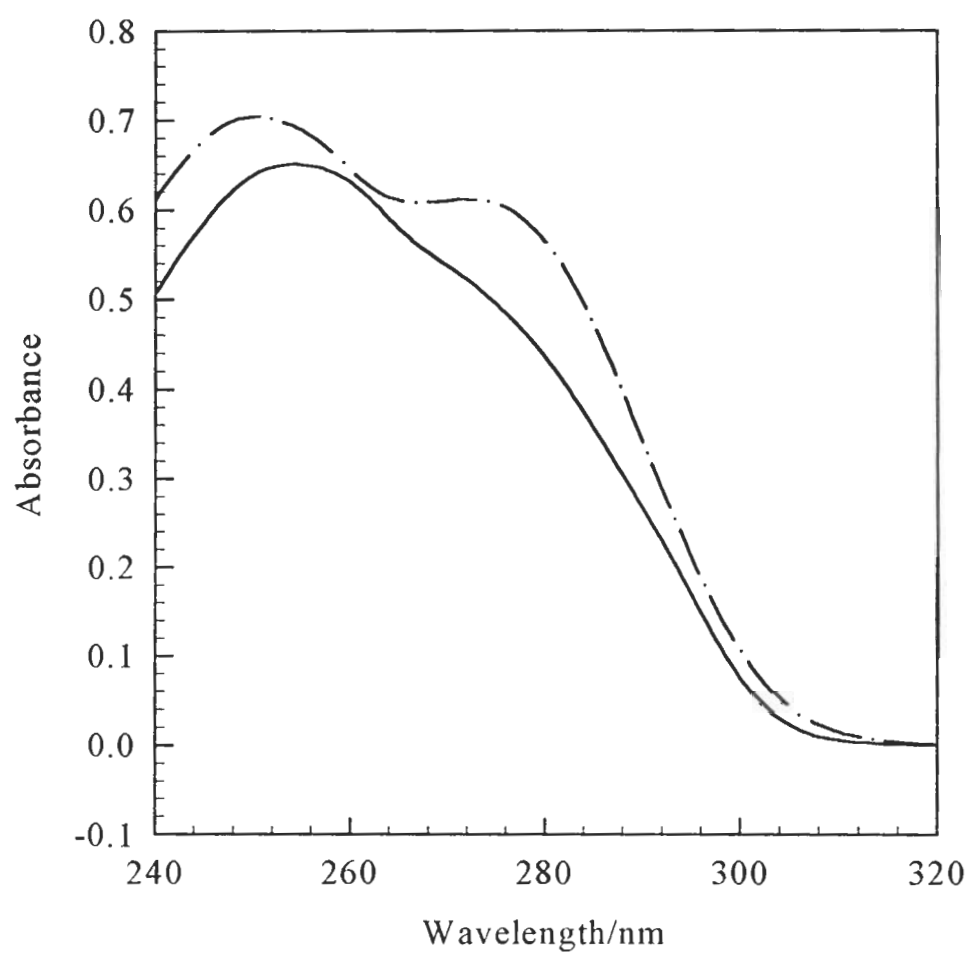
94

Figure 32. UV Spectra of Untreated **Z8** at 25 °C and 95 °C

The effect of temperature on UV absorption spectra of untreated **Z8.** The difference between the 25 °C (solid) and the 95 °C (dash-dot) spectra is due to hyperchromic shift. The concentration of DNA for these data was ca. 4.3×10^{-5} M in base pairs.

95

Figure 33. UV Spectra of Treated **Z8**; 250 μM [Co(NH$_3$)$_5$(OH$_2$)]$^{3+}$ at 25 °C and 95 °C

The effect of temperature on UV absorption spectra of **Z8** which was incubated with 250μM [Co(NH$_3$)$_5$(OH$_2$)]$^{3+}$ at 37 °C for 48 hours, and then exhaustively dialyzed. The difference between the 25 °C (solid) and the 95 °C (dash-dot) spectra is due to the hyperchromic shift. The concentration of DNA for these data was ca. 4.3 x 10^{-5} M in base pairs.
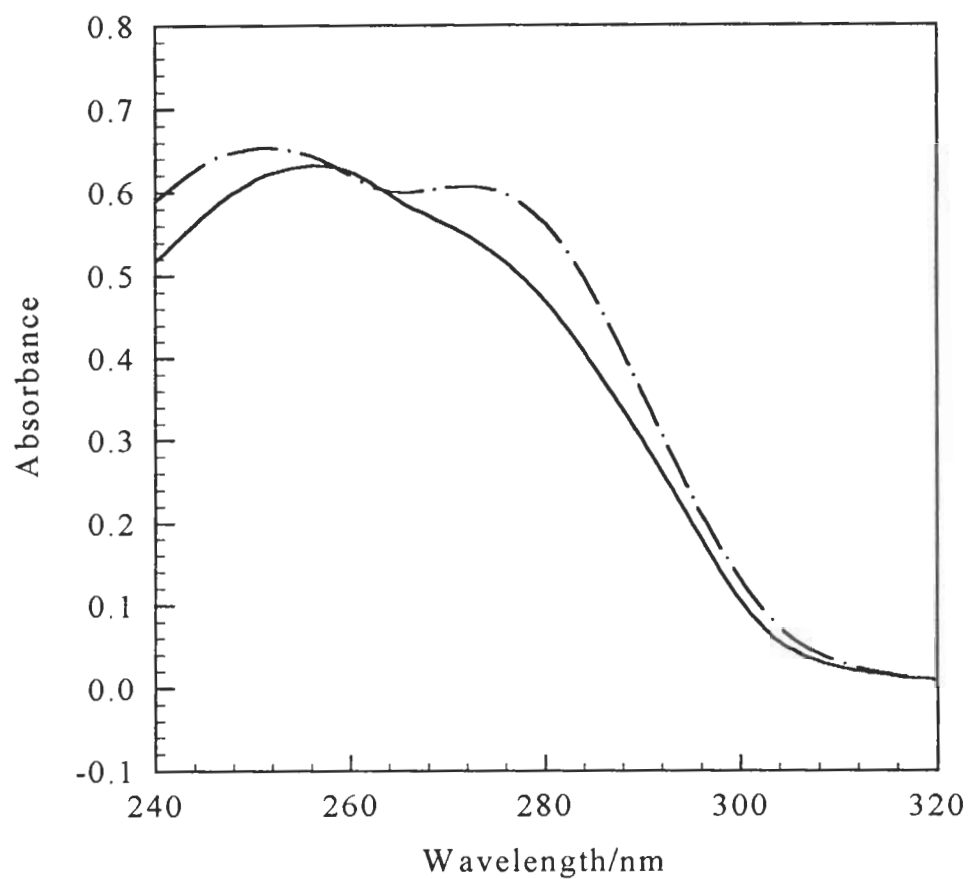
Figure 34. UV Spectra of Treated **Z8**; 300 μM $[Co(NH_3)_5(OH_2)]^{3+}$ at 25 °C and 95 °C

The effect of temperature on UV absorption spectra of **Z8** which was incubated with 300μM $[Co(NH_3)_5(OH_2)]^{3+}$ at 37 °C for 48 hours, and then exhaustively dialyzed. The difference between the 25 °C (solid) and the 95 °C (dash-dot) spectra is due to the hyperchromic shift. The concentration of DNA for these data was ca. 4.3×10^{-5} M in base pairs.
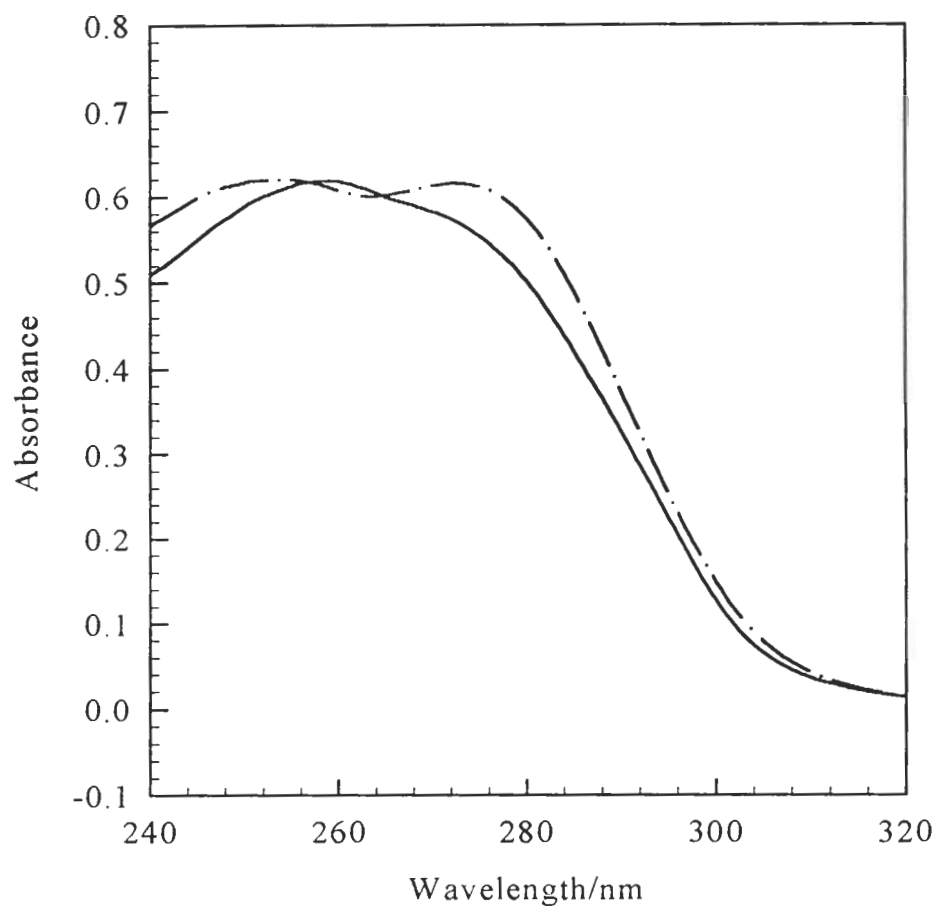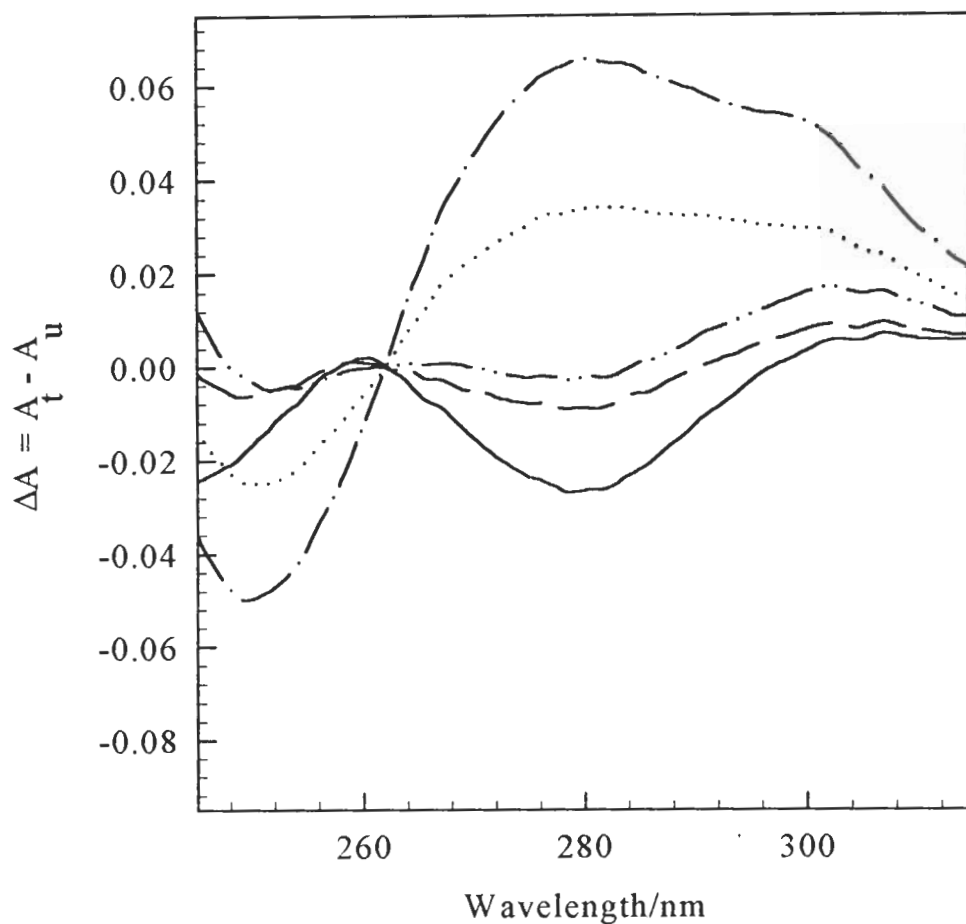
97

Figure 35. UV Difference Spectra at 25 °C of Treated and Untreated **Z8**

The effect of increasing the concentration of $[Co(NH_3)_5(OH_2)]^{3+}$ in the incubation of **Z8** at 37 °C for 48 hours, followed by exhaustive dialysis, on UV absorption spectra of the oligomer in standard buffer with 200 mM NaCl at 25 °C. The UV absorption difference spectra are plotted as: $\Delta A = A_t - A_u$, where A_t and A_u are the absorbances of treated and untreated oligomer, respectively. The concentrations of $[Co(NH_3)_5(OH_2)]^{3+}$ in the incubation were 100 µM (solid), 200 µM (dash), 250 µM (dot), 300 µM (dash-dot), and 400 µmM (dash-dot-dot). The concentration of DNA for these data was ca. 4.3 x 10^{-5} M in base pairs. The spectra were normalized at 260 nm before calculating their differences.
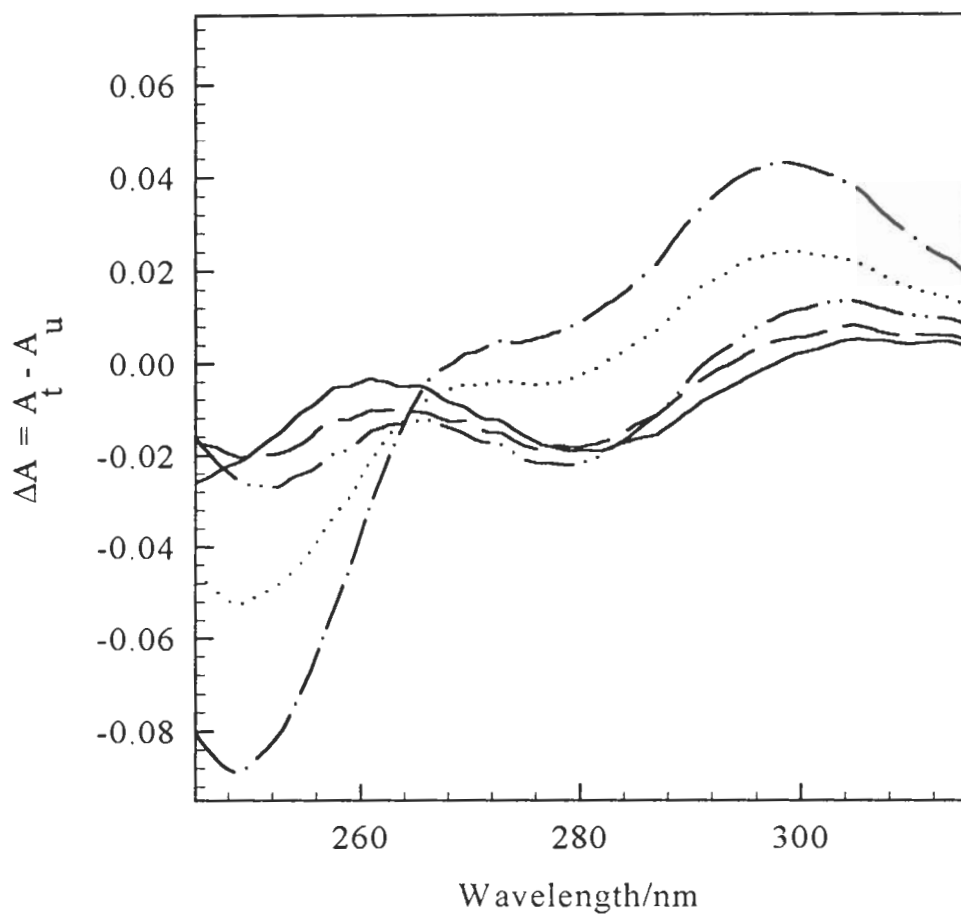
98

Figure 36. UV Difference Spectra at 95 °C of Treated and Untreated **Z8**

The effect of increasing the concentration of $[Co(NH_3)_5(OH_2)]^{3+}$ in the incubation of **Z8** at 37 °C for 48 hours, followed by exhaustive dialysis, on UV absorption spectra of the oligomer in standard buffer with 200 mM NaCl at 95 °C, which is at denaturing conditions. The UV absorption difference spectra is plotted as: $\Delta A = A_t - A_u$, where A_t and A_u are the absorbances of treated and untreated oligomer, respectively. The concentrations of $[Co(NH_3)_5(OH_2)]^{3+}$ in the incubation were 100 μM (solid), 200 μM (dash), 250 μM (dot), 300 μM (dash-dot), and 400 μmM (dash-dot-dot). The concentration of DNA for these data was ca. 4.3 x 10^{-5} M in base pairs. The 95 °C spectra were normalized at 260 nm, according to the 25 °C spectra, before calculating their differences.

99
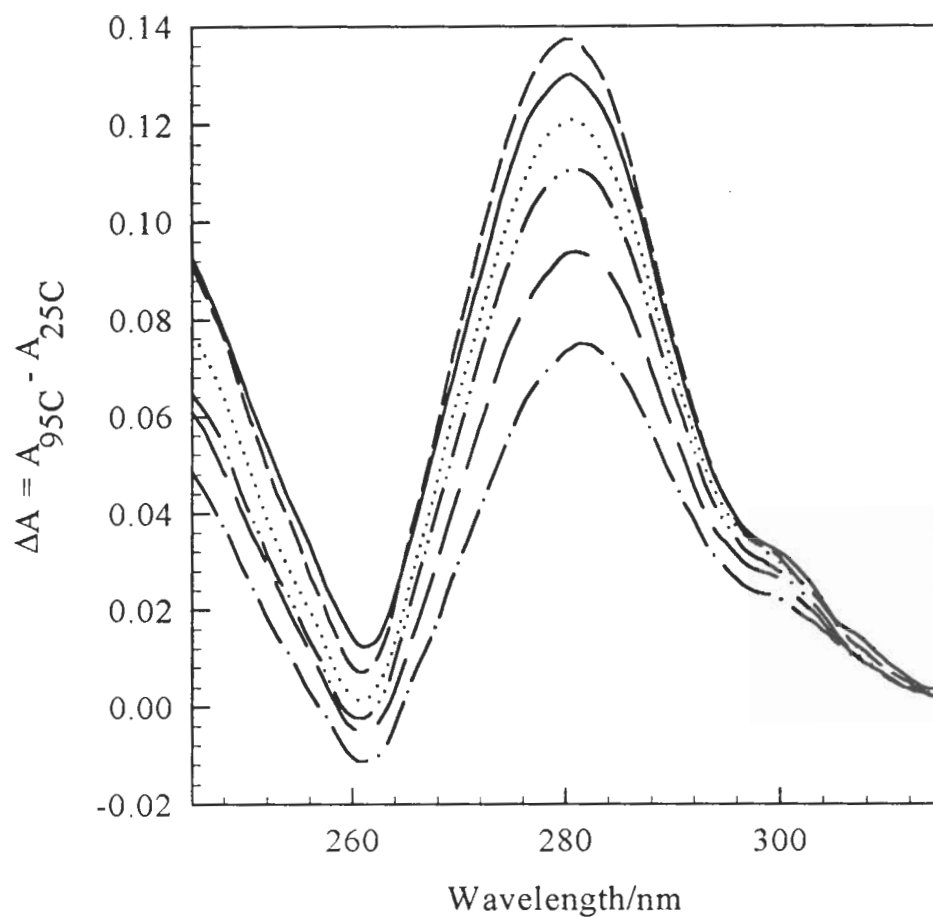
Figure 37. UV Temperature Difference Spectra for Incubated **Z8**

The effect of increasing the concentration of $[Co(NH_3)_5(OH_2)]^{3+}$ in the incubation of **Z8** at 37 °C for 48 hours, followed by exhaustive dialysis, on UV absorption spectra. The UV temperature difference spectra for untreated and treated **Z8** are plotted as: $\Delta A = A_{95C} - A_{25C}$, where the subscripts designate the temperature at which the spectra were recorded. The concentrations of $[Co(NH_3)_5(OH_2)]^{3+}$ in the incubation were 0 (solid), 100 μM (short dash), 200 μM (dot), 250 μM (long dash), 300 μM (dash-dot), and 400 μM (dash-dot-dot). The concentration of DNA for these data was ca. 4.3×10^{-5} M in base pairs.

100

Figure 38. CD Spectra of **Z8** Incubated with Various Concentrations of $[Co(NH_3)_5(OH_2)]^{3+}$

The effect of increasing the concentration of $[Co(NH_3)_5(OH_2)]^{3+}$ in the incubation of **Z8** at 37 °C for 48 hours, followed by exhaustive dialysis, on CD spectra. The concentrations of $[Co(NH_3)_5(OH_2)]^{3+}$ in the incubation were 0 (bottom line at 255 nm), 100 µM, 200 µM (middle line at 255 nm), 400 µM, and 300 µM (top line at 255 nm). For the CD spectra, the samples were kept at 25 °C.

Figure 39. CD Difference Spectra at 25 °C of Treated and Untreated **Z8**

The effect of increasing the concentration of $[Co(NH_3)_5(OH_2)]^{3+}$ in the incubation of **Z8** at 37 °C for 48 hours, followed by exhaustive dialysis, on the molar ellipticity of the oligomer in standard buffer with 200 mM NaCl at 25 °C. The CD difference spectra are plotted as: $\Delta\theta = \theta_t - \theta_u$, where θ_t and θ_u are the molar ellipticities of treated and untreated oligomer, respectively. The concentration of $[Co(NH_3)_5(OH_2)]^{3+}$ in the incubation was 100 μM (solid), 200 μM (dash), 250 μM (dot), 300 μM (dash-dot), and 400 μM (dash-dot-dot). The concentration of DNA for these data was ca. 4.3×10^{-5} M in base pairs.
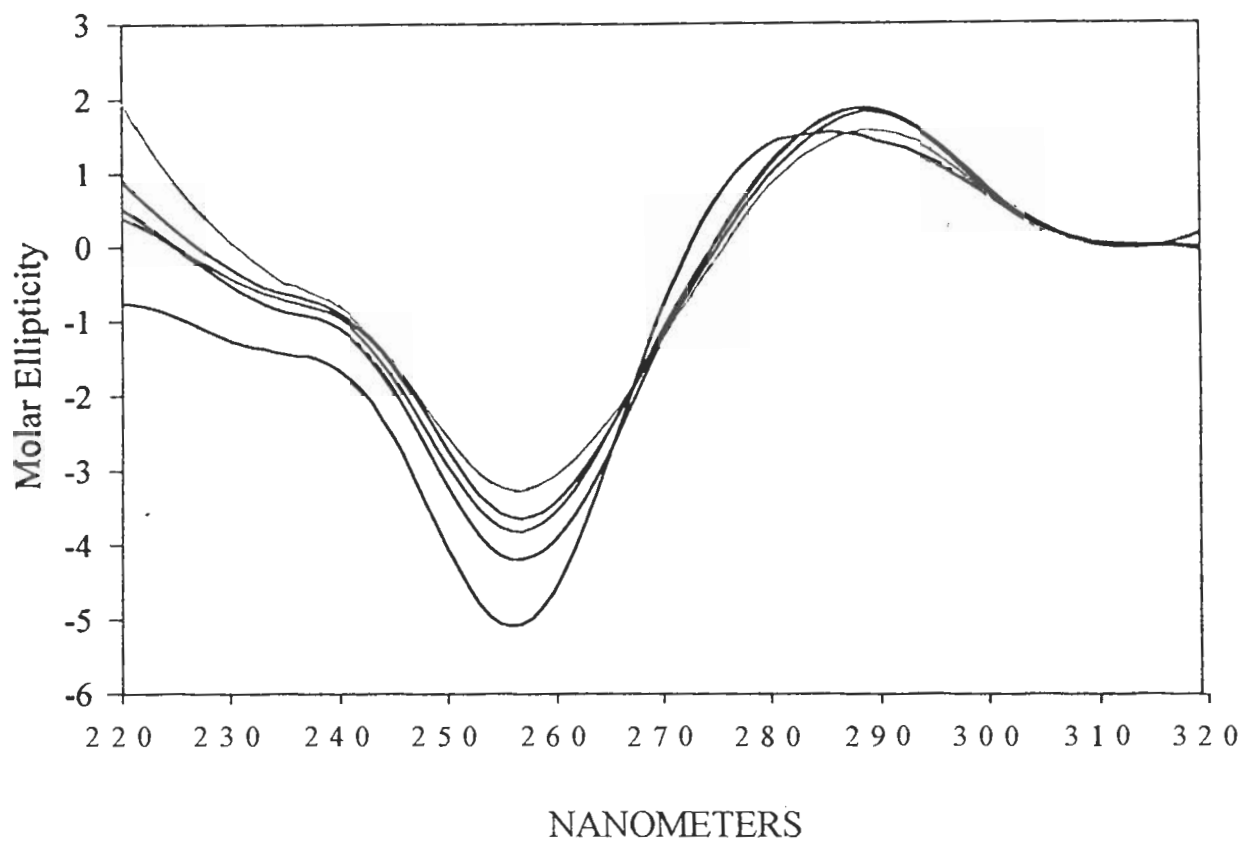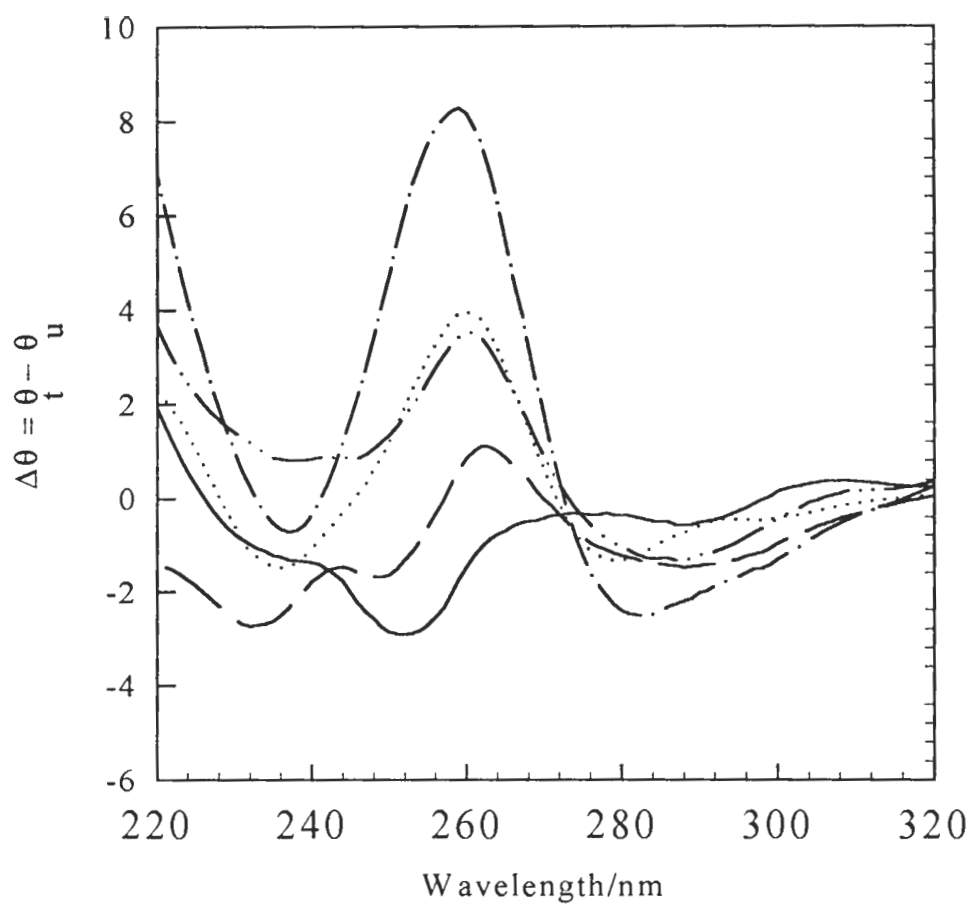
102

Figure 40. CD Difference Spectra at 95 °C of Treated and Untreated **Z8**

The effect of increasing the concentration of $[Co(NH_3)_5(OH_2)]^{3+}$ in the incubation of **Z8** at 37 °C for 48 hours, followed by exhaustive dialysis, on the molar ellipticity of the oligomer in standard buffer with 200 mM NaCl at 95 °C, which is at denaturing conditions. The CD difference spectra are plotted as: $\Delta\theta = \theta_t - \theta_u$, where θ_t and θ_u are the molar ellipticities of treated and untreated oligomer, respectively. The concentration of $[Co(NH_3)_5(OH_2)]^{3+}$ in the incubation was 100 µM (solid), 200 µM (dash), 250 µM (dot), 300 µM (dash-dot), and 400 µM (dash-dot-dot). The concentration of DNA for these data was ca. 4.3 x 10^{-5} M in base pairs.
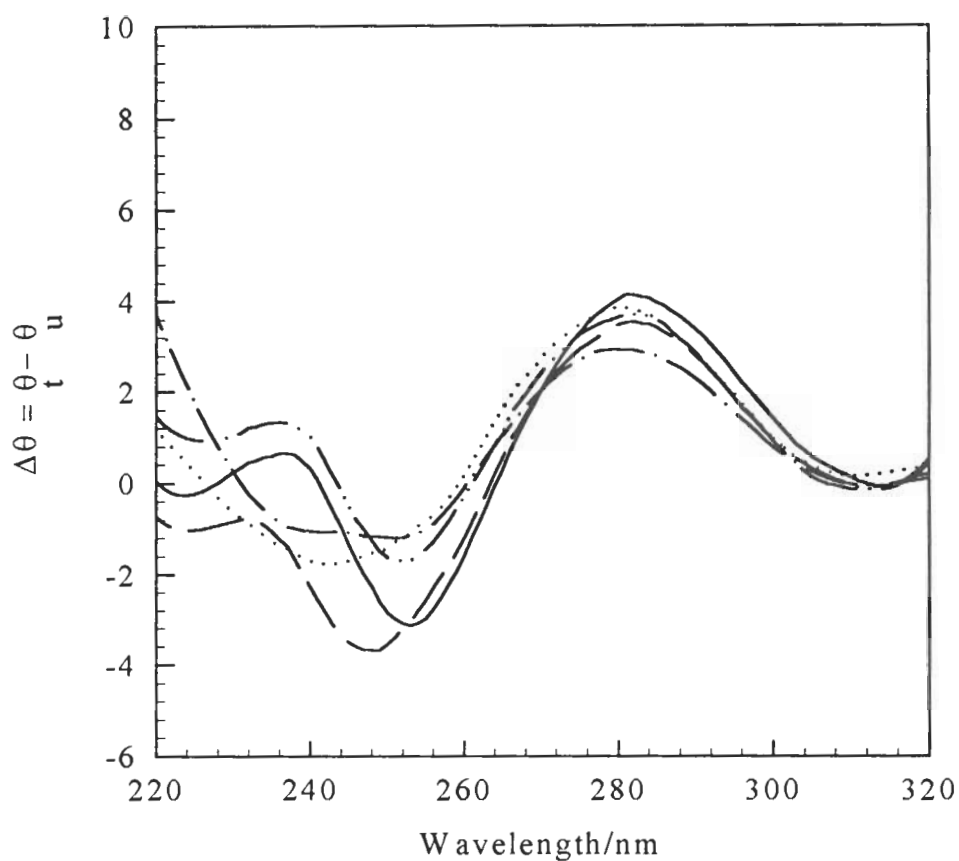
103

Figure 41. CD Temperature Difference Spectra for Incubated **Z8**

The effect of increasing the concentration of $[Co(NH_3)_5(OH_2)]^{3+}$ in the incubation of **Z8** at 37 °C for 48 hours, followed by exhaustive dialysis, on the molar ellipticity of the oligomer in standard buffer with 200 mM NaCl. The CD temperature difference spectra for untreated and treated **Z8** are plotted as: $\Delta\theta = \theta_{95C} - \theta_{25C}$, where the subscripts designate the temperature at which the spectra were recorded. The concentration of $[Co(NH_3)_5(OH_2)]^{3+}$ in the incubation was 0 (solid), 100 μM (short dash), 200 μM (dot), 250 μM (long dash), 300 μM (dash-dot), and 400 μM (dash-dot-dot). The concentration of DNA for these data was ca. 4.3×10^{-5} M in base pairs.
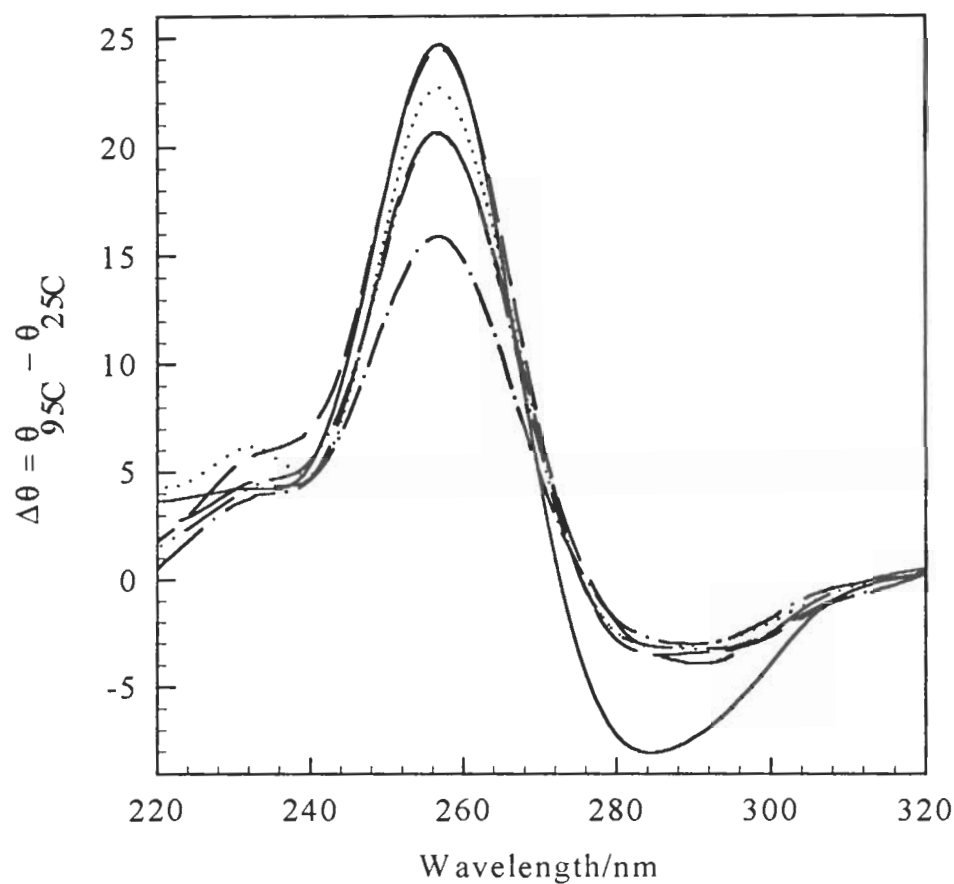
104
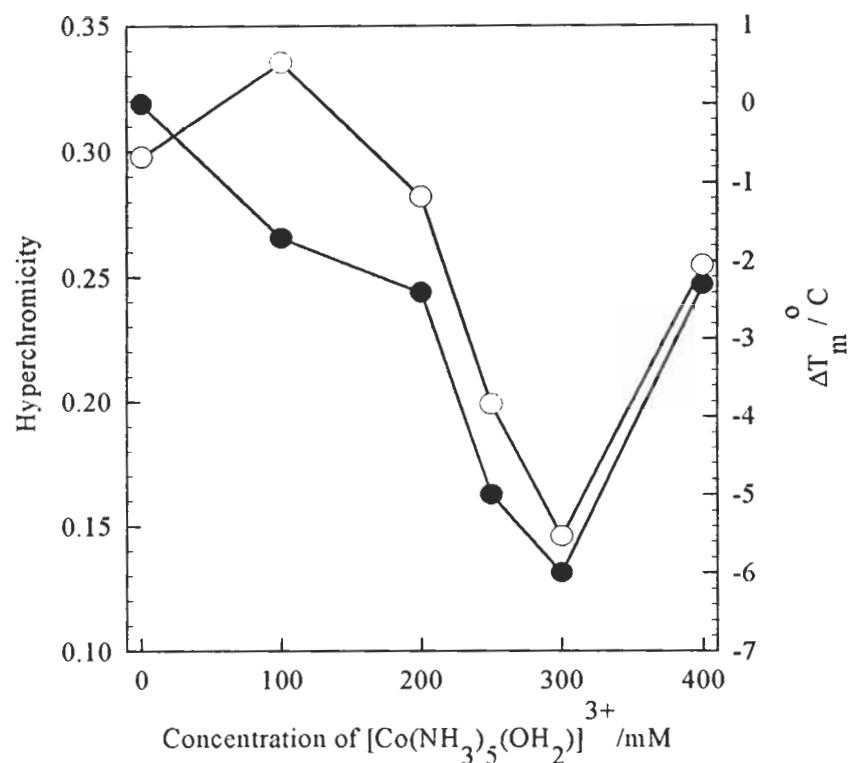
Figure 42. Dependence of the Hyperchromicity and ΔT_m of Incubated **Z8** on the Concentration of $[Co(NH_3)_5(OH_2)]^{3+}$

The effect of increasing the concentration of $[Co(NH_3)_5(OH_2)]^{3+}$ in the incubation of **Z8** at 37 °C for 48 hours, followed by exhaustive dialysis, on the thermal denaturation. Thermal denaturation studies were carried out in standard buffer with 200 mM NaCl. Hyperchromicity (open circle) is calculated as $(A_{280,95C} - A_{280,25C})/A_{280,25C}$, where $A_{280,95C}$ and $A_{280,25C}$ are the absorbances of the sample at 280 nm at 95 °C and 25 °C, respectively. The change in thermal denaturation temperature (filled circle), ΔT_m, is $T_{m,t} - T_{m,u}$ where $T_{m,t}$ and $T_{m,u}$ are the thermal denaturation temperatures of treated and untreated samples, respectively. The T_m values were determined as the inflection point of absorbance versus temperature plots via first derivatives (Godiff software, Turbo-Basic). The DNA concentration for all samples for these data was ca. 4.3×10^{-4} M in base pairs.

105
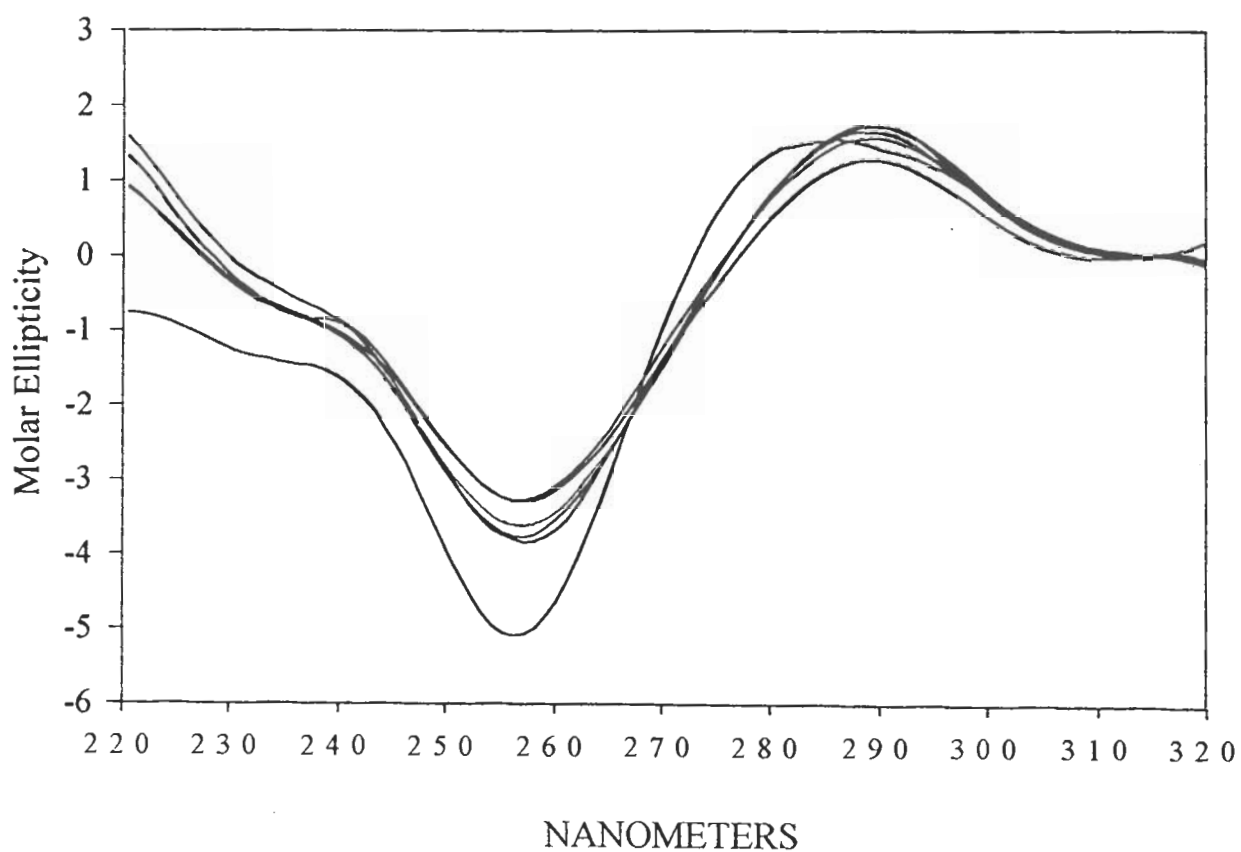
Figure 43. CD Spectra of **Z8** Incubated with $[Co(NH_3)_5(OH_2)]^{3+}$ for Various Reaction Times

The effect of increasing the reaction time in the incubation of **Z8** at 37 °C with 200 μM $[Co(NH_3)_5(OH_2)]^{3+}$, followed by exhaustive dialysis, on CD spectra. The incubation times were 0 (bottom line at 255 nm), 6 hours, 13 hours, 27 hours, 51 hours, and 76 hours. For the CD spectra, the samples were kept at 25 °C.

106
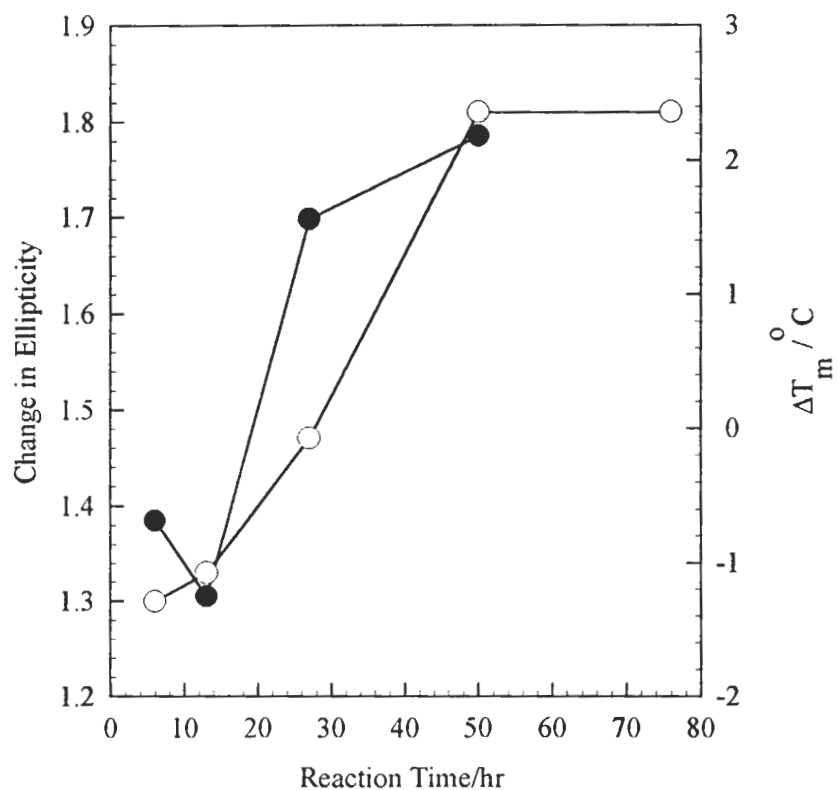
Figure 44. Dependence of Δ Molar Ellipticity and ΔT_m of Z8 upon Incubation Reaction Time

The effect of increasing the reaction time in the incubation of **Z8** at 37 °C with 200 μM $[Co(NH_3)_5(OH_2)]^{3+}$, followed by exhaustive dialysis, on thermal denaturation and CD molar ellipticity at 255 nm. Thermal denaturation studies were carried out in standard buffer with 200 mM NaCl. The T_m values (filled circles) were determined as the inflection point of absorbance versus temperature plots via first derivatives (Godiff software, Turbo-Basic). CD spectra were carried out at 25 °C in standard buffer with 200 mM NaCl, and the B-trough values at 255 nm were replotted (open circles) as a measure of distortion and lessening of the right-handed helix. The DNA concentration for all samples for these data was ca. 4.3×10^{-4} M in base pairs.
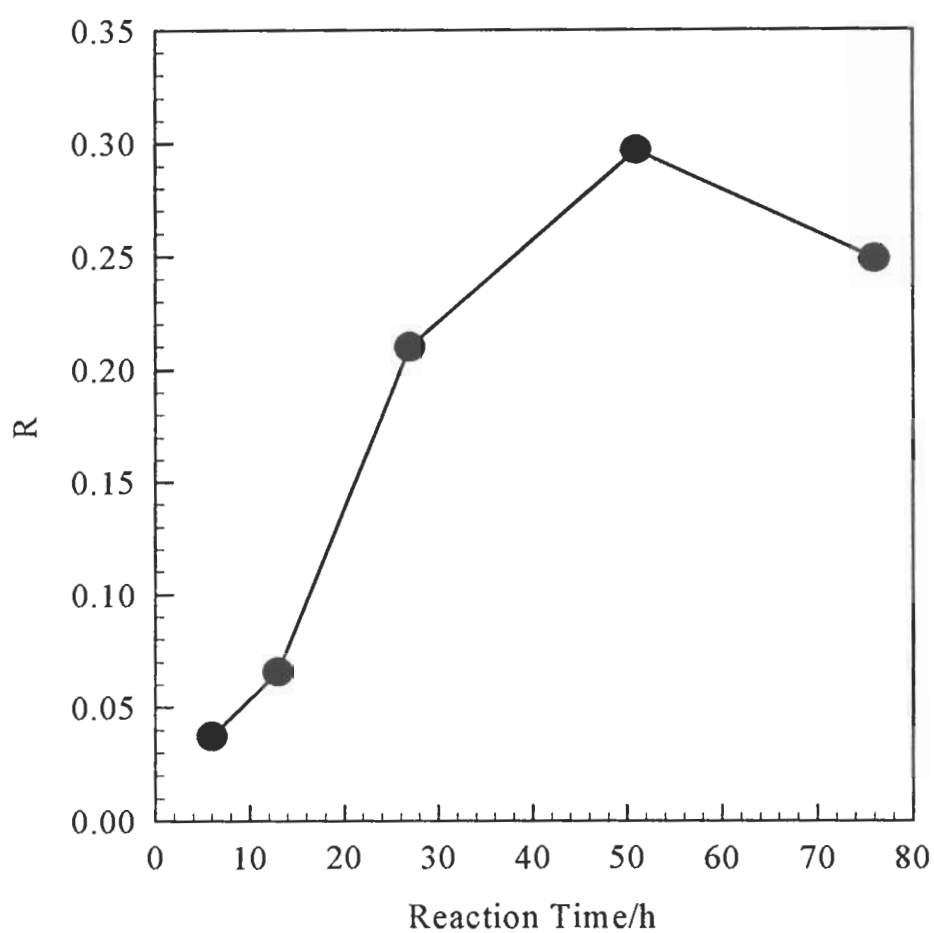
Figure 45. Dependence of Cobalt Uptake by **Z8** on Incubation Reaction Time

The effect of incubation time for cobalt binding to **Z8** treated with 200 μM $[Co(NH_3)_5(OH_2)]^{3+}$ at 37 °C, followed by exhaustive dialysis. The binding ratio, **R**, is determined as the number of atoms of cobalt bound per base pair of DNA. The concentration of cobalt was determined by graphite furnace atomic absorption spectroscopy as detailed in Materials and Methods.
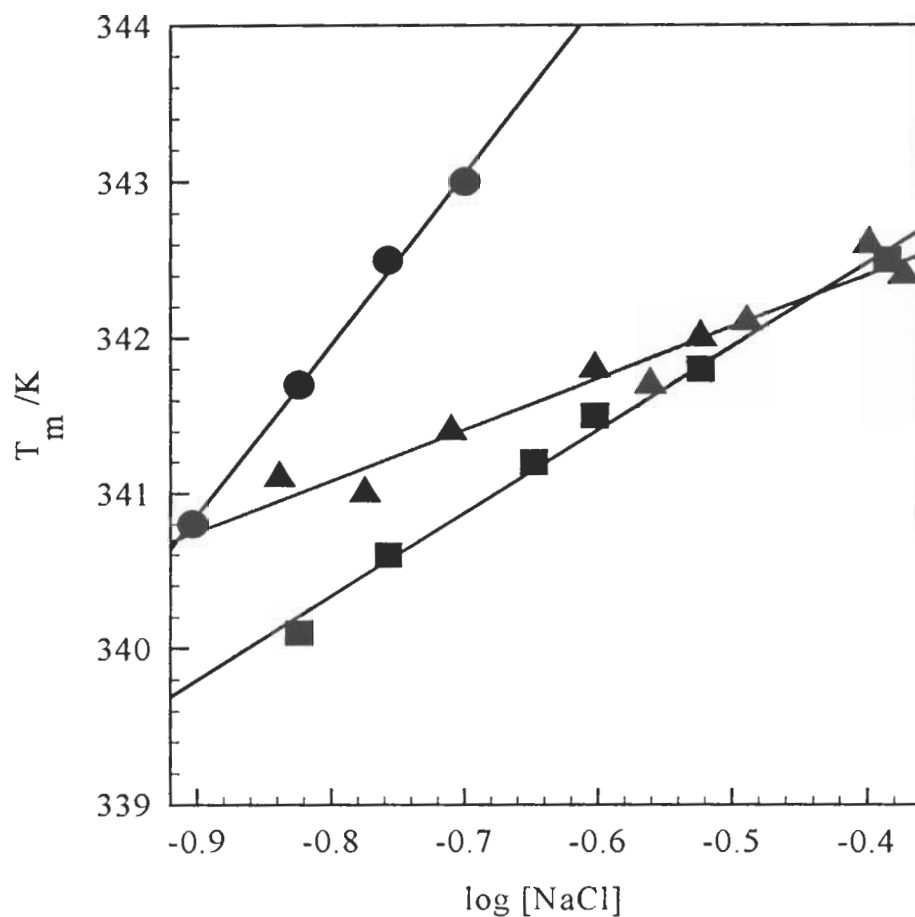
Figure 46. T_m versus Log [NaCl] for **Z8** under Various Cobalt Treatments

Plots of T_m versus log [NaCl] for the **Z8** samples {1} untreated **Z8** (circles); {2} **Z8** heat-annealed in the presence of 200 μM $[Co(NH_3)_5(OH_2)]^{3+}$, followed by exhaustive dialysis (squares); {3} **Z8** incubated with 200 μM $[Co(NH_3)_5(OH_2)]^{3+}$ at 37 °C for 48 hours, followed by exhaustive dialysis (triangles). All DNA samples were prepared in 5 mM phosphate buffer, pH 7.0, with NaCl added to give [NaCl] ranging from 125 to 400 mM ([DNA] = 4.3 x 10^{-4} M in base pairs). Thermal denaturation studies and T_m determinations were carried out as described in Materials and Methods.

109

CHAPTER IV

CONCLUSIONS

The data presented here indicate that $[Co(NH_3)_5(OH_2)]^{3+}$ does not, in the manner of $[Co(NH_3)_6]^{3+}$, induce the B to Z-form transition in the alternating purine-pyrimidine oligomer $(5medC-dG)_4$, or **Z8**, but the complex with a labile ligand apparently does modify the oligomer. The degree of modification depends upon the concentration of the cobalt complex, the method of treatment (with respect to temperature), and the length of incubation. The UV and CD spectral data presented (Figures 6 & 7) suggest that heat-annealing **Z8** in the presence of $[Co(NH_3)_5(OH_2)]^{3+}$ modifies the oligomer to an altered B-like conformation. Since the heat annealing was carried out at 80 °C for 2 minutes, it is likely that most of the oligomer was single stranded during that treatment. In order to investigate the interaction of $[Co(NH_3)_5(OH_2)]^{3+}$ with duplex DNA, the oligomer was incubated in the presence of the cobalt complex at 37 °C (the T_m of **Z8** under the conditions used is about 70 °C). As evidenced by the UV and CD difference spectra (Figures 37 & 41), such incubation of **Z8** in the presence of increasing concentrations of $[Co(NH_3)_5(OH_2)]^{3+}$ also leads to modification to a B-like conformation even after exhaustive dialysis.

Upon heating, $[Co(NH_3)_5(OH_2)]^{3+}$ in solution reacts with itself, forming a red powdery inorganic precipitate as a result of dimerization and polymerization (Cotton & Wilkinson, 1988). However, for the protocols used at the concentrations of 200-300 μM in cobalt complex, binding to and modification of the DNA occurs before much cobalt to cobalt chemistry.

110

Other oligomers are modified by the cobalt complex upon the heating and annealing treatment. The dodecamer $[(CG)_2ATAT(CG)_2]_2$, **12-mer**, showed reduced UV hyperchromicity after heat treatment. A pair of oligomers, which showed selectivity for cross-linking by cis-Pt$(NH_3)_2Cl_2$ (Hopkins et al., 1991), were modified by treatment with $[Co(NH_3)_5(OH_2)]^{3+}$. These oligomers are 17 bases long, with 8 adenines and 7 thymines in a strand as well as a pair of guanines and cytosines. In the self-complementary 14 base region, one oligomer has a core sequence of -AGCT- (designated **GC-site**) and the other has -ACGT- at its center (**CG-isomer**). Reduced UV hyperchromicity upon denaturation of treated oligomers, exhibited strongly for **Z8** and **GC-site**, coincides with GpC as part of the sequence. There are three such steps in **Z8**. In the case of the 17-mers, modification of the central GpC site in **GC-site** causes a stabilization of the helix (higher T_m) which is not exhibited with **CG-isomer** under the same conditions. This is consistent with the GN7 to GN7 crosslink results reported with cis-Pt$(NH_3)_2Cl_2$ (Hopkins et al., 1991). A 24-mer oligomer, $[(ACTG)_6]:[(TGAC)_6]$, which contains 12 isolated guanines, has some reduced UV hyperchromicity after heat treatment with the complex, but showed no significant change in the temperature of thermal denaturation. This indicates that the separated guanines in the 24-mer are modified, but only by cobalt complexes which are non-bridging.

The data presented clearly demonstrate that the treated oligomers **Z8**, **12-mer**, and **GC-site**, are conformationally distinct from untreated oligomer in both the native (i.e., at 25 °C) and denatured (i.e. at 95 °C) states. The melting profiles indicate complete thermally induced transitions for both treated and untreated oligomers, as evidenced by establishment on an upper baseline at the high-end temperatures (Figures 22-24 & 26).

111

Treatment of sonicated calf thymus DNA with $[Co(NH_3)_5(OH_2)]^{3+}$ via incubation at 37 °C for 48 hours with 400 µM and 200 µM complex (140 - 560 µM DNA), followed by dialysis, modifies the natural polymer. Subsequent thermal denaturations show distorted DNA with lower T_m's with increasing complex (Figure 30). However, the sample of DNA which was incubated at the highest concentration of complex (and of DNA) did not fully melt. Upon reannealing and remelting, that sample exhibited some sigmoidal nature in its thermal transition profile (Figure 31). This is in contrast to the other samples (and control) which appeared only as a random-coil structure. The incubation with $[Co(NH_3)_5(OH_2)]^{3+}$ modifies natural DNA, and the results are consistent with the earlier heat treatment studies of oligomers (Calderone et al., 1995).

Z8 was incubated with 200 µM $[Co(NH_3)_5(OH_2)]^{3+}$, dialyzed and then monitored by thermal denaturation and CD spectropolarimetry. The modification of **Z8** by incubation reduces UV hyperchromism and distorts CD spectra to an extent proportional to time of incubation and concentration of complex (Figures 42 & 44). During the incubation with 200 µM $[Co(NH_3)_5(OH_2)]^{3+}$, Z8 binds cobalt with time, up to one cobalt for every 4 base pairs after two days, as shown directly by atomic absorption (Figure 45). The salt dependence of melting temperature is shown for three oligomer samples: **Z8** control, **Z8** heat-treated and dialyzed, and **Z8** incubated and dialyzed (Figure 46). From the slopes of the T_m versus log [NaCl] plot, the differential ion binding term, Δn, can be calculated. The Δn term represents the release of counterions per duplex upon denaturation (in that double stranded DNA has a higher charge density than single stranded DNA). For the oligomers **Z8** control, **Z8** heat-treated, and **Z8** incubated, the Δn terms are 0.92, 0.48, and 0.28, respectively. This is indirect

112

evidence that the two methods of modification result in cobalt being tightly bound to the DNA. The incubated sample has more bound metal (is more modified) in that fewer sodium ions are released upon melting.

A covalent bond between N-7 of guanine and the Co (III) center, via displacement of the water, is highly likely. The data for **Z8**, **12-mer**, **GC-site**, and calf thymus DNA are also consistent with cobalt mediated interstrand crosslinking. At high concentrations of $[Co(NH_3)_5(OH_2)]^{3+}$ and long reaction times, the modification was more prevalent. As with $cis\text{-}Pt(NH_3)_2Cl_2$, the GpC sequence provides the crosslinkable site. Crosslinking through cobalt would only be possible through loss of one of the ammines. The interaction of $[Co(NH_3)_5(OH_2)]^{3+}$ with **Z8**, **12-mer**, and **GC-site** modifies the conformational properties of the DNA oligomer at both 25 °C and 95 °C. The results suggest that other simple cobalt (III) complexes may have surprisingly interesting DNA binding properties.

113

References

Basolo, F. & Murmann, R. K. (1953). Acidopentamminecobalt(III) Salts. *Inorg. Syn. 4*, 171-176.

Behe, M. J. & Felsendfeld G. (1981). Effects of Methylation on a Synthetic Polynucleotide: B-Z Transition in Poly(dG-m^{5}dC). *Proc. Natl. Acad. Sci. USA 78*, 112-118.

Blackburn, G. M. & Gait, M. J. (1996). **Nucleic Acids in Chemistry and Biology** (second edition). Oxford University Press, New York.

Blundell, T. L. & Johnson, L. N. (1976). **Protein Crystallography.** Academic Press, New York.

Brabek, V., Reedijk, J. & Leng, M. (1992). Sequence-Dependent Distortions Induced in DNA by Monofunctional Platinum(II) Binding. *Biochemistry 31*, 12397-12402.

Braunlin, W. H., Anderson, C. F. & Record, Jr., M. T. (1987). Competitive Interactions of Co(NH$_3$)$_6$$^{+3}$ and Na$^+$ with Helical DNA Probed by ^{59}Co and ^{23}Na NMR. *Biochemistry 26*, 7724-7731.

Braunlin, W. H. & Xu, Q. (1992). Hexaamminecobalt (III) Binding Environments on Double-Helical DNA. *Biopolymers 32*, 1703-1711.

Bruhn, S. L., Toney, J. H. & Lippard, S. J. (1990). Biological Processing of DNA Modified by Platinum Complexes. *Prog. Inorg. Chem. 38*, 477-516.

Buckingham, D. A., Cresswell, P. J., Dellaca, R. J., Dwyer, M., Gainsford, G. J., Marzilli, L. G., Maxwell, I. E., Robinson, W. T., Sargeson, A. M. & Turnbull, K. R. (1974). Structure, Conformational Analysis, and Properties of Diastereoisomeric Forms of β_1-Glycinato triethylenetetraminecobalt(III) Ions. *J. Amer. Chem. Soc. 96*, 1713-1725.

Calderone, D. M., Mantilla, E. J., Hicks, M., Huchital, D. H., Murphy, W. R., Jr., & Sheardy, R. D. (1995). Binding of Co(III) to a DNA Oligomer via Reaction of [Co(NH$_3$)$_5$(OH$_2$)]$^{+3}$ with (5medC-dG)$_4$. *Biochemistry 34*, 13841-13846.

Calladine, C. R., Drew, H. R. & McCall, M. J. (1988). Intrinsic curvature of DNA in solution. *J. Mol. Biol., 210*, 127-137.

Cantor, C. R. & Warshaw, M. M. (1970). Oligonucleotide Interactions. III. Circular Dichroism Studies of the Conformation of Deoxyoligonucleotides. *Biopolymers 9*, 1059-1077.

114

Cantor, C. R. & Schimmel, P. R. (1980). **Biophysical Chemistry Part III: The Behavior of Biological Macromolecules**. W. H. Freeman and Company, New York.

Caruthers, M. H. (1985). Gene Synthesis Machines: DNA Chemistry and Its Uses. *Science, 230*, 281-285.

Carlson, D. L., Huchital, D. H., Mantilla, E. J., Sheardy, R. D. & Murphy, Jr., W. R. (1993). A New Class of DNA Metallobinders Showing Spectator Ligand Size Selectivity: Binding of Ligand Bridged Bimetallic Complexes of Ru(II) to Calf Thymus DNA. *J. Amer. Chem. Soc. 115*, 6424-6425.

Chaires, J. B., Fox, K. R., Herrera, J. E., Britt, M. & Waring, M. J. (1987). Site and Sequence Specificity of the Daunomycin-DNA Interaction. *Biochemistry, 26*, 8227-8236.

Chaires, J. B. (1990). Biophysical Chemistry of the Daunomycin-DNA Interaction. *Biophys. Chem. 35*, 191-202.

Chaires, J. B., Priebe, W., Graves, D. & Burke, T. G. (1993). Dissection of the Free Energy of Anthracycline Antibiotic Binding to DNA: Electrostatic Contributions. *J. Amer. Chem. Soc. 115*, 5360-5364.

Clarke, M. J. & Taube, H. (1974). Pentaammineruthenium-Guanine Complexes. *J. Amer. Chem. Soc. 96*, 5413-5419.

Clarke, M. J. & Taube, H. (1975). Nitrogen-Bound and Carbon-Bound Xanthine Complexes of Ruthenium Ammines. *J. Amer. Chem. Soc. 97*, 1397-1403.

Clarke, M. J. (1977). Linkage Isomers of Pentaammineruthenium-Hypoxanthine Complexes. *Inorg. Chem. 16*, 738-744.

Clarke, M. J. (1980). The Potential of Ruthenium in Anticancer Pharmaceutical. In **Inorganic Chemistry in Biology and Medicine**, edited by A. E. Miller. American Chemical Society, Washington, DC. 157-180.

Clarke, M. J., Jansen, B., Marx, K. A. & Kruger, R. (1986). Biochemical Effects of Binding $[(H_2O)(NH_3)_5Ru^{II}]^{+2}$ to DNA and Oxidation to $[(NH_3)_5Ru^{III}]_n$-DNA. *Inorg. Chim. Acta 124*, 13-28.

Cornelius, R. D., Hart, P. A. & Cleland, W. W. (1977). Phosphorus-31 NMR Studies of Complexes of Adenosine Triphosphate, Adenosine Diphosphate, Tripolyphosphate, and Pyrophosphate with Cobalt(III) Ammines. *Inorg. Chem. 16*, 2799-2805.

Cotton, A. F. & Wilkinson, G. (1988). **Advanced Inorganic Chemistry** (fifth edition).

John Wiley & Sons, New York. 732-738.

Crothers, D. M., Haran, T. E., & Nadeau J. G. (1990). Intrinsically Bent DNA. *J. Biological Chemistry 265*, 7093-7096.

de Meester, P., Goodgame, D. M. L., Jones, T. J., & Skapski, A. C. (1974). X-Ray Evidence for Metal-N-7 Bonding in a Hydrated Manganese Derivative of Guanosine 5'-Monophosphate. *Biochem. J. 139*, 791-792.

Dickerson, R. E. (1989). Definitions and Nomenclature of Nucleic Acid Structure Parameters. *J. Mol. Biol. 205*, 787-791.

Dickerson, R. E. (1992). DNA Structure from A to Z. *Methods In Enzymology 211*, 67-111.

Dickerson, R. E., Goodsell, D. S., & Neidle, S. (1994). "...the tyranny of the lattice..." *Proc. Natl. Acad. Sci. USA 91*, 3579-3583.

Dixon, N. E., Jackson, W. G., Lancaster, M. J., Lawrance, G. A., & Sargeson, A. M. (1981). Labile (Trifluoromethanesulfonato)cobalt(III) Amine Complexes. *Inorg. Chem. 20*, 470-476.

Drew, H. R. & Dickerson, R. E. (1981). Structure of a B-DNA Dodecamer III. Geometry of Hydration. *J. Mol. Biol. 151*, 535-556.

Eastman, A. (1983). Characterization of the Adducts Produced in DNA by *cis*-diamminedichloroplatinum(II) and *cis*-dichloro(ethylenediamine)Pt(II). *Biochemistry 22*, 3927-3933.

Eastman, A. (1986). Reevaluation of Interaction of *cis*-dichloro(ethylenediamine)Pt(II) with DNA. *Biochemistry 25*, 3912-3915.

Eisenberg, D. (1970). X-ray Crystallography and Enzyme Structure. In **The Enzymes** (third edition), edited by P. D. Boyer. Academic Press, New York. vol. I, 1-89.

Ezaz-Nikpay, K. & Verdine, G. L. (1992). Aberrantly Methylated DNA: Site-Specific Introduction of N7-methyl-2'-deoxyguanosine into the Dickerson/Drew Dodecamer. *J. Amer. Chem. Soc. 114*, 6562-6563.

Fichtinger-Schepman, A. M. J., van der Veer, J. L., Lohman, P. H. M. & Reedijk, J. (1984). A Simple Method for the Inactivation of Monofunctionally DNA-Bound *cis*-Diamminedichloroplatinum(II). *Journal of Inorganic Biochemistry 21*, 103-112.

Fichtinger-Schepman, A. M. J., van der Veer, J. L., den Hartog, J. H. J., Lohman, P. H. M. & Reedijk, J. (1985). Adducts of the Antitumor Drug *cis*-Diamminedichloroplatinum(II) with

116

DNA: Formation, Identification, and Quantitation. *Biochemistry 24*, 707-713.

Friedman, R. A. G. & Manning, G. S. (1984). Polyelectrolyte Effects on Site-Binding Equilibria with Application to the Intercalation of Drugs into DNA. *Biopolymers 23*, 2671-2714.

Geiduschek, P. (1961). "Reversible" DNA. *Proc. Natl. Acad. Sci. USA 47*, 950-955.

Gessner, R. V., Quigley, G. J., Wang, A. H.-J., van der Marel, G. A., van Boom, J. H. & Rich, A. (1985). Structural Basis for Stabilization of Z-DNA by Cobalt Hexaammine and Magnesium Cations. *Biochemistry 24*, 237-240.

Hicks, M., Wharton, G. F., III, Huchital, D. H., Murphy, W. R., Jr., & Sheardy, R. D. (1997a). Assessing the Sequence Specificity in the Binding of Co(III) to DNA via A Thermodynamic Approach. *Biopolymers*, in press.

Hicks, M., Xiao, B., Pantano, T., Sheardy, R. D., Huchital, D. H., & Murphy, W. R., Jr. (1997b). Reduced BamH I Activity due to the Irreversible Coordination of Pentaammineaquocobalt(III) to d(-GG-) Oligomeric Nucleic Acids. Manuscript in preparation.

Hopkins, P. B., Millard, J. T., Woo, J., Weidner, M. F., Kirchner, J. J., Sigurdsson, S. T. & Raucher, S. (1991). Sequence Preferences of DNA Interstrand Cross-Linking Agents: Importance of Minimal DNA Structural Reorganization in the Cross-Linking Reactions of Mechlorethamine, Cisplatin, and Mitomycin C. *Tetrahedron 47*, 2475-2489.

Huang, H., Zhu, L., Reid, B. R., Drobny, G. P., & Hopkins, P. B. (1993). Solution Structure of a Cisplatin-Induced DNA Interstrand Cross-Link. *Science 270*, 1842-1845.

Jack, A., Ladner, J. E., Rhodes, D., Brown, R. S., & Klug, A. (1977). A Crystallographic Study of Metal-binding to Yeast Phenylalanine Transfer RNA. *J. Mol. Biol. 111*, 315-328.

Kabsch, W., Sander, C. & Trifonov, E. N. (1982). The ten helical twist angles of B-DNA. *Nucleic Acids Res. 10*, 1097-1104.

Karpel, R. L., Miller, N. S., Lesk, A. M., & Fresco, J. R. (1975). Stabilization of the Native Tertiary Structure of Yeast tRNA$_3^{Leu}$ by Cationic Metal Complexes. *J. Mol. Biol. 97*, 519-532.

Kopka, M. L., Yoon, C., Goodsell, D., Pjura, P., & Dickerson, R. E. (1985). The molecular origin of DNA-drug specificity in netropsin and distamycin. *Proc. Natl. Acad. Sci. USA 82*, 1376-1380.

Kozelka, J. & Chottard, J.-C. (1990). How does cisplatin alter DNA structure? A molecular mechanics study on double-stranded oligonucleotides. *Biophys. Chem. 35*, 165-178.

Kristenmacher, T. J., Marzilli, L. G. & Chang, C.-H. (1973). Crystal and Molecular Structure of a Cobalt(III) Complex Containing Adenine as a Unidentate Ligand. *J. Amer. Chem. Soc. 95*, 5817-5819.

Lefebvre, A., Mauffret, O., Hartmann, B., Lescot, E., & Fermandjian, S. (1995). Structural Behavior of the CpG Step in Two Related Oligonucleotides Reflects Its Malleability in Solution. *Biochemistry 34*, 12019-12028.

Lu, M., Guo, Q., Kallenbach, N. R. & Sheardy, R. D. (1992). Conformational Properties of B-Z Junctions in DNA. *Biochemistry 31*, 4712-4719.

Malinge, J.M., Perez, C., & Leng, M. (1994). Base Sequence-independent Distortions Induced by Interstrand Cross-links in *cis*-Diamminedichloroplatinum(II) Modified DNA. *Nuc. Acid Res. 22*, 3834-3839.

Manning, G. S. (1978). The molecular Theory of Polyelectrolyte Solutions with Applications to the Electrostatic Properties of Polynucleotides. *Q. Rev. Biophys. 11*, 179-246.

Marky, L. & Breslauer, K. (1987). Calculating Thermodynamic Data for Transitions of any Molecularity from Equilibrium Melting Curves. *Biopolymers 26*, 1601-1620.

Marzilli, L. G., Kristenmacher, T. J. & Chang, C.-H. (1973). Intramolecular Hydrogen Bonding in Metal-Purine Systems. Synthesis and Structure of a Cobalt(III)-Theophylline Complex. *J. Amer. Chem. Soc. 95*, 7507-7508.

Marzilli, L. G., Kristenmacher, T. J., Darcy, P. E., Szalda, D. J. & Beer, M. (1974). Nucleoside Complexing. Interligand Interactions between Purine and Pyrimidine Exocyclic Groups and Polyamines. The Importance of Both Hydrogen Bonds and Nonbonding Repulsions. *J. Amer. Chem. Soc. 96*, 4686-4688.

Marzilli, L. G., Epps, L. A., Sorrell, T., & Kistenmacher, T. J. (1975). Reaction of Coordinated Purines. A Facile, High Yield Synthetic Route to N(7)-Alkylated Xanthines and Hypoxanthines. The Structure of [Bis(dimethylglyoximato)(xanthinato)-(tri-*n*-butyl phosphine)cobalt(III)] and the Trans Influence in Cobalt(III) Chemistry. *J. Amer. Chem. Soc. 97*, 3351-3358.

Marzilli, L. G. (1977). Metal-Ion Interactions with Nucleic Acids and Nucleic Acid Derivatives. *Prog. Inorg. Chem. 23*, 225-378.

Marzilli, L. G. (1981). Metal Complexes of Nucleic Acid Derivatives and Nucleotides:

118

Binding Sites and Structures. In **Metal Ions in Genetic Information Transfer,** edited by G. L. Eichorn & L. G. Marzilli. Elsevier, New York. 47-85.

Matthews, B. W. (1977). X-ray Structure of Proteins. In **The Proteins** (third edition), edited by H. Neurath & R. L. Hill. Academic Press, New York. vol. **3, pp.** 404-590.

Muller, J. G., Chen, X., Dadiz, A. C., Rokita, S. E., & Burrows, C. (1992). Ligand Effects Associated with the Intrinsic Selectivity of DNA Oxidation Promoted by Nickel(II) Macrocyclic Complexes. *J. Amer. Chem. Soc. 114*, 6407-6411.

Murray, V., Motyka, H., England, P. R., Wickham, G., Lee, H. H., Denny, W. A. & McFadyen, W. D. (1992). An Investigation of the Sequence-Specific Interaction of *cis*-Diamminedichloroplatinum(II) and Four Analogues, Including Tow Acridine-Tethered Complexes, with DNA in Human Cells. *Biochemistry 31*, 11812-11822.

Pelton, J. G. & Wemmer, D. E. (1989). Structural characterization of a 2:1 distamycin A∘d(CGCAAATTGGC) complex by two-dimensional NMR. *Proc. Natl. Acad. Sci. USA 86*, 5723-5727.

Pett, V. B., Sorof, J. M., Fenderson, M. B., & Zeff, L. A. (1985). The Effect of Cr(III) upon the Thermal Denaturation of DNA. *Bioorganic Chemistry 13*, 24-33.

Pinto, A. L & Lippard, S. J. (1985). Binding of the Antitumor Drug cis-Diamminedichloroplatinum(II) to DNA. *Biochem. Biophys. Acta 780*, 167-180.

Rahmouni, A. & Leng, M. (1987). Reaction of Nucleic Acids with *cis*-Diamminedichloroplatinum(II) Interstrand Crosslinks. *Biochemistry 26*, 7229-7234.

Record, M. T., Jr., Anderson, C. F., & Lohman, T. M. (1978). Thermodynamic Analysis of Ion Effects on the Binding and Conformational Equilibria of Proteins and Nucleic Acids: The Roles of Ion Association or Release, Screening, and Ion Effects on Water Activity. *Q. Rev. Biophys. 11*, 102-178.

Saenger, W. (1984). **Principles of Nucleic Acid Structure**. Springer-Verlag, New York.

Saenger, W., Hunter, W. N. & Kennard, O. (1986). DNA conformation is determined by economics in the hydration of phosphate groups. *Nature 324*, 385-388.

Seeman, N. C., Rosenberg, J. M. & Rich, A. (1976). Sequence Specific Recognition of Double Helical Nucleic Acids by Proteins. *Proc. Natl. Acad. Sci. USA, 73*, 804-808.

Sheardy, R. D. (1988). Preliminary Spectroscopic Characterization of a Synthetic DNA Oligomer Containing a B-Z Junction at High Salt. *Nucleic Acids Res. 16*, 1153-1167.

119

Sheardy, R. D. (1991). Monitoring Conformational Transitions in Synthetic DNA Oligomers Using Circular Dichroism. *Spectroscopy, 6*, 14-17.

Sheardy, R. D., Levine, N., Marotta, S., Suh, D. & Chaires, J. B. (1994). A Thermodynamic Investigation of the Melting of B-Z Junction Forming DNA Oligomers. *Biochemistry, 33*, 1385-1391.

Sorrell, T., Epps, L. A., Kristenmacher, T. J. & Marzilli, L. G. (1977). Stereoselectivity in the Binding of the Bis(acetylacetonato)(nitro)cobalt(III) Moiety to Purines and Pyrimidines and Their Nucleosides, an Evaluation of the Role of Interligand Interactions in Stereoselectivity, and the Molecular and Crystal Structure of the Bis(acetylacetonato) (nitro)(deoxyadenosine) cobalt(III) Complex. *J. Amer. Chem. Soc. 99*, 2173-2179.

Tajmir-Riahi, H. A. (1991). Interaction of Purine Nucleotides with Cobalt-Hexammine, Cobalt-Pentammine and Cobalt-Tetrammine Cations. Evidence for the Rigidity of Adenosine and Flexibility of Guanosine and Deoxyguanosine Sugar Conformations. *J. Biomol. Struct. Dyn. 8*, 1169-1186.

Tajmir-Riahi, H. A., Naoui, M. & Ahmad, R. (1993). Effects of Cobalt-Hexaammine and Cobalt-Pentammine Cations on Solution Structure of Calf-Thymus DNA, DNA Condensation and Structural Features by FTIR Difference Spectra. *J. Biomol. Struct. Dyn. 11*, 83-93.

Takahara, P. M., Rosenzweig, A. C., Frederick, C. A., & Lippard, S. J. (1995). X-ray Crystal Structure of Cisplatin bound to GpG. *Nature 377*, 649.

Thomas, T. J. & Bloomfield, V. A. (1983). Collapse of DNA Caused by Trivalent Cations: pH and Ionic Specificity Effects. *Biopolymers 22*, 1097-1106.

Watson, J. D. & Crick, F. H. C. (1953). A structure for deoxyribose nucleic acid. *Nature 171*, 737-738.

Winkle, S. A. & Sheardy, R. D. (1990). Anomalous Gel Migration of DNA Oligomers Containing Multiple Conformational Junctions. *Biochemistry 29*, 6514-6521.

Winkle, S. A., Aloyo, M. C., Lee-Chee, T., Morales, N., Zambrano, T. Y. & Sheardy, R. D. (1992). The Interface Between an Alternating CG Motif and a Random Sequence Motif Displays Altered Nuclease Activity. *J. Biomol. Struct. Dyn. 10*, 389-402.

Xu, Q., Shoemaker, R. K. & Braunlin, W. H. (1993). Induction of a B-A Transition of Deoxyoligonucleotides by Multivalent Cations in Dilute Aqueous Solutions. *Biophys. J. 65*, 1039-1049.

Yohannes, P. G., Zon, G., Doetsch, P. W. & Marzilli, L. G. (1993). DNA Hairpin Formation in Adducts with Platinum Anticancer Drugs: Gel Electrophoresis Provides New Information and a Caveat. *J. Amer. Chem. Soc. 115*, 5105-5110.